University of Potsdam
Institute of Earth and Environmental Science

Turning a problem into a solution: heterogeneities in soil hydrology

Cumulative dissertation
for the degree of "doctor rerum naturalium" (Dr. rer. nat.)
in Geoecology/Hydrology

submitted to the
Faculty of Mathematics and Natural Sciences
at the University of Potsdam, Germany

by
Tobias Ludwig Hohenbrink

Potsdam, March 17th, 2016

Published online at the
Institutional Repository of the University of Potsdam:
URN urn:nbn:de:kobv:517-opus4-101485
http://nbn-resolving.de/urn:nbn:de:kobv:517-opus4-101485

Turning a problem into a solution: heterogeneities in soil hydrology

Dissertation submitted to the Faculty of Mathematics and Natural Sciences at the University of Potsdam, Germany, for the degree of Doctor of Natural Sciences (Dr. rer. nat.) in Geoecology/Hydrology

Potsdam, March 17th, 2016

Author: **Tobias Ludwig Hohenbrink**
University of Potsdam, Institute of Earth and Environmental Science, Germany
Leibniz Centre for Agricultural Landscape Research (ZALF), Institute of Landscape Hydrology, Eberswalder Str. 84, 10567 Müncheberg, Germany
Email: hohenbrink@zalf.de

Supervisor: **Prof. Dr. Gunnar Lischeid**
1. Referee *University of Potsdam, Institute of Earth and Environmental Science, Germany*
Leibniz Centre for Agricultural Landscape Research (ZALF), Institute of Landscape Hydrology, Eberswalder Str. 84, 10567 Müncheberg, Germany

2. Referee: **Prof. Dr. Hannes Flühler**
Swiss Federal Institute of Technology in Zurich *(ETH Zürich)*
Institute of Terrestrial Ecosystems, Switzerland

3. Referee **Prof. Dr. Sascha Oswald**
University of Potsdam, Institute of Earth and Environmental Science, Germany

Acknowledgements

First of all, I would like to thank my supervisor Gunnar Lischeid who encouraged me to use unconventional approaches to answer soil hydrological questions. He opened my mind for an extended perspective on the meaning of data, processes and modelling.

Thanks to my colleagues at the Institute of Landscape Hydrology at ZALF for the pleasant working atmosphere and for supporting me scientifically and organizationally. I thank Uwe Schindler for acquiring funding for my position and for inspiring conversations. Especially, I thank my colleagues Björn Thomas, Christian Lehr, Gabriela Onandia, Florian Reverey, Helene Rieckh, Marcus Fahle, Miaomiao Ma, Philipp Rauneker and Steven Böttcher for helpful discussions and proofreading my manuscripts. I am still amazed about the team spirit and openness. It was a great fun to spend time with you.

I greatly thank my family and my friends for mental support and taking my mind off things. My parents always encouraged me to follow my own way. Finally, I thank my partner Anne and our son Anton for being there for me.

Summary

It is commonly recognized that soil moisture exhibits spatial heterogeneities occurring in a wide range of scales. These heterogeneities are caused by different factors ranging from soil structure at the plot scale to land use at the landscape scale. There is an urgent need for efficient approaches to deal with soil moisture heterogeneity at large scales, where management decisions are usually made. The aim of this dissertation was to test innovative approaches for making efficient use of standard soil hydrological data in order to assess seepage rates and main controls on observed hydrological behavior, including the role of soil heterogeneities.

As a first step, the applicability of a simplified Buckingham-Darcy method to estimate deep seepage fluxes from point information of soil moisture dynamics was assessed. This was done in a numerical experiment considering a broad range of soil textures and textural heterogeneities. The method performed well for most soil texture classes. However, in pure sand where seepage fluxes were dominated by heterogeneous flow fields it turned out to be not applicable, because it simply neglects the effect of water flow heterogeneity. In this study a need for new efficient approaches to handle heterogeneities in one-dimensional water flux models was identified.

As a further step, an approach to turn the problem of soil moisture heterogeneity into a solution was presented: Principal component analysis was applied to make use of the variability among soil moisture time series for analyzing apparently complex soil hydrological systems. It can be used for identifying the main controls on the hydrological behavior, quantifying their relevance, and describing their particular effects by functional averaged time series. The approach was firstly tested with soil moisture time series simulated for different texture classes in homogeneous and heterogeneous model domains. Afterwards, it was applied to 57 moisture time series measured in a multifactorial long term field experiment in Northeast Germany.

The dimensionality of both data sets was rather low, because more than 85 % of the total moisture variance could already be explained by the hydrological input signal and by signal transformation with soil depth. The perspective of signal transformation, i.e. analyzing how hydrological input signals (e.g., rainfall, snow melt) propagate through the vadose zone, turned

out to be a valuable supplement to the common mass flux considerations. Neither different textures nor spatial heterogeneities affected the general kind of signal transformation showing that complex spatial structures do not necessarily evoke a complex hydrological behavior. In case of the field measured data another 3.6% of the total variance was unambiguously explained by different cropping systems. Additionally, it was shown that different soil tillage practices did not affect the soil moisture dynamics at all.

The presented approach does not require a priori assumptions about the nature of physical processes, and it is not restricted to specific scales. Thus, it opens various possibilities to incorporate the key information from monitoring data sets into the modeling exercise and thereby reduce model uncertainties.

Zusammenfassung

Es ist allgemein anerkannt, dass Bodenfeuchte auf verschiedenen Raumskalen räumliche Heterogenitäten aufweist. Diese Heterogenitäten werden durch verschiedene Faktoren verursacht, die auf den unterschiedlichen Skalen wirken. Dies können z.B. die Bodenstruktur auf Plotskala oder die Landnutzung auf Landschaftsskala sein. Es werden dringend effiziente Ansätze benötigt, um mit den Heterogenitäten der Bodenfeuchte umzugehen. Dies gilt besonders für große Skalen, auf denen in der Regel weitreichende Managemententscheidungen getroffen werden. Das Ziel dieser Dissertation war es, effiziente Methoden zu testen, die es ermöglichen auf Basis bodenhydrologischer Daten sowohl Sickerwasserraten als auch die Haupteinflussfaktoren der Bodenfeuchtedynamik zu bestimmen. Dies bezieht Effekte von Bodenheterogenitäten mit ein.

In einem ersten Schritt wurde die Eignung einer vereinfachten Buckingham-Darcy Methode zur Abschätzung von Sickerwasserflüssen auf Grundlage punktuell gemessener Zeitreihen der Bodenfeuchte untersucht. Hierzu wurde eine Simulationsstudie durchgeführt, in der ein breites Spektrum an Bodentexturen und Texturheterogenitäten berücksichtigt wurde. Die Methode lieferte gute Ergebnisse für die meisten Texturklassen. In reinem Sand jedoch stellte sie sich als nicht anwendbar heraus, da hier Sickerwasserflüsse von heterogenen Fließfeldern dominiert wurden. In dieser Studie wurde ein Bedarf an neuen effizienten Ansätzen für den Umgang mit Heterogenitäten in eindimensionalen Wasserflussmodellen identifiziert.

In einem weiteren Schritt wurde ein Ansatz vorgestellt, um aus dem Problem der Bodenfeuchteheterogenität eine Lösung zu machen: In einer Hauptkomponentenanalyse wurde die Variabilität zwischen Bodenfeuchtezeitreihen genutzt, um die wahre Komplexität bodenhydrologischer Systeme zu analysieren. Auf diesem Weg ist es möglich die Haupteinflussfaktoren des hydrologischen Verhaltens zu identifizieren, ihre Relevanz zu quantifizieren und ihre jeweiligen Effekte als funktional gemittelte Zeitreihen zu beschreiben. Der Ansatz wurde zunächst mit simulierten Bodenfeuchtezeitreihen für unterschiedliche Texturklassen im homogenen und heterogenen Fall getestet. Anschließend wurde die Methode auf 57 Bodenfeuchtezeitreihen angewendet, die in einem Langzeitfeldexperiment in Nordostdeutschland gemessen wurden.

Die Dimensionalität beider Datensätze war gering, da mehr als 85 % der gesamten Bodenfeuchtevarianz bereits durch das hydrologische Eingangssignal und die Transformation dieses

Signals mit zunehmender Bodentiefe erklärt werden konnten. Analysen der Signaltransformation haben sich als wertvolle Ergänzung zu den weit verbreiteten Massenflussbetrachtungen herausgestellt. Hierbei wird untersucht, wie sich hydrologische Eingangssignale (z.B. Niederschlag oder Schneeschmelze) in der vadosen Zone fortpflanzen. Die generellen Muster der Signaltransformation wurden weder durch verschiedene Bodentexturen noch durch räumliche Heterogeneitäten beeinfluss. Dies zeigt, dass komplexe räumliche Strukturen nicht zwangsläufig ein komplexes hydrologisches Verhalten hervorrufen. Im Fall der Felddaten wurden weitere 3,6 % der Gesamtvarianz durch verschiedene Fruchtfolgen erklärt. Darüber hinaus konnte gezeigt werden, dass die Bodenbearbeitung keinen Einfluss auf die Bodenfeuchtedynamik hatte.

Der vorgestellte Ansatz erfordert keine Vorannahmen über physikalische Prozesse und ist nicht auf eine bestimmte Skala begrenzt. Dadurch ergeben sich viele Möglichkeiten, wichtige Informationen aus Monitoringdatensätzen in die Modellbildung einzubeziehen und damit Modellunsicherheiten zu verringern.

Contents

Acknowledgements……iii

Summary……v

Zusammenfassung……vii

Contents……ix

1. Introduction 1
1.1. Motivation and central objective 1
1.2. Scientific background 2
1.2.1. Spatial heterogeneities of soil moisture 2
1.2.2. Analyzing the hydrological behavior of soils 4
1.2.3. Challenges and opportunities: turning a problem into a solution 6
1.3. Objectives and methodological approaches 7
1.4. Outline of the thesis 8
References 10

2. Texture-depending performance of an in situ method assessing deep seepage 15
Summary 15
2.1. Introduction 17
2.2. Methods 18
2.2.1. Buckingham-Darcy method to estimate deep seepage 18
2.2.2. Generating model data 21
2.2.3. Assessing the performance of the Buckingham-Darcy method 25
2.3. Results 26
2.3.1. Performance of the Buckingham-Darcy method 26
2.3.2. Influence of particle size distribution and textural heterogeneity 29
2.4. Discussion 32
2.4.1. Using simulated data to test the Buckingham-Darcy method 32
2.4.2. Performance of the Buckingham-Darcy method 33
2.4.3. Influence of particle size distribution and textural heterogeneity 35
2.5. Conclusions 37
Acknowledgements 38
References 39

3. Does textural heterogeneity matter? Quantifying transformation of hydrological signals in soils 45
Summary 45
3.1. Introduction 47
3.2. Methods 50
3.2.1. Simulating soil moisture time series 51
3.2.2. Functional analysis of simulated soil moisture time series 57

3.3. Results 61
3.3.1. Autocorrelation, cross-correlation and power spectrum 61
3.3.2. Principal Components 62
3.3.3. Signal transformation behavior assessed by PCA 65
3.4. Discussion 68
3.4.1. Analyzing simulated soil moisture time series by PCA 68
3.4.2. Signal transformation in homogeneous soils with different textures 70
3.4.3. Effects of random noise and textural heterogeneity 72
3.4.4. Potential fields of application 73
3.5. Conclusions 74
Acknowledgements 75
References 76
4. Disentangling the effects of land management and soil heterogeneity on soil moisture dynamics 83
Summary 83
4.1. Introduction 85
4.2. Methods 87
4.2.1. Field experiment 87
4.2.2. Data preparation 88
4.2.3. Principal component analysis of time series 90
4.3. Results 93
4.3.1. Mean behavior of soil moisture and effect of soil depth 93
4.3.2. Effect of cropping system 96
4.3.3. Effect of soil tillage 99
4.3.4. Considering data from different soil depths 100
4.4. Discussion 100
4.4.1. Decomposing the soil moisture variance 100
4.4.2. Signal transformation behavior 101
4.4.3. Effects of cropping system and soil tillage 103
4.5. Conclusions 105
Acknowledgements 106
References 107
5. Synthesis 111
5.1. Achievements of the thesis 111
5.1.1. Using point information of moisture dynamics for seepage estimation 111
5.1.2. Analyzing the signal transformation behavior of soils 112
5.1.3. Identifying the controls on observed soil moisture dynamics 114
5.2. Implications for modeling and further research needs 117
5.2.1. Reducing uncertainties in large scale modeling 117
5.2.2. Experimental evidence for signal transformation characteristics 118
5.3. Conclusions 119
References 120
Author's declaration 123

1. Introduction

1.1. Motivation and central objective

Soil moisture is a key variable for ecosystem functioning in the earth's critical zone, i.e. the near-surface environment where rock, soil, water, air, and life interact (Brooks et al., 2015). Soil moisture dynamics, for example, regulate nutrition (Rodriguez-Iturbe and Porporato, 2004) and transpiration of plants (Wu et al., 2011). Moreover, they affect habitat conditions for soil biota (Lavelle, 2013) and control any kind of redox processes in the soil (Dutta et al., 2015). Based on this, soil moisture dynamics play an important role for the provision of numerous ecosystem services (Adhikari and Hartemink, 2016; Calzolari et al., 2016). Agricultural food production strongly depends on plant available soil water. This is reflected by the fact that enormous efforts are spent on irrigation in many parts of the world (Siebert et al., 2015; Thenkabail et al., 2009). The agricultural sector accounts for 69% of the global water withdrawal amount of 3,763 $km^3\ y^{-1}$ (FAO, 2014). The quantity and quality of groundwater available for freshwater production is also affected by soil moisture because processes like groundwater recharge (de Vries and Simmers, 2002) and filtering of seepage water (Keesstra et al., 2012) depend on soil moisture states. Soil moisture is also a key variable for the climatic system (Seneviratne et al., 2010). It controls, for example, processes of energy exchange between land and atmosphere, such as latent heat fluxes (Jung et al., 2010). Furthermore, the emission of greenhouse gases like carbon dioxide (Mi et al., 2015) and nitrous oxide (Ciarlo et al., 2007; Rubol et al., 2012) from soils is strongly associated with soil moisture states (Jaeger and Seneviratne, 2011; le Roux et al., 2013).

The importance of soil moisture for most environmental processes makes it an interface variable linking disciplines such as pedology, hydrology, ecology and meteorology (Legates et al., 2011). However, soil moisture exhibits great spatial heterogeneities at various scales (Vereecken et al., 2014). Thus, it is often difficult to break down the large amount of moisture

information resulting from intensive monitoring campaigns to a concise and manageable description of the most relevant soil moisture dynamics.

At small scales soil heterogeneities can explicitly be considered to model soil moisture dynamics (e.g. Abdou and Flury, 2004; Schlüter et al., 2012; Vogel et al., 2006), but it is still a great challenge to consider the effects of heterogeneities at the field scale or at larger scales. There is an urgent need for efficient approaches to deal with soil moisture variability at large scales, where management decisions are usually made.

Common approaches to investigate the effects of heterogeneities on soil moisture dynamics follow the concept of using explicit descriptions of spatial heterogeneities to simulate time series of soil hydrological variables, e.g. soil moisture or matric head. However, the inverse approach, i.e. identifying and quantifying the determining factors by analyzing observed soil hydrological time series, has not been considered so far. This approach is promising, since it is applicable at the scale of interest of water resources management (Lischeid et al., 2010), and it is even applicable if the controls on observed moisture dynamics occur in a continuum of several scales. For that reasons the central aim of this dissertation was: to introduce and test inverse data-based approaches to make more efficient use of field soil hydrological time series at the scale of management.

1.2. Scientific background

1.2.1. Spatial heterogeneities of soil moisture

It is commonly recognized that soil moisture exhibits spatial heterogeneities occurring in a wide range of scales (Vereecken et al., 2014). A large variety of controls on the spatial soil moisture distribution exist at different scales. Typical examples from the plot scale are soil structure due to, e.g. drying, freezing or burrowing of soil organisms (Bastardie et al., 2005; Bronick and Lal, 2005) and the distribution of plant roots (Moradi et al., 2011). At the field scale soil types with different horizon sequences can be observed (Rieckh et al., 2012). At the landscape scale the topography or rainfall variability can affect the soil moisture distribution (Qiu et al., 2014). However, single factors cannot always be assigned to one specific scale. For example, spatial heterogeneities of soil texture have been observed at several scales (e.g. Delbari et al., 2011; Heil and Schmidhalter, 2012; Liu et al., 2012). It is rather the case that the

factors controlling the spatial soil moisture distribution occur in a continuum of scales. Thus, soil moisture distributions observed at any scale can substantially be affected by factors having their origin at smaller scales. For example, the hydraulic conductivity of soils is determined by the subscale structure (Samouelian et al., 2007; Vogel and Roth, 2003).

The effects of single controls on soil moisture dynamics can be investigated by soil physical approaches at small scales. At the plot scale, for instance, it is possible to explicitly consider detailed descriptions of soil heterogeneities or plant root distributions as an input for two- or three-dimensional process based water flux models (e.g. Dunbabin et al., 2013; Schlüter et al., 2012; Vogel et al., 2006). This approach requires a high spatial model discretization to meet the conditions under which the physically based model equations, e.g. the Richards Equation, can be applied (Vogel and Ippisch, 2008). Thus, it is not applicable at larger scales where detailed information about soil heterogeneity are not accessible (Beven, 2001).

At larger scales hydrological response units are usually derived from spatial information about land use, management, topography, and soil characteristics (Flügel, 1996). Single units are then treated as homogeneous in spatially distributed hydrological models, e.g. the SWAT model (e.g. Arnold et al., 2012). This way it is assumed that the spatial distribution of the hydrological response units determines the spatial soil moisture variability. This approach, therefore, ignores that small scale heterogeneities can substantially affect the hydraulic behavior at larger scales. A pragmatic approach to generalize the effects of small scale heterogeneities at larger scale is treating the physical flux equations (e.g. the Darcy law and the Richards Equation) as conceptual models at larger scale and estimating effective soil hydraulic parameters through model calibration. However many authors doubted the predictive performance of such models (e.g. Beven, 2001; Kirchner, 2006), not least because of the equifinality problem.

Despite the spatial variability of absolute soil moisture values, it has been frequently observed that the relative spatial soil moisture patterns are often stable in time (Vachaud et al., 1985; Vanderlinden et al., 2012). This phenomenon is called temporal stability or rank stability of soil moisture patterns. Continuous efforts have been spent on characterizing, interpolating and mapping spatial soil moisture patterns by a variety of geostatistical approaches such as variograms (e.g. Baroni et al., 2013; Joshi and Mohanty, 2010), wavelet analyses (e.g. Biswas, 2014; Peng et al., 2013) or fractal analysis (Korres et al., 2015). With regard to the large number of geostatistical articles published since the late 1970s, Baveye and Laba (2015) recently argued that “insensibly, this application of geostatistics appears to have become an end in itself, and

the reasons why one should be concerned about the spatial heterogeneity of soil properties are rarely, if ever made clear anymore". According to that, heterogeneities only have to be taken into account, if they really affect the hydrological behavior in a manner that is relevant for one's individual research question. Therefore, it is useful to identify the main controls on soil moisture dynamics in the first steps of data evaluation.

1.2.2. Analyzing the hydrological behavior of soils

The hydrological behavior of soils determines the way how changes of system state variables are processed within the vadose zone between the soil surface and the groundwater table. Central state variables of soil hydrological systems are for example soil water pressure head, soil temperature or soil moisture. The latter was exclusively considered in this dissertation. Thus, the hydrological behavior of soils is reflected by the characteristics of soil moisture time series observed at different locations in the vadose zone. Two opposite approaches exist to examine and model hydrological behavior: the reductionist bottom-up approach and the empirical top-down approach (Sivapalan et al., 2003).

- The basic idea of the bottom-up approach is to model single processes that can be described by universal physical laws and are expected to be deterministic for the system behavior. By combining several of such physically based model components the system behavior is modeled at the scale of interest. Usually the scale of interest is larger than the scale of the physical process descriptions. A soil hydrological example is the coupling of the Richards Equation and the advection dispersion equation at the continuum scale in order to simultaneously model water flow and solute leaching through a porous medium at the pedon scale (e.g. van Genuchten et al., 2014). Such physically based modelling approaches have been recently prevalent in the field of soil hydrology because they are expected to be suitable for making predictions for unobserved system states. The scaleway approach to predict flow and transport in structured materials (Vogel and Roth, 2003) illustrates very well the principles of the bottom-up idea because it provides a consistent transition from one scale to the next larger scale. In this study, effective parameters to solve the Richards Equation at the continuum scale have been predicted by explicitly considering the structure at the smaller pore scale. By this, an effective process model at the scale of observation was not needed. However, examples for such consequent applications of the bottom-up principles are very

rare. From the bottom-up perspective the consequences of soil moisture variability can be described by a causal chain: local variability of soil moisture cause spatial gradients in the soil water energy status, which are compensated by transient water fluxes (Jury and Horton, 2004). In the case of textural heterogeneities the spatial variation of soil hydraulic properties causes heterogeneous water flow fields (Roth, 1995; Schlüter et al., 2012).

- The top down approach was introduced to the hydrological community by Klemes (1983). Thus, it is a relatively new phenomenon in this discipline, although it is based on long established principles of empirical research, i.e. systematic learning from observed data. Sivapalan et al. (2003) emphasized that in the sense of the top-down idea learning from data does not mean deriving simple input-output relationships in a most efficient manner by ignoring any kind of underlying physical processes. On the contrary, it is the primary aim of the top-down approach to derive information about the governing processes from observed data.

  In the last three decades especially catchment hydrologists showed growing interest in the top-down idea. As a first step towards analyzing hydrological system behavior by the top-down approach patterns in data observed at the scale of interest are identified. Descriptions of lower scale processes contributing to the system behavior at the scale of interest are then deduced from the results. Usually, for this purpose parsimonious models with only few parameters are used (Sivapalan et al., 2003). In several opinion papers the top-down approach was suggested as a promising way to deal with spatial heterogeneities (Savenije, 2009) and to overcome shortcomings of the established bottom-up approach, such as the lack of physically based process descriptions at larger scales or the equifinality problem due to over-parameterization of complex models (e.g. Kirchner, 2006; McDonnell et al., 2007). Strongly related to the top-down approach is the dominant processes concept, where only the most important processes determining main features of the system behavior are considered (Grayson and Blöschl, 2000).

Although the introduction of the top-down idea was often accompanied by criticism about the bottom-up approach, Sivapalan et al. (2003) emphasized that both approaches should be considered as complementary and not competing. Various authors stated that largest benefit could be gained from combining both approaches (e.g. Savenije, 2009; Sivapalan et al., 2003).

Examples can be found in the field of modelling complex ecological systems by the pattern-oriented modelling approach (Grimm et al., 2005). However, examples from hydrology are scare.

1.2.3. Challenges and opportunities: turning a problem into a solution

Predicting the hydrological behavior of soils using the common model approaches is still very difficult due to the effects of spatial heterogeneities (cf. Vereecken et al., 2007). Hence, efficient ways to account for spatial heterogeneities of the controls on water fluxes across different scales are needed (Asbjornsen et al., 2011). Adapting the top-down approach to typical soil hydrological problems might open up new possibilities to handle soil moisture heterogeneities. The variability among observed soil moisture time series can be used to identify and quantify the dominant factors and processes controlling soil moisture dynamics. This way advantage could be taken of the heterogeneous nature of soil moisture, which is usually seen as the main problem. Adapting the top-down idea to soil hydrological problems would primarily require (i) large soil hydrological monitoring data sets, (ii) powerful tools for data analyses, and (iii) creative approaches to grasp the hydrological behavior of soils from new perspectives.

The first mentioned large soil moisture data sets exist today and are mostly accessible for researchers, since numerous extensive soil water monitoring projects have been established in recent years to gather data sets about spatial distribution and temporal dynamics of soil hydrological variables at different scales (e.g. Bogena et al., 2010; Dorigo et al., 2011; Zacharias et al., 2011). Vereecken et al. (2014) proclaimed that we have now entered the ‘‘big data’’ era in the field of soil moisture sensing providing unique opportunities to study soil water dynamics. At the same time it was pointed out that this opportunity is naturally associated with challenges in managing, sharing, analyzing, and visualizing soil moisture data.

Concerning the need for powerful tools, Romano (2014) reported about an upcoming trend in the soil hydrological community to set-up interpretative and forecasting techniques that “let the data speak for themselves”. Some innovative multivariate data analyzing techniques such as artificial neural networks (Selle et al., 2008) and information and complexity measures (Pan et al., 2011) have been successfully applied for soil hydrological purposes in recent years. However, these promising approaches are not yet established in the soil hydrological community, and there is still a need for robustly and easily applicable tools that allow a wide range of applications at different scales.

The last mentioned demand of new creative approaches that are suitable to elucidate the overall system behavior at the field scale or larger has been raised many times (e.g. Kirchner, 2006; McDonnell et al., 2007). But the demand still maintains since new methodological concepts are rare and do not belong to the standard toolkit of most soil hydrologists. Soil hydrology could strongly benefit from new methodological concepts supplementing to the common perspective of mass flux considerations.

1.3. Objectives and methodological approaches

The aim of this dissertation was to test innovative approaches for making efficient use of standard soil hydrological data in order to assess seepage rates and main controls on observed hydrological behavior, including the role of soil textural heterogeneities. For this purpose the following three objectives were defined that build on each other:

1. Investigating the effects of soil texture and textural heterogeneities on the applicability of one-dimensional approaches for water flux quantification by the example of a simple method based on the Buckingham-Darcy law.

2. Testing a theoretical concept of low-dimensional transformation of hydrological signals (e.g. rainfall, snow melt) propagating through heterogeneous soils and a related efficient method to describe these dynamics.

3. Applying principal component analysis (PCA) for identifying the main controls on soil moisture dynamics observed in a multifactorial long-term field experiment and describing their particular contributions to these dynamics.

The following concepts and assumptions were used throughout the whole dissertation to achieve these objectives.

Relative spatiotemporal dynamics of soil moisture were investigated. Each single time series was scaled to zero mean and unit variance (z-transformation). It is worth noting that no conclusions about the absolute levels and amplitudes of soil moisture fluctuations can be drawn in this way.

It was assumed that temporal dynamics are the result of various soil processes and effects. Each of these controls (e.g. textural heterogeneity) specifically contributes to the hydrological behavior of soils. The time series of a monitoring data set were considered to be composed by

superposition of uncorrelated temporal patterns. The spatial variability among single soil moisture time series from different sites is termed functional heterogeneity in this dissertation (cf. Basu et al., 2010; Lischeid et al., 2010). The functional heterogeneity of soil moisture time series was analyzed by (i) running two-dimensional distributed water flux models with a large number of possible soil heterogeneity realizations and by (ii) analyzing soil moisture time series with dimensionality reduction techniques in terms of principal component analysis. The latter approach enables to identify temporal patterns in monitoring data sets, which can then be traced back to their specific causes.

The perspective of signal transformation followed in this dissertation can be considered as a valuable supplement to the common mass flux investigations.

Several methods and concepts of data analysis suggested in this dissertation have not been used for soil hydrological questions, yet. Consequently, there was a lack of practical experiences and it was thus necessary to assess the methods' performances theoretically before applying them to measured field data. For this purpose numerical experiments were performed, i.e. testing a method with theoretical data sets simulated exclusively with a process based model. This has the advantage that all factors controlling the modeled system behavior are known exactly. The transferability of these theoretically achieved results and the applicability of the respective methodological approach to real world situations was tested using an extensive field data set.

1.4. Outline of the thesis

This dissertation is structured into five Chapters. The general introduction (Chapter 1) gives a thematic and methodological overview about the current state of research on soil moisture heterogeneity and the hydrological behavior of soils. Additionally, the main objectives of this dissertation are introduced. The following three chapters address these objectives successively. They contain single studies that have been published in scientific journals. Their contents build on each other in the following way:

- **"Texture-depending performance of an in situ method assessing deep seepage"** (Hohenbrink and Lischeid, 2014, Chapter 2): This study aimed at investigating the applicability of a simplified Buckingham-Darcy method to estimate deep seepage fluxes in heterogeneous soils, which are generally difficult to determine in situ. Schindler and

Müller (1998) introduced that method as a promising approach requiring low monitoring costs. However, it has only been tested with data from a small number of lysimeters (Schindler et al., 2008; Schindler and Müller, 2005). The applicability of that method was investigated by a numerical experiment explicitly considering the whole range of soil textures and different intensities of textural heterogeneities. A key issue was the transferability of soil moisture dynamics measured at a distinct position in a soil profile to a larger area. In this publication a need for new efficient approaches to handle soil textural heterogeneities in one-dimensional water flux models was identified.

- **"Does textural heterogeneity matter? Quantifying transformation of hydrological signals in soils"** (Hohenbrink and Lischeid, 2015, Chapter 3): A data-based approach to analyze and handle the effects of textural heterogeneity on soil moisture dynamics was introduced to the field of soil hydrology. It was illustrated and tested by simulated time series from a numerical experiment. The basic idea of that approach was to describe and quantify the transformation characteristics of hydrological signals propagating through a vadose zone. A central question was if heterogeneous water flow induces specific temporal moisture patterns that could not occur under uniform flow conditions.
- **"Disentangling the Effects of Land Management and Soil Heterogeneity on Soil Moisture Dynamics"** (Hohenbrink et al., 2016, Chapter 4): The previously introduced approach was applied for the first time on measured soil moisture time series and thus tested for measured "real world" data. The main objective was to disentangle and describe the specific contributions of soil heterogeneity and land management practices to the observed temporal soil moisture dynamics.

In Chapter 5 general conclusions are drawn. The theoretical and methodological achievements are discussed with regard to possible scientific and practical applications. Additionally, further research needs are identified.

References

Abdou, H.M., Flury, M., 2004. Simulation of water flow and solute transport in free-drainage lysimeters and field soils with heterogeneous structures. Eur J Soil Sci, 55(2): 229-241.

Adhikari, K., Hartemink, A.E., 2016. Linking soils to ecosystem services - A global review. Geoderma, 262: 101-111.

Arnold, J.G. et al., 2012. Swat: Model Use, Calibration, and Validation. T ASABE, 55(4): 1491-1508.

Asbjornsen, H. et al., 2011. Ecohydrological advances and applications in plant-water relations research: a review. J Plant Ecol, 4(1-2): 3-22.

Baroni, G., Ortuani, B., Facchi, A., Gandolfi, C., 2013. The role of vegetation and soil properties on the spatio-temporal variability of the surface soil moisture in a maize-cropped field. J Hydrol, 489: 148-159.

Bastardie, F., Capowiez, Y., Cluzeau, D., 2005. 3D characterisation of earthworm burrow systems in natural soil cores collected from a 12-year-old pasture. Appl Soil Ecol, 30(1): 34-46.

Basu, N.B. et al., 2010. Parsimonious modeling of hydrologic responses in engineered watersheds: Structural heterogeneity versus functional homogeneity. Water Resour Res, 46, W04501.

Baveye, P.C., Laba, M., 2015. Moving away from the geostatistical lamppost: Why, where, and how does the spatial heterogeneity of soils matter? Ecol Model, 298: 24-38.

Beven, K., 2001. How far can we go in distributed hydrological modelling? Hydrol Earth Syst Sc, 5(1): 1-12.

Biswas, A., 2014. Scaling analysis of soil water storage with missing measurements using the second-generation continuous wavelet transform. Eur J Soil Sci, 65(4): 594-604.

Bogena, H.R. et al., 2010. Potential of Wireless Sensor Networks for Measuring Soil Water Content Variability. Vadose Zone J, 9(4): 1002-1013.

Bronick, C.J., Lal, R., 2005. Soil structure and management: a review. Geoderma, 124(1-2): 3-22.

Brooks, P.D. et al., 2015. Hydrological partitioning in the critical zone: Recent advances and opportunities for developing transferable understanding of water cycle dynamics. Water Resour Res, 51(9): 6973-6987.

Calzolari, C. et al., 2016. A methodological framework to assess the multiple contributions of soils to ecosystem services delivery at regional scale. Geoderma, 261: 190-203.

Ciarlo, E., Conti, M., Bartoloni, N., Rubio, G., 2007. The effect of moisture on nitrous oxide emissions from soil and the $N_2O/(N_2O+N_2)$ ratio under laboratory conditions. Biol Fert Soils, 43(6): 675-681.

de Vries, J.J., Simmers, I., 2002. Groundwater recharge: an overview of processes and challenges. Hydrogeol J, 10(1): 5-17.

Delbari, M., Afrasiab, P., Loiskandl, W., 2011. Geostatistical analysis of soil texture fractions on the field scale. Soil Water Res, 6(4): 173-189.

Dorigo, W.A. et al., 2011. The International Soil Moisture Network: a data hosting facility for global in situ soil moisture measurements. Hydrol Earth Syst Sc, 15(5): 1675-1698.

Dunbabin, V.M. et al., 2013. Modelling root-soil interactions using three-dimensional models of root growth, architecture and function. Plant Soil, 372(1-2): 93-124.

Dutta, T. et al., 2015. Vadose zone oxygen (O_2) dynamics during drying and wetting cycles: An artificial recharge laboratory experiment. J Hydrol, 527: 151-159.

FAO, 2014. AQUASTAT database. Food and Agriculture Organization of the United Nations. http://www.fao.org/nr/aquastat.

Flügel, W.A., 1996. Hydrological Response Units (HRUs) as modeling entities for hydrological river basin simulation and their methodological potential for modeling complex environmental process systems. Die Erde, 127: 42-62.

Grayson, R., Blöschl, B., 2000. Summary of Pattern Comparison and Concluding Remarks. In: Grayson, R., Blöschl, B. (Eds.), Spatial Patterns in Catchment Hydrology: Observations and Modelling. Cambridge University Press, Cambridge, UK, pp. 355.

Grimm, V. et al., 2005. Pattern-oriented modeling of agent-based complex systems: Lessons from ecology. Science, 310(5750): 987-991.

Heil, K., Schmidhalter, U., 2012. Characterisation of soil texture variability using the apparent soil electrical conductivity at a highly variable site. Comput Geosci, 39: 98-110.

Hohenbrink, T.L., Lischeid, G., 2014. Texture-depending performance of an in situ method assessing deep seepage. J Hydrol, 511: 61-71.

Hohenbrink, T.L., Lischeid, G., 2015. Does textural heterogeneity matter? Quantifying transformation of hydrological signals in soils. J Hydrol, 523: 725-738.

Hohenbrink, T.L., Lischeid, G., Schindler, U., Hufnagel, J., 2016. Disentangling the effects of land management and soil heterogeneity on soil moisture dynamics. Vadose Zone J, 15(1).

Jaeger, E.B., Seneviratne, S.I., 2011. Impact of soil moisture-atmosphere coupling on European climate extremes and trends in a regional climate model. Clim Dynam, 36(9-10): 1919-1939.

Joshi, C., Mohanty, B.P., 2010. Physical controls of near-surface soil moisture across varying spatial scales in an agricultural landscape during SMEX02. Water Resour Res, 46, W12503.

Jung, M. et al., 2010. Recent decline in the global land evapotranspiration trend due to limited moisture supply. Nature, 467(7318): 951-954.

Jury, W.A., Horton, R., 2004. Soil Physics. John Wiley & Sons, Inc., Hoboken, New Jersy, 370 pp.

Keesstra, S.D. et al., 2012. Soil as a filter for groundwater quality. Curr Opin Env Sust, 4(5): 507-516.

Kirchner, J.W., 2006. Getting the right answers for the right reasons: Linking measurements, analyses, and models to advance the science of hydrology. Water Resour Res, 42(3).

Klemes, V., 1983. Conceptualization and scale in hydrology. J Hydrol, 65(1-3): 1-23.

Korres, W. et al., 2015. Spatio-temporal soil moisture patterns – A meta-analysis using plot to catchment scale data. J Hydrol, 520: 326-341.

Lavelle, P., 2013. Soil as a Habitat. In: Wall, D. (Ed.), Soil Ecology and Ecosystem Services. Oxford Univ Press, New York, USA, pp. 7-27.

le Roux, P.C., Aalto, J., Luoto, M., 2013. Soil moisture's underestimated role in climate change impact modelling in low-energy systems. Global Change Biol, 19(10).

Legates, D.R. et al., 2011. Soil moisture: A central and unifying theme in physical geography. Prog Phys Geog, 35(1): 65-86.

Lischeid, G. et al., 2010. Assessing coupling between lakes and layered aquifers in a complex Pleistocene landscape based on water level dynamics. Adv Water Resour, 33(11): 1331-1339.

Liu, F., Geng, X.Y., Zhu, A.X., Fraser, W., Waddell, A., 2012. Soil texture mapping over low relief areas using land surface feedback dynamic patterns extracted from MODIS. Geoderma, 171: 44-52.

McDonnell, J.J. et al., 2007. Moving beyond heterogeneity and process complexity: A new vision for watershed hydrology. Water Resour Res, 43(7).

Mi, J., Li, J.J., Chen, D.M., Xie, Y.C., Bai, Y.F., 2015. Predominant control of moisture on soil organic carbon mineralization across a broad range of arid and semiarid ecosystems on the Mongolia plateau. Landscape Ecol, 30(9): 1683-1699.

Moradi, A.B. et al., 2011. Three-dimensional visualization and quantification of water content in the rhizosphere. New Phytol, 192(3): 653-663.

Pan, F., Pachepsky, Y.A., Guber, A.K., Hill, R.L., 2011. Information and complexity measures applied to observed and simulated soil moisture time series. Hydrolog Sci J, 56(6): 1027-1039.

Peng, J., Shen, H., He, S.W., Wu, J.S., 2013. Soil moisture retrieving using hyperspectral data with the application of wavelet analysis. Environ Earth Sci, 69(1): 279-288.

Qiu, J.X., Mo, X.G., Liu, S.X., Lin, Z.H., 2014. Exploring spatiotemporal patterns and physical controls of soil moisture at various spatial scales. Theor Appl Climatol, 118(1-2): 159-171.

Rieckh, H., Gerke, H.H., Sommer, M., 2012. Hydraulic properties of characteristic horizons depending on relief position and structure in a hummocky glacial soil landscape. Soil Till Res, 125: 123-131.

Rodriguez-Iturbe, I., Porporato, A., 2004. Ecohydrology of Water-Controlled Ecosystems: Soil Moisture and Plant Dynamics. Cambridge University Press, Cambridge, UK.

Roth, K., 1995. Steady state flow in an unsaturated, two-dimensional, macroscopically homogeneous, Miller-similar medium. Water Resour Res, 31(9): 2127-2140.

Rubol, S., Silver, W.L., Bellin, A., 2012. Hydrologic control on redox and nitrogen dynamics in a peatland soil. Sci Total Environ, 432: 37-46.

Samouelian, A., Vogel, H.J., Ippisch, O., 2007. Upscaling hydraulic conductivity based on the topology of the sub-scale structure. Adv Water Resour, 30(5): 1179-1189.

Savenije, H.H.G., 2009. HESS Opinions "The art of hydrology". Hydrol Earth Syst Sc, 13(2): 157-161.

Schindler, U., Fank, J., Müller, L., 2008. Alternativlösung zur Quantifizierung der Tiefensickerung in situ, 13. Gumpensteiner Lysimetertagung. Lehr- und Forschungszentrum für Landwirtschaft Raumberg-Gumpenstein, Gumpenstein, pp. 93-98.

Schindler, U., Müller, L., 1998. Calculating deep seepage from water content and tension measurements in the vadose zone at sandy and loamy soils in North-East Germany. Archives of Agronomy and Soil Science 43(3): 233-243.

Schindler, U., Müller, L., 2005. Comparison of deep seepage estimations of a virtual with a real lysimeter by means of TDR-measurements. International Agrophysics, 19(1): 69-73.

Schlüter, S. et al., 2012. Virtual soils: Assessment of the effects of soil structure on the hydraulic behavior of cultivated soils. Vadose Zone J, 11(4).

Selle, B., Lischeld, G., Huwe, B., 2008. Effective modelling of percolation at the landscape scale using data-based approaches. Comput Geosci, 34(6): 699-713.

Seneviratne, S.I. et al., 2010. Investigating soil moisture-climate interactions in a changing climate: A review. Earth-Sci Rev, 99(3-4): 125-161.

Siebert, S. et al., 2015. A global data set of the extent of irrigated land from 1900 to 2005. Hydrol Earth Syst Sc, 19(3): 1521-1545.

Sivapalan, M., Blöschl, G., Zhang, L., Vertessy, R., 2003. Downward approach to hydrological prediction. Hydrol Process, 17(11): 2101-2111.

Thenkabail, P.S. et al., 2009. Global irrigated area map (GIAM), derived from remote sensing, for the end of the last millennium. Int J Remote Sens, 30(14): 3679-3733.

Vachaud, G., Desilans, A.P., Balabanis, P., Vauclin, M., 1985. Temporal stability of spatially measured soil-water probability density-function. Soil Sci Soc Am J, 49(4): 822-828.

van Genuchten, M.T., Naveira-Cotta, C., Skaggs, T.H., Raoof, A., Pontedeiro, E.M., 2014. The Use of Numerical Flow and Transport Models in Environmental Analyses. In: Teixeira, W.G., Ceddia, M.B., Donnagema, G.K., Ottoni, M.V. (Eds.), Application of Soil Physics in Environmental Analyses. Springer International Publishing.

Vanderlinden, K. et al., 2012. Temporal stability of soil water contents: A review of data and analyses. Vadose Zone J, 11(4).

Vereecken, H. et al., 2014. On the spatio-temporal dynamics of soil moisture at the field scale. J Hydrol, 516: 76-96.

Vereecken, H., Kasteel, R., Vanderborght, J., Harter, T., 2007. Upscaling hydraulic properties and soil water flow processes in heterogeneous soils: A review. Vadose Zone J, 6(1): 1-28.

Vogel, H.J., Cousin, I., Ippisch, O., Bastian, P., 2006. The dominant role of structure for solute transport in soil: experimental evidence and modelling of structure and transport in a field experiment. Hydrol Earth Syst Sc, 10(4): 495-506.

Vogel, H.J., Ippisch, O., 2008. Estimation of a critical spatial discretization limit for solving Richards' equation at large scales. Vadose Zone J, 7(1): 112-114.

Vogel, H.J., Roth, K., 2003. Moving through scales of flow and transport in soil. J Hydrol, 272(1-4): 95-106.

Wu, Y.Z., Huang, M.B., Gallichand, J., 2011. Transpirational response to water availability for winter wheat as affected by soil textures. Agr Water Manage, 98(4): 569-576.

Zacharias, S. et al., 2011. A network of terrestrial environmental observatories in Germany. Vadose Zone J, 10(3): 955-973.

2. Texture-depending performance of an in situ method assessing deep seepage[1]

Summary

Deep seepage estimation is important for water balance investigations of groundwater and the vadose zone. A simplified Buckingham-Darcy method to assess time series of deep seepage fluxes was proposed by Schindler and Müller [*Schindler, U., Müller, L., 1998. Calculating deep seepage from water content and tension measurements in the vadose zone at sandy and loamy soils in North-East Germany. Archives of Agronomy and Soil Science 43(3): 233-243*]. In the method dynamics of water fluxes are calculated by a soil hydraulic conductivity function. Measured soil moistures and matric heads are used as input data. Resulting time series of flux dynamics are scaled to realistic absolute levels by calibration with the areal water balance. An assumption of the method is that water fluxes at different positions exhibit identical dynamics although their absolute values can differ. The aim of this study was to investigate uncertainties of that method depending on the particle size distribution and textural heterogeneity in non-layered soils. We performed a numerical experiment using the two-dimensional Richards Equation. A basic model of transient water fluxes beneath the root and capillary zone was set up and used to simulate time series of soil moisture, matric head, and seepage fluxes for 4221 different cases of particle size distribution and intensities of textural heterogeneity. Soil hydraulic parameters were predicted by the pedotransfer function Rosetta. Textural heterogeneity was modeled with Miller & Miller scaling factors arranged in spatial random fields. Seepage fluxes were calculated with the Buckingham-Darcy method from simulated soil moisture and matric head time series and compared with simulated reference fluxes. The median of Root Mean Square Error was about 0.026 cm d^{-1} and the median of maximum cross correlation was 0.96 when the method was calibrated adequately. The method's performance was mainly influenced by (i) the soil textural class and (ii) the time period used for flux calibration. It per-

formed best in sandy loam while hotspots of errors occurred in case of sand and silty texture. Calibrating the method with time periods that exhibit high variance of seepage fluxes yielded the best performance. The geostatistical properties of the Miller & Miller scaling field influenced the performance only slightly. However, the Miller & Miller scaling procedure generated heterogeneous flow fields that were addressed as main reason for mismatches of simulated reference fluxes and fluxes obtained with the Buckingham-Darcy method.

Keywords: Vadose zone, Deep percolation flux, Buckingham-Darcy law, Soil heterogeneity, Temporal stability of soil water fluxes, Numerical experiment

[1] An article with equivalent content has been published as:

Hohenbrink, T.L., Lischeid, G., 2014. Texture-depending performance of an in situ method assessing deep seepage. Journal of Hydrology, 511: 61-71. DOI: 10.1016/j.jhydrol.2014.01.011.

2.1. Introduction

Assessment of groundwater recharge is important for sustainable use of groundwater resources. Overviews of numerous studies on determining groundwater recharge are given by de Vries and Simmers (2002) and Scanlon et al. (2002). Groundwater recharge can result from different processes like infiltration from rivers or lateral inflows from other regions but it is often dominated by deep seepage. Deep seepage comprises all downward water fluxes in the vadose zone that reach the groundwater table.

Many methods to estimate deep seepage such as direct measurements with drainage lysimeters (Meissner et al., 2010a) and passive wick-samplers (Gee et al., 2009; Meissner et al., 2010b), conceptual (Bethune et al., 2008), mechanistic (Jimenez-Martinez et al., 2009; Lu et al., 2011) and empirical (Selle et al., 2008; Wessolek et al., 2008) modeling approaches and tracer balance calculations (Fragala and Parkin, 2010; Perkins et al., 2011) have been developed and applied at different scales. However, in many cases it is still a challenge to quantify deep seepage with adequate time and effort (cf. Sanford, 2002).

Schindler and Müller (1998) introduced a simplified method to obtain deep seepage fluxes from measured soil moisture and matric head time series at sites with a large distance to groundwater. Their method is based on the Buckingham-Darcy law. In contrast to complex monitoring and modeling procedures the simplified method can be applied with low effort in measuring and data evaluation. Schindler et al. (2008) tested the method with lysimeter data from Northeast Germany and Southeast Austria and showed that it performed properly in loamy and sandy soils. Obtained seepage fluxes were in close agreement with measured lysimeter outflow data. However, these conclusions have been drawn from only few example cases. Further research regarding a more widespread range of soil texture and soil heterogeneity is needed to obtain more general information about the method's benefits and limitations.

When flux dynamics from point locations are related to larger scales of interest like the field scale, it is assumed that water flux time series at different locations are synchronous and might differ with respect to absolute values. This assumption called temporal stability of spatial patterns of soil water dynamics is a crucial point when the Buckingham-Darcy method – and also many other methods – are applied. A large body of literature on the characterization of temporal stability of soil moisture patterns exists (e.g. Mittelbach and Seneviratne, 2012;

Pachepsky et al., 2005; Vachaud et al., 1985; Vanderlinden et al., 2012). Guber et al. (2008b) showed that temporal stability can hold for soil water flux patterns as well.

Numerical experiments allow the analysis of a method's performance with respect to different influencing factors. Any combination of influencing factors can be tested in a consistent way (Mirus et al., 2011). Such approaches have been applied to water flux problems at the soil core scale (Peters and Durner, 2008), at the scale of several meters (Schelle et al., 2013; Schlüter et al., 2012), at the hillslope scale (Weiler and McDonnell, 2004), and at the catchment scale (Mirus et al., 2011).

The aim of this study was to identify conditions of particle size distribution and textural heterogeneity under which the simplified Buckingham-Darcy method can be used to obtain deep seepage fluxes. This also comprises the question which texture conditions facilitate the occurrence of temporal stability in water flux patterns. In a numerical experiment we simulated time series of soil moisture $\theta(t)$ [L^3 L^{-3}], matric head $h(t)$ [L] and water fluxes $q(t)$ [L T^{-1}] considering a wide range of soil properties and applied the Buckingham-Darcy method to this data. Afterwards, we evaluated the performance of the Buckingham-Darcy method with respect to single textural classes. In this study we concentrated on non-layered soils at a scale that would also be represented by a lysimeter.

2.2. Methods

2.2.1. Buckingham-Darcy method to estimate deep seepage

Required data

The Buckingham-Darcy method aims at assessing seepage fluxes at a soil depth z_1 [L] far beneath the rooting zone and far above the groundwater table. The horizontal plane in this observation depth is defined as the plane of interest. The plane of interest must be located beneath the root and capillary zone where upward water fluxes never occur. In this permanent seepage zone processes like evaporation or root water uptake that are difficult to control do not occur (Fig. 2.1). Thus, soil moisture changes are caused only by deep seepage fluxes. Time series of soil moisture $\theta_{z1}(t)$ and matric head $h_{z1}(t)$ measured in the plane of interest are required. As a rule of thumb for Central Europe it is suggested to install the probes at a depth of $z_1 = 3$ m at arable sites and pasture and in $z_1 = 5$ m at forest sites (Schindler et al., 2008;

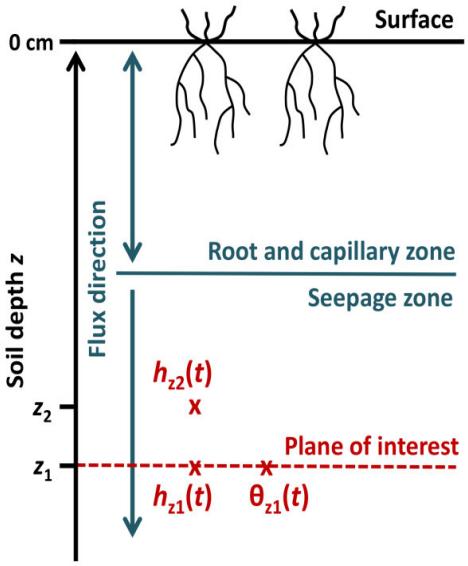

Figure 2.1. Positions of sensors (x) to measure time series of soil moisture $\theta(t)$ and matric head $h(t)$ in the permanent seepage zone underneath the root and capillary zone.

Schindler and Müller, 2005). However, an adequate installation depth depends on climatic, edaphic, and vegetational conditions of each specific site. The sign of the hydraulic gradient $i(t)$ [L L^{-1}] must be monitored to ensure that measurements are performed deep enough where only downward flux occurs. This requires a second matric head time series $h_{z2}(t)$ measured at another depth z_2. Schindler et al. (2008) suggested using daily data. The Buckingham-Darcy method involves a calibration procedure (see next section). For that issue the total amount of groundwater recharge Q_{cal} [L] at the investigation site must be estimated with an independent method for a representative calibration period. This can, for instance, be done by water balance calculations during winter periods when evapotranspiration can be assumed to be negligible.

Data evaluation

Relative fluxes q_r describing the flux dynamics can be computed from the measured water content data θ_{z1} for each time interval T by the Buckingham-Darcy law

$$q_{r_T} = -k_r(\theta_{z1_T}) \cdot i_T \,. \qquad (2.1)$$

The relative hydraulic conductivity $k_r(\theta)$ [L T^{-1}] is the quotient of the actual conductivity $k(\theta)$ depending on θ and the conductivity of the saturated soil k_s. Schindler and Müller (1998) suggested to assume a unit gradient $I = 1$ in Eq. 2.1 so that q_r is only controlled by $k_r(\theta_{z1})$. They

argue that assuming a unit gradient affects q_r less strongly than calculating $i(t)$ from measured matric head data because of measuring inaccuracies of $h_{z1}(t)$ and $h_{z2}(t)$ that cannot be avoided.

The relation between k_r and θ can be described by van Genuchten (1980) and Mualem (1976)

$$k_r(\theta) = \Theta^{\tau}\left[1-\left(1-\Theta^{1/m}\right)^m\right]^2. \qquad (2.2)$$

The effective saturation Θ [-] is defined as $\Theta = (\theta-\theta_r)/(\theta_s-\theta_r)$. In the Buckingham-Darcy method the tortuosity parameter τ [-] is assumed to be 0.5. The parameters saturated and residual water content θ_s and θ_r, and the shape parameter m [-] can be determined by fitting the parameters of the van Genuchten model of soil water retention (van Genuchten, 1980) to the measured time series $\theta_{z1}(t)$ and $h_{z1}(t)$

$$\theta(h) = \theta_r + \frac{(\theta_s-\theta_r)}{\left[1+\left|\alpha\cdot h\right|^n\right]^m} \qquad (2.3)$$

$$\text{with} \quad m = 1-1/n.$$

The parameter α [L^{-1}] denotes the inverse of the matric head at the air entry point and n [-] is a shape-parameter. Parameter fitting of soil hydraulic properties can be performed with specific software like *RETC* (van Genuchten et al., 1991) or *SHYPFIT* (Peters and Durner, 2006). It is also possible to describe $k_r(\theta)$ by other models (e.g. Brooks and Corey, 1964; Kosugi, 1996). Resulting time series of q_r reflect relative changes of seepage fluxes at the position where the soil moisture probe is installed. Hence, temporal stability of spatial soil water flux patterns must be assumed in order to assign q_r to the whole investigation site. Time series of q_r are then converted to realistic absolute values by linear scaling. The scaling factor β_{cal} can be calculated from the independently derived groundwater recharge amount during the calibration period Q_{cal} and the obtained cumulative relative seepage amount $Q_r = \sum q_{rT}$ during the same period

$$\beta_{cal} = \frac{Q_{cal}}{Q_r}. \qquad (2.4)$$

Absolute seepage fluxes at the investigation site q_{obt} can then be calculated as follows

$$q_{obt} = \beta_{cal}\cdot q_r. \qquad (2.5)$$

The application scale of the Buckingham-Darcy method depends on (i) site conditions influencing validity of the temporal stability assumption and on (ii) the method used to estimate Q_{cal}.

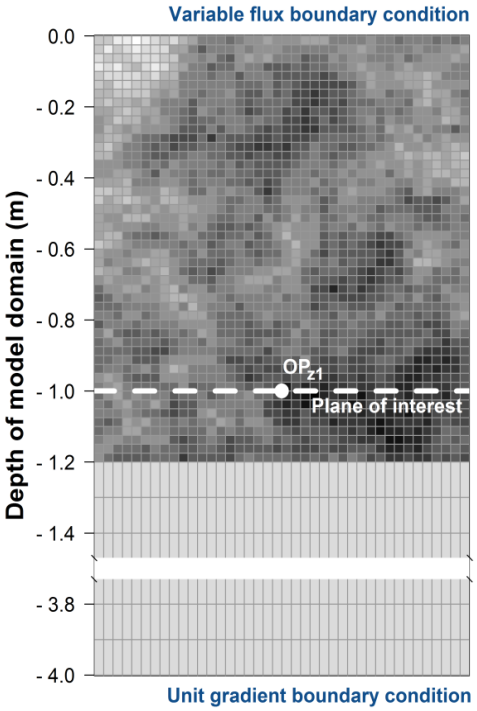

Figure 2.2. Model domain. Gray colors indicate spatial correlated Miller & Miller scaling factors from an example realization. Scaling factors were always 1 beneath 1.2 m depth. The observation point OP_z defines the location where time series of θ, h, and q_{ref} were simulated.

2.2.2. Generating model data

A test data set comprising simulated time series for 4221 cases of different particle size distribution and intensities of textural heterogeneity was generated by a simulation model. For each case the simulated variables were $\theta_{z1}(t)$, $h_{z1}(t)$ and the reference flux rates through the entire plane of interest $q_{ref}(t)$. For this purpose we (i) defined one basic model set up and (ii) ran this basic model for all 4221 cases, varying the soil hydraulic properties and the geostatistical properties characterizing textural heterogeneity.

Basic model setup

The basic model set up represented a boundary and initial value problem defining the following general water flux scenario. Gravity driven flow through one soil layer located in the unsaturated seepage zone was modeled with the two-dimensional Richards Equation. The latter was solved numerically with the *Hydrus-2D* code (Simunek et al., 2011).

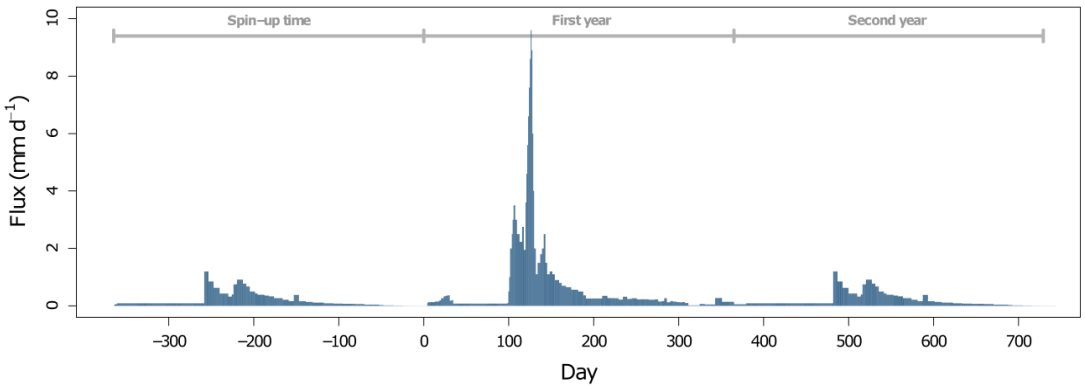

Figure 2.3. Seepage fluxes at the upper boundary.

The model domain represented a rectangular section of a non-layered soil profile that was fully located in the permanent seepage zone (Fig. 2.2). Hence, the upper boundary did not represent the soil surface. The model domain was 1 m wide and 4 m deep. Dye tracer experiments showed that correlation lengths of water pathways were much smaller than 1 m (Bogner et al., 2008; van Schaik, 2009; Weiler and Flühler, 2004). This demonstrates that the actual range of flux rates was covered by a 1 m wide model domain. Spatial discretization was achieved by 3157 nodes arranged in a rectangular grid. In the upper 1.2 m node spacing was 0.025 m in both directions. Between -1.2 m and -4 m node spacing in z-direction was set to 0.1 m. The plane of interest was defined at -1 m depth of the model domain. An observation point OP_{z1} was inserted at the depth of the plane of interest (z_1) corresponding to the sensor locations for matric head and water content measurements. Time series of the output variables $\theta_{z1}(t)$, $h_{z1}(t)$, and $q_{ref}(t)$ were generated at this position. It was not necessary to simulate $h_{z2}(t)$ at a second position to monitor hydraulic gradients because the model scenario did not include upward water fluxes at all. Hence, it was ensured in the simulations that the plain of interest was always located in the permanent seepage zone. Time series of lysimeter discharge measured during the hydrologic years 2002 and 2003 at a Research Station in Dedelow (Federal State of Brandenburg, Germany) were used to define a 730 days inflow scenario at the upper boundary of the model domain. The inflow scenario included time periods with both large and small seepage flux rates as well as abrupt changes in flux intensity (Fig. 2.3). The variable inflow was implemented by a flux boundary condition. It was not necessary to consider processes like evapotranspiration and root water up take because the model domain did not include the root and capillary zone. Realistic initial conditions of matric head were achieved by modeling the seepage scenario from 2003 as spin-up period.

At the lower boundary free drainage conditions were modeled with a unit gradient boundary condition as recommended by McCord (1991). We previously conducted test simulations to investigate possible effects of this boundary condition on time series simulated at the plane of interest. Therefore time series of soil moisture and actual hydraulic gradients from model domains with different vertical extents were compared to those from a reference case with a large distant to the groundwater. The reference case was simulated with a 21 m deep model domain. A constant groundwater level in 21 m depth was modeled by a first type lower boundary condition (constant head) with $h = 0$. All texture classes were considered. Mean Percent Errors (MPE) of soil moisture (MPE < 0.4 %) and actual hydraulic gradients (MPE < 3.75 %) were small when the distance between the plane of interest and the lower boundary was at least 3 m. For that reason a 4 m deep model domain was used although only the upper 1 m was of interest (Fig. 2.2).

Modeling spatial heterogeneities of soil texture

The soil water retention curve $\theta(h)$ and the hydraulic conductivity curve $k(h)$ that are needed to solve the Richards Equation were parameterized by the models of Mualem (1976) and van Genuchten (1980). The formulation of $\theta(h)$ is described by Eq. 2.3. The $k(h)$ value arises from Eq. 2.2 and Eq. 2.3 scaled by k_s. In this way hydraulic characteristics of different soil textures were expressed by the six soil hydraulic parameters θ_s, θ_r, α, n, τ and k_s.

The texture triangle was discretized by a grid with a resolution of 1 % texture fraction in each of the three directions resulting in 4221 different combinations of soil texture fractions (Fig. 2.4). The points represent all investigated cases of particle size distribution. For each combination the fractions of sand, silt, and clay were used to predict soil hydraulic parameters by the pedotransfer function *Rosetta* (Schaap et al., 2001). *Rosetta* involves an artificial neural network that was trained to a large data set of soil hydraulic parameters measured in the laboratory. Soil textures with more than 40 % of clay along with a silt content less than 30 % were not considered because (i) they are rarely found in natural soils (cf. Schindler and Müller, 2010; Twarakavi et al., 2009; Woesten et al., 1998) and (ii) we did not trust in the estimated parameters in this part of the texture triangle because the data set underlying *Rosetta* contains only few data points in this texture range (Schaap et al., 2001).

Textural heterogeneity was implemented in the upper 1.2 m of the model domain where the observation point was located (Fig. 2.2). The scaling approach of Miller and Miller (1956) was

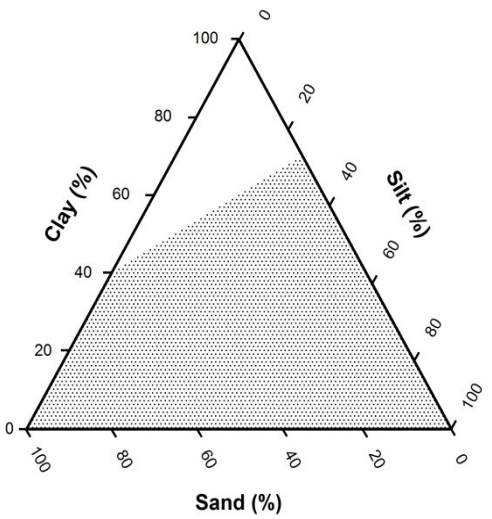

Figure 2.4. Textural fractions considered in the model study. Each dot symbol represents one of 4221 different texture realizations.

used to define spatially variable soil hydraulic properties. Relationships of soil hydraulic properties of two porous media with similar internal geometry but different scales are described in this theory. Thus, it is possible to predict soil hydraulic properties of a porous medium from a Miller similar reference medium. This is done by scaling the soil hydraulic functions of the reference medium $h^*(\theta)$ and $k^*(\theta)$ with specific scaling factors φ_θ, φ_h and φ_k [-]. Accordingly to Abdou and Flury (2004) and Vogel et al. (1991) the scaling factors for matric head and hydraulic conductivity were related $\varphi_h = \varphi_k^{-0.5}$, and soil moisture was not scaled $\varphi_\theta = 1$. Using this relationship it is possible to consider spatial heterogeneity in soil water dynamics by defining one single scaling parameter φ_{xy} for each node in the model domain. Thereby, the reference soil hydraulic properties $h^*(\theta)$ and $k^*(h)$ are modified locally by

$$h_{x,z}(\theta) = \frac{h^*(\theta)}{\sqrt{\varphi_{x,z}}} \tag{2.6}$$

and

$$k_{x,z} = \varphi_{x,z} \cdot k^*(h)\,. \tag{2.7}$$

In this study the reference soil hydraulic properties were given by the *Rosetta* outputs as described above. In each of the 4221 cases different spatial distributions of all φ_{xy} in a scaling field Φ were defined and Φ was assigned to the upper 1.2 m of the model domain (Fig. 2.2). We arranged all $\varphi_{x,z}$ in Φ to be log-normally distributed. The distribution of scaling factors φ

can then be described by $\varphi = 10^b$ with normally distributed exponents b. The mean of b was kept constant $\bar{b} = 0$ so the median of φ in a realization of Φ was zero ($\tilde{\varphi} = 0$). Within Φ all $b_{x,z}$ were arranged to be spatially correlated. The spatial correlation between any two values $b_{x1,z1}$ and $b_{x2,z2}$ with a distance of l [L] was defined by an exponential covariance function C

$$C(l) = \sigma^2(b) e^{-\frac{l}{range}}. \tag{2.8}$$

The variance $\sigma^2(b)$ is termed *sill* [-] in this paper. The parameter *range* [L] describes the strength of the decrease of covariance with increasing distance between two positions of $b_{x1,z1}$ and $b_{x2,z2}$. Detailed descriptions of the geostatistical concepts are given by Burgess and Webster (1980) and Goovaerts (1999). For each of the 4221 texture realizations *sill* and *range* were drawn independently from uniform distributions. The bounds of these two geostatistical parameters were set to 0.1 and 1.65 (*sill*), and 2.3 cm and 27.5 cm (*range*). Gaussian random fields of b were generated using the R packages *geoR* (Paulo et al., 2001) and *RandomFields* (Schlather, 2011).

2.2.3. Assessing the performance of the Buckingham-Darcy method

For each of the 4221 model runs the seepage flux passing the plane of interest was calculated with the Buckingham-Darcy method. The simulated time series of $\theta_{z1}(t)$, $h_{z1}(t)$, $h_{z2}(t)$ were treated as measured data with daily resolution and evaluated (see section 2.1):

1. The software *SHYPFIT 2.0* (Peters and Durner, 2006) was used to fit the parameters θ_r, θ_s, α and n in Eq. 2.3 to simulated water retention data $\theta(h)$.
2. Relative seepage fluxes q_r during the two years were computed by Eq. 2.1 with the simulated time series $\theta_{z1}(t)$ assuming a constant unit gradient $I = 1$.
3. Simulated cumulative fluxes through the entire plane of interest were assigned to Q_{cal} (Eq. 2.4) in order to calibrate local water fluxes by Eq. 2.5. Data from three different periods were used for calibration: (i) both years of the total simulation time, (ii) the first year and (iii) the second year (Fig. 2.3). In the first year large water fluxes occurred, whereas the second year was much dryer.

The performance of the Buckingham-Darcy method was evaluated with three quality criterions. The Root Mean Square Error *RMSE* [L T^{-1}] was used to evaluate the accuracy of obtained flux rates q_{obt}

$$RMSE = \sqrt{\frac{1}{t_{\max}} \sum_{t=1}^{t_{\max}} \left(q_{obt,t} - q_{ref,t} \right)^2} \,. \tag{2.9}$$

It measures the mean deviation of q at defined positions on the time-axis. Large deviations are weighted more strongly due to the square. Secondly, the similarity of the shapes of q_{ref} and q_{obt} was measured by the maximum value of the cross correlation function CC_{max} [-]

$$CC_{\max} = \frac{\mathrm{cov}(q_{ref}(t), q_{obt}(t - Lag))}{\sigma_{q_{ref}} \cdot \sigma_{q_{obt}}} \,. \tag{2.10}$$

The cross correlation function describes the Pearson correlation of two time series that are shifted relatively to each other by different time lags. The time lag *Lag* [T] that corresponds to CC_{max} was used as third quality criterion measuring the extent of time shift between q_{ref} and q_{obt}. The R software (R Development Core Team, 2010) was used to arrange all simulation runs automatically, to calculate water fluxes with the Darcy-Buckingham method for each scenario and to compute the quality criterions.

2.3. Results

2.3.1. Performance of the Buckingham-Darcy method

Each of the 4221 simulations generated specific seepage dynamics due to different fractions of sand, silt and clay (soil hydraulic parameters) and different geostatistical properties of the scaling factor distribution (*sill* and *range*). The Miller & Miller scaling of soil hydraulic properties resulted in a specific heterogeneous flow field for each simulated case. The flow fields were generally characterized by a few vertical water pathways surrounded by more passive regions. It is not possible to illustrate them here due to their large number. Simulated cumulative reference fluxes Q_{ref} increased mainly between the days 100 and 200 and, although less strongly, between the days 500 and 600 (Fig. 2.5a). The majority of time series ran close to the median curve. Only in the upper range between the 90th and 100th percentiles (p_{90} and p_{100}) Q_{ref} differed more strongly from the median in times of high flux rates. Simulated reference flux rates q_{ref} were maximal (maximum of median curve: 0.4 cm d^{-1}) and varied in the widest range (between 0.28 and 0.75 cm d^{-1}) during the main peak between the days 100 and 150 (Fig. 2.5b). High flux intensities at the plane of interest were related to high inflows through the upper boundary condition (see Fig. 2.3).Relative time series $q_r(t)$ had to be scaled with θ_{cal} to match

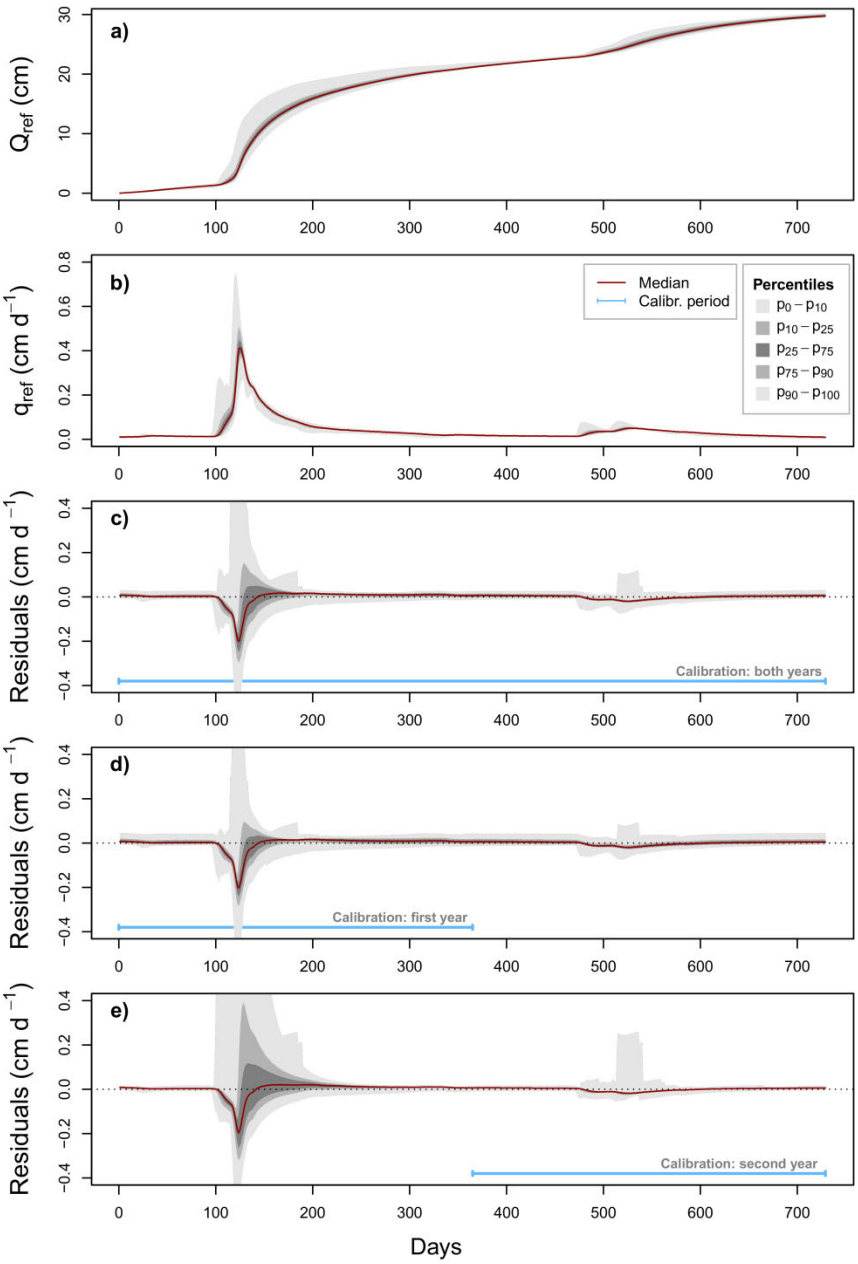

Figure 2.5. Global reference time series of cumulative fluxes Q_{ref} (a) and flux rates q_{ref} (b). Time series of deviations between q_{ref} and obtained fluxes q_{obt} (residuals) calibrated with data from both years (c), first year (d), and second year (e). Red lines display the median. Gray areas indicate different percentiles of all 4221 time series. The spin-up period is not included.

the order of magnitude of q_{ref}. The median p_{50} of θ_{cal} was about 31. In less than 10 % of all cases $q_r(t)$ had to be reduced by θ_{cal} smaller than 1 (p_{10}: about 1.4). Large θ_{cal} values occurred in sandy textures (p_{90}: about 4000). The *RMSE* distribution differed when the different calibration periods both years, first year, and second year were used (Fig. 2.6). The smallest deviations

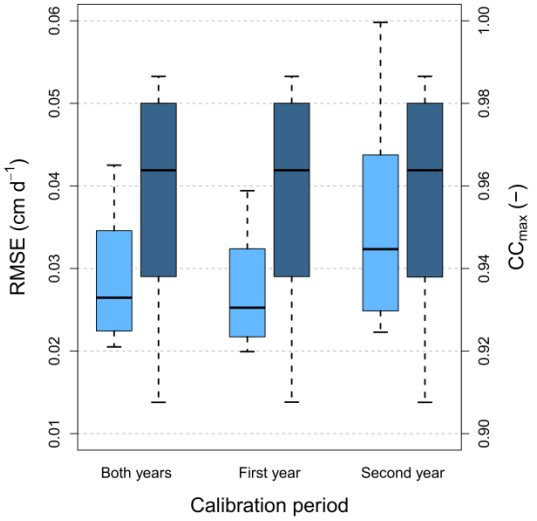

Figure 2.6. Distribution of Root Mean Square Error evaluating mismatches of obtained flux rates q_{obt} (*RMSE*, lightblue). Distribution of maximum cross correlation of obtained fluxes q_{obt} and reference fluxes q_{ref} (CC_{max}, darkblue). Boxes confine the 25th and 75th percentiles and whiskers indicate the 10th and 90th percentiles.

between q_{ref} and q_{obt} were achieved by calibrating with data from the first year when highest seepage fluxes occurred. Here, the median p_{50} of *RMSE* was 0.025 cm d^{-1} and in 10 % of all cases *RMSE* exceeded 0.039 cm d^{-1} (p_{90}). Calibration with data from both years increased *RMSE* (p_{50}: 0.026 cm d^{-1}, p_{90}: 0.043 cm d^{-1}) and expanded their range. Using the last year for calibration resulted in high *RMSE* indicating poor accordance of q_{ref} and q_{obt} (p_{50}: 0.032 cm d^{-1}, p_{90}: 0.06 cm d^{-1}). All three distributions were positively skewed, i.e. asymmetrical with higher variability for large percentiles. The other two quality criterions CC_{max} and *Lag* were not affected by the calibration period because linear scaling of q_r (Eq. 2.5) influenced not the shape of q_{obt}. The distribution of CC_{max} was slightly negatively skewed. The median of CC_{max} was 0.964 and p_{10} was 0.908 (Fig. 2.6). In every case q_{obt} lagged behind q_{ref}. Time shifts *Lag* varied between 0 d and 10 d and were nearly normal distributed (p_{50}: 4 d, p_{90}: 6 d). Residuals calculated as difference between q_{obt} and q_{ref} varied with time. For most realizations of particle size distribution and textural heterogeneity seepage fluxes q_{obt} were underestimated during the first seepage phase between the days 100 and 140 when actual seepage fluxes were high. The maximum deviation between q_{obt} and q_{ref} occurred at day 124 when the median of the residuals was -0.2 cm d^{-1} in all calibration cases. This accounts for 50 % of q_{ref} (Fig. 2.5c-e). In the following period reference fluxes were slightly overestimated with maximum residuals around day 170 (both years calibration: 0.017 cm d^{-1}, first year: 0.015 cm d^{-1},

second year: 0.021 cm d^{-1}) that converge to 0 cm d^{-1} until the next seepage event started. The magnitude of residuals for all 4221 cases varied for the different calibration periods even when their median values were very similar (Fig. 2.5c–e). Analogous to the *RMSE* distributions (Fig. 2.6) the smallest range of residuals was found for the first year calibration where 80 % of all residual time series (between p_{10} and p_{90}) did not differ by more than 0.21 cm d^{-1} from the median. Wider distributions of residuals resulted from the second year calibration. The second seepage event (starting at day 480) showed the same pattern of under- and overestimation of q_{ref} as the first seepage event. However, seepage fluxes and residuals were much smaller due to smaller input fluxes at the upper boundary of the model domain (cf. Fig. 2.3).

2.3.2. Influence of particle size distribution and textural heterogeneity

The influence of particle size distribution and textural heterogeneity on the performance of the Buckingham-Darcy method is only presented for the case of first year calibration. Findings for both years calibration hardly differed.

Both *RMSE* and CC_{max} varied in dependence of the particle size distribution. They were correlated inversely (r = -0.76) and showed similar spatial distributions in the texture triangle (Fig. 2.7a-c). By far the largest *RMSE* arose from time series that were simulated for sandy soils (up to 0.123 cm d^{-1}). In the textural class sand 95 % of all realizations yielded *RMSE* located in the upper quartile of all *RMSE* (in the following called: poor *RMSE* quartile). Large *RMSE* also occurred in the region of silty loam and silt with 61 % and 32 % in the poor *RMSE* quartile. Around sandy clay both large and small *RMSE* occurred. In the remaining parts of the texture triangle smaller *RMSE* dominated. Smallest CC_{max} were located in silty loam and silt with 69 % and 55 % in the lower poor CC_{max} quartile. In contrast to *RMSE* poor CC_{max} did not prevail in sandy soils.

Regions in the texture triangle where more than 25 % of model realizations were located in the poor quartiles of either *RMSE* or CC_{max} were defined as hotspots of errors with poor performance of the Buckingham-Darcy method. Two hotspots of errors were detected in the texture classes (i) sand as well as (ii) silty loam and silt (Fig. 2.8). The best performance of the Buckingham-Darcy method could be achieved in sandy loam. Here only 5.9 % (*RMSE*) and 6.5 % (CC_{max}) were part of the poor quartiles.

The third quality criterion *Lag* was not used to define the hotspot of errors because time lags were small (p_{50} = 4 d). The spatial distribution of *Lag* differed from those of RMSE and CC_{max}

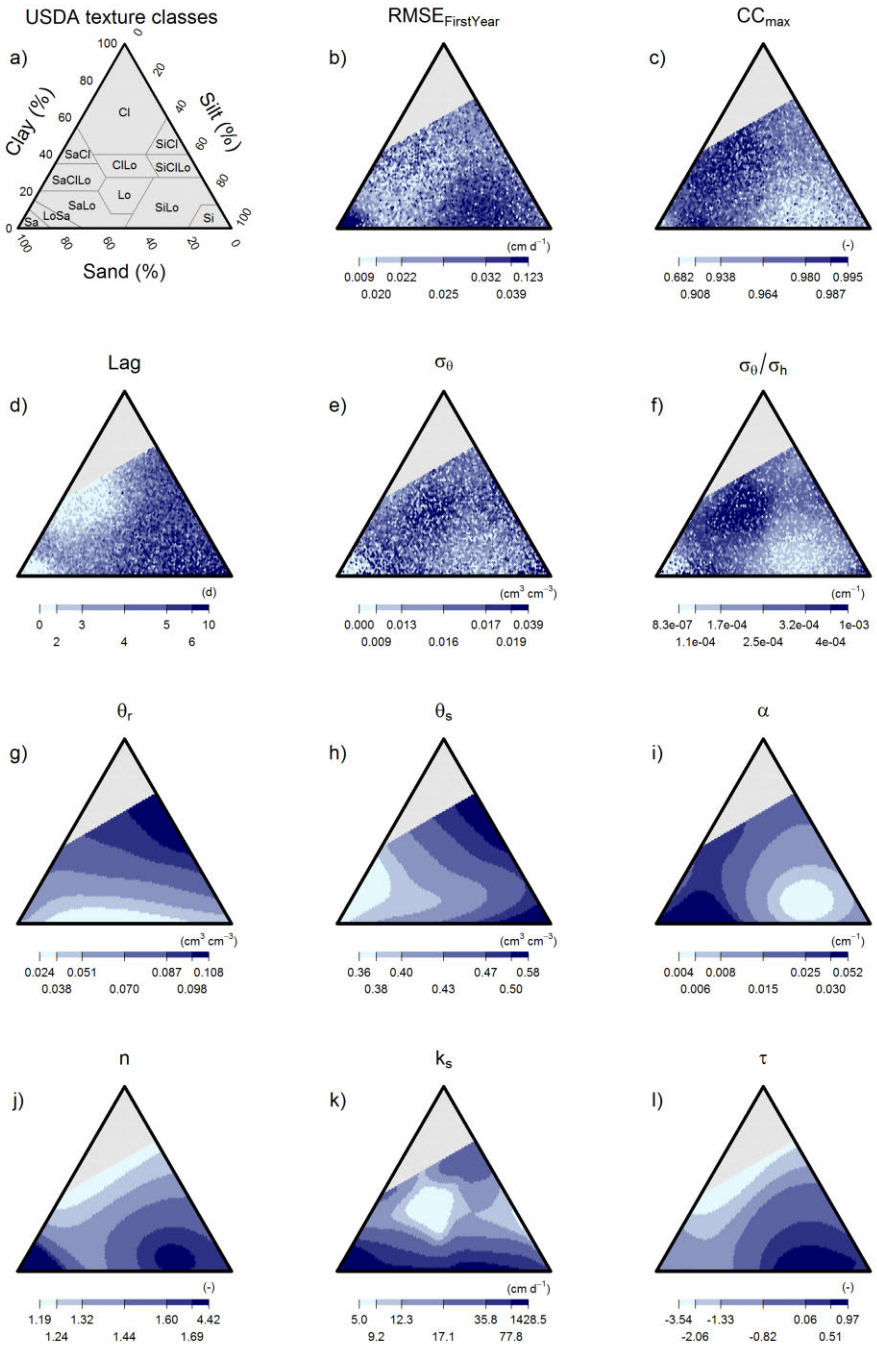

Figure 2.7. Soil texture triangles colored after Root Mean Square Error *RMSE* (b), the maximum cross correlation CC_{max} (c) at the time shift *Lag* (d), the standard deviation σ_θ of $\theta_{z1}(t)$ (e), and its quotient σ_θ/σ_h with the standard deviation σ_h of h_{z1} (f), and the soil hydraulic parameters θ_r, θ_s, α, n, k_s, and τ arising from the *Rosetta* pedotransfer function (g - l). Panel (a) shows the USDA texture classes for orientation.

(Fig. 2.7d). Largest *Lag* occurred in the right part of the texture triangle (silt and loam soils) including the second hotspot of errors. Smallest *Lag* prevailed in the first hotspot of errors (sand) and around sandy clay.

Two variables arising from the input time series were closely related to *RMSE* and CC_{max} (i) the standard deviation σ_θ of the simulated input time series $\theta_{z1}(t)$ and, (ii) its quotient σ_θ/σ_h with the standard deviation σ_h of the simulated input time series $h_{z1}(t)$ (Fig. 2.7e-f). Small temporal variance of $\theta_{z1}(t)$ caused poor performance of the Buckingham-Darcy method because small values of σ_θ prevailed in the hotspots of uncertainties. The correlation between σ_θ and RMSE was r = -0.47 and between σ_θ and CC_{max} was r = 0.31. The relation σ_θ/σ_h is used to assess the steepness of the retention curve in the range of values which was effective in each simulation. The spatial distribution of σ_θ/σ_h in the texture triangle was similar to the global patterns of *RMSE* and CC_{max}. Both quality criterions were correlated with σ_θ/σ_h (*RMSE*: r = -0.52, CC_{max}: r = 0.56). Small values of σ_θ/σ_h prevailed in the hotspots of errors. This shows that shallow sections of the retention curves were active in cases with poor performance of the Buckingham-Darcy method.

The influence of soil texture on *RMSE* and CC_{max} can also be investigated by means of the six soil hydraulic parameters. They implicitly contain the same information like the texture because they have been predicted from texture fractions by the pedotransfer function *Rosetta*. The nonlinear structure of the artificial neural network underlying *Rosetta* becomes apparent when the texture triangle is colored according to each single parameter (Fig. 2.7g-l). The *RMSE* was correlated with the parameters n (r = 0.60) and K_s (r = 0.50). Large values of n predominated in both hotspots of uncertainties. The criterion CC_{max} was mainly affected by the parameters τ (r = -0.58) and α (r = 0.55).

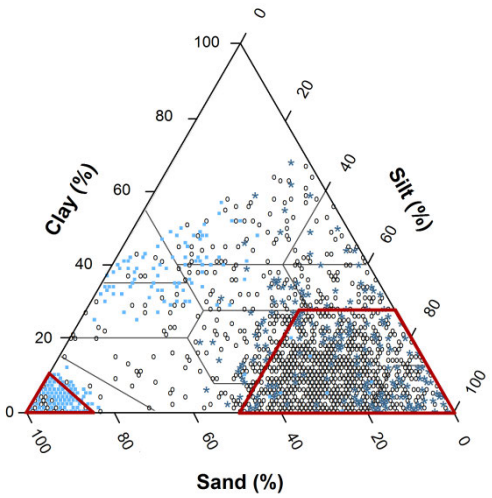

Figure 2.8. Texture of model realizations laying in the poor quartile of *RMSE* (lightblue dots), CC_{max} (darkblue stars) or both (black circles). Texture classes with more than 25 % in the poor quartile of *RMSE* or CC_{max} are defined as hotspots of errors (marked by red polygons).

Table 2.1. Pearson correlation r between the geostatistical parameter sill and the quality criterions Root Mean Square Error (*RMSE*), maximum of the cross correlation function *CCmax*, and time lag *Lag* for the global range of textures (All) and for each specific texture class. Only significant correlations (significance level: 0.95) are shown.

	All	Sa	SiLo	LoSa	Si	SaCl	SiClLo	Lo	SaClLo	ClLo	Cl	SiCl	SaLo
RMSE	0.11	-	-	-	-	0.29	0.17	-	0.32	0.21	0.23	-	0.21
CC_{max}	-	-	-	-0.17	-	-0.28	-	-	-0.16	-	-	-	-
Lag	-0.25	0.32	-0.39	-	-0.45	-0.32	-0.64	-0.57	-0.46	-0.35	-0.29	-0.76	-0.40

The geostatistical parameter *sill* characterizing the spatial variance of the Miller and Miller scaling factors influenced *Lag* significantly (confidence level: 0.95). Strongest negative correlations were found in silty clay (r = -0.76) and silty clay loam (r = -0.64) (Tab. 2.1). Significant correlations between *sill* and *RMSE* occurred in six textural classes. Maximal correlation was found in sandy clay loam (r = 0.32). Correlations between *sill* and CC_{max} were significant in only three texture classes. In sandy clay the correlation was strongest (r = -0.28). The parameter *range* was not correlated with the three quality criterions at all.

2.4. Discussion

2.4.1. Using simulated data to test the Buckingham-Darcy method

We followed a numerical modeling approach because theoretical approaches with simulated data enable drawing more general conclusions than case studies with real measured data that are only valid for a few specific cases. It is worth noting that transferability of theoretically obtained results to field conditions is limited due to model simplifications.

Our strategy to investigate a couple of first order control parameters describing particle size distribution and textural heterogeneity simultaneously minimized the risk to miss basic patterns in systems behavior that result from interactions of parameters. However, working with simulated data required a couple of simplifications about the investigated processes *a priori*. This involves the risk to neglect processes that are critical in real field situations. To simulate time series of soil moisture, matric head, and reference water fluxes we made the following assumptions: (i) transient water fluxes in an unsaturated soil can be modeled adequately using the Richards Equation, (ii) soil hydraulic properties can be modeled with the van Genuchten/Mualem model in a proper way, (iii) textural heterogeneity can be reproduced by varying

reference soil hydraulic properties with Miller & Miller scaling factors that are arranged in a Gaussian random field. Numerous more advanced physically based approaches exist to model water flow through structured soils with the Richards Equation (cf. Köhne et al., 2009). Most of them highlight one specific aspect like multimodal pore size distribution (eg. Durner, 1994), nonequilibrium between θ and h (Ross and Smettem, 2000), macropore flow (eg. Gerke and van Genuchten, 1993; Jarvis et al., 1991) or hysteresis (Kool and Parker, 1987). There are also more sophisticated geostatistical approaches to predict spatial heterogeneity in soils: Schlüter and Vogel (2011) for example used different morphological descriptors like Minkowski functions and chord length distributions in order to generate random fields that exhibit more realistic pore connectivity. Fleckenstein and Fogg (2008) used geostatistical indicator simulations based on transition probabilities and Markov chains to characterize alluvial hydrofacies. We concentrated on non-layered soils and adopted less complex but commonly accepted and verified models to cope with acceptable computation times and adequate numbers of model parameters.

The results are only valid for magnitudes of seepage fluxes occurring in the simulations. However, the implemented upper boundary condition was composed of measured seepage fluxes from both a wet and a dry year (cf. section 2.2). Thus, a wide range of realistic seepage flux dynamics was covered.

2.4.2. Performance of the Buckingham-Darcy method

Comparing global reference fluxes q_{ref} and calibrated local fluxes q_{obt} revealed that the Buckingham-Darcy method is valid in many cases. Overall *RMSE* amounted to approximately 7.5 % of the maximal median flow rate of 0.4 cm d^{-1}. Absolute values of q_{ref} and q_{obt} were in the same order of magnitude due to the calibration procedure where the integral of q_{obt} was set to be identical to the integral of q_{ref}. The dynamics of $q_{ref}(t)$ and $q_{obt}(t)$ were very similar. The median of CC_{max} was 0.964. This means that 93 % (CC_{max}^2 = 0.93) of the temporal variance of q_{ref} could be reproduced when q_{obt} was shifted in time by *Lag*. Time lags of about 4 d (median of *Lag*) are mostly negligible when groundwater recharge is monitored for years or decades.

Nevertheless, the Buckingham-Darcy method showed also limited performance in the hotspot of errors. The reasons might be as follows. Poor performance occurred in the model when flux dynamics obtained from one single position were not synchronous with fluxes through the entire plane of interest. In the model heterogeneous flow fields were dominated by preferen-

tial funneled flow (Kung, 1990) through a network of distinct pathways. Water fluxes in such pathways were not only higher than those in more passive regions but also differed with respect to temporal dynamics. In the latter case actual flux dynamics through the entire plane of interest resulted from a non-linear interplay of various local fluxes. Under these conditions spatial patterns of water fluxes were not stable in time. In the calibration procedure flux dynamics obtained at one single position q_r were scaled linearly to match the overall flux dynamics through the plane of interest q_{ref}. In the hotspots of errors q_r and q_{ref} were not linearly related. This yielded errors in determining flux rates with the Buckingham-Darcy method. In literature there are hardly any studies about temporal stability that were referred explicitly to the permanent seepage zone. It was discussed that processes in the root zone like root water uptake decrease temporal stability (Cassel et al., 2000; Hupet and Vanclooster, 2002). Many other authors also found that spatial homogeneity of soil water dynamics increased with depth (e.g. Guber et al., 2008a; Kamgar et al., 1993). This confirms the findings of Schindler and Müller (1998) who suggested concentrating on the permanent seepage zone where relative soil moisture dynamics are not influenced by root zone processes and less variable in space. In a recent, but still unpublished study, we use soil moisture time series measured with many spatial replicates to investigate the spatial synchronicity of seepage fluxes obtained with the Buckingham-Darcy method.

The shape of the median time series of residuals followed a systematical pattern (Fig. 2.5c-e). The strong underestimation during the flux peak and the slight overestimation in the following 350 days corresponds to our findings that q_{obt} lagged behind q_{ref}. A systematical time shift between q_{obt} and q_{ref} contributes to the high residuals during the main peak. Two possible reasons can explain this pattern. Firstly, dynamics of flux through the plane of interest were dominated by high flow rates that occurred only at very view locations in the model domain. These preferred pathways are rarely matched by sampling points. Thus, it is likely that $\theta_{z1}(t)$ was simulated in a region of the profile where water fluxes were delayed. This would cause systematic underestimation of the flow dynamics. Secondly, the unit gradient assumption of the Buckingham-Darcy method can be a reason for the dynamics of residuals. At a seepage front during the wetting phase it can be expected that the actual hydraulic gradient is underestimated by assuming unit gradient conditions. This would cause an underestimation of seepage fluxes. In the drainage phase actual gradients are expected to be smaller than 1 cm cm^{-1} which would cause an overestimation of seepage fluxes.

The selection of the calibration period impacts *RMSE* strongly. In the simulated flow scenarios 71 % of total seepage occurred in the first year (Fig. 2.5a). The main flux peak with maximal residuals also took place in the same year. Thus, calibrating with data from the most important first year resulted in smallest *RMSE* whereas calibrating with the second year data yielded maximal *RMSE*. In the second case the variance of the water flux data was smaller during the calibration period than during the whole observed period. Thus, the essential range of system status was not fully considered in the calibration procedure which yielded large uncertainties.

Schindler and Müller (2005) tested the Buckingham-Darcy method with time series measured in lysimeters at the ZALF Research Station, Dedelow in the year 2002. The plane of interest (at 1.85 m depth) was in a sand layer under a 1.15 m thick layer of sandy loam. Their study was conducted under identical meteorological boundary conditions like in the first year input data of our model study. In a second study they applied the method to data measured in the same lysimeter in the years 2001 to 2008 (Schindler et al., 2008). They used only one winter season of 3.5 months for calibration. In both studies they found even smaller flux residuals than we would expect from the background of our theoretical findings. A possible explanation could be that the flow field in their lysimeters could have been less heterogeneous than those in our simulations.

Da Silva et al. (2007) compared deep seepage flux data, obtained from a water balance equation, with those calculated by the Buckingham-Darcy equation without calibration. They claimed that using the Buckingham-Darcy equation does not yield consistent results under field conditions and that errors of estimated fluxes can be in the range of several orders of magnitudes if no calibration is applied. This corresponds to our findings that especially in sandy substrates large β_{cal} were needed to transform the observed flux dynamics to a realistic absolute level. By calibrating calculated seepage fluxes with the water balance as suggested by Schindler and Müller (1998), both methods that da Silva et al. (2007) investigated are merged. In this way both magnitudes and dynamics of water fluxes could be obtained.

2.4.3. Influence of particle size distribution and textural heterogeneity

The most important influencing factors σ_θ and σ_θ/σ_h are known when the Buckingham-Darcy method is applied to field data. Our findings about the distributions of resulting *RMSE,* CC_{max}, and *Lag* can be used to evaluate the reliability of obtained seepage time series under specific site conditions. Reliable results can be expected for instance at investigation sites with sandy

loam where measured water content data exhibit large standard deviations and the relation σ_θ/σ_h is large.

Both hotspots of errors were located in regions of the texture triangle where *n* was large. Large values of *n* involve steep slopes of $k_r(\theta)$. In such cases small errors resulting from temporal and spatial averaging of soil moisture data can lead to large uncertainties in determining $k_r(\theta)$. These uncertainties affect flux calculations directly because $q(\theta)$ is linearly related to $k_r(\theta)$ when unit gradients are assumed (Eq. 2.1). Several authors have shown that Darcy-flux methods can be highly sensitive to measurement errors due to strong non-linear characteristics of $k_r(\theta)$ (da Silva et al., 2007; Ghiberto et al., 2011; Reichardt et al., 1998). The parameters K_s, α, and τ were correlated with single quality criterions but showed no general tendency in both hotspots of errors. Rocha et al. (2006) analyzed the sensitivity of soil hydraulic parameters on subsurface water flows under furrows in a numerical experiment. They also found that the parameter *n* has the largest impact on soil water fluxes.

Mohanty and Skaggs (2001) investigated spatio-temporal patterns of near surface soil moisture by air-borne passive microwave remote sensing at a scale of 0.5 km^2. Consistent with our findings at smaller scale they found that soil moisture patterns were more stable in time in sandy loam than in silty loam. With regard to the Buckingham-Darcy method which requires temporal stability, we also allocated silty loam to the hotspot of errors and found the best performance in sandy loams.

Influences of soil hydraulic parameters on *RMSE,* CC_{max} and *Lag* were analyzed in a bivariate and linear way. This entailed that correlations among influencing factors were not considered when effects of each single influencing factor were evaluated. In most texture classes large *sill* values yielded small *Lags* (Tab. 2.1). It can only be speculated that this phenomenon arises from flow fields that are more variable in space and time when *sill* is large. Both parameters *sill* and *range* could not be used to predict the applicability of the Buckingham-Darcy method in field situations because in real soils they cannot be assessed easily.

The occurrence of poor performance could not be explained fully by the variables we investigated in this study. There was still an irregular component in the distribution of the quality criterions in the texture triangle (Fig. 2.7b-d). This fraction of *RMSE* variance could also not be explained fully by *sill* and *range*. We assume that the individual characteristics of each scaling field at the positions of the observation point also have an impact on the performance (cf.

Fig. 2.2). It happened randomly if the time series $\theta_{z1}(t)$, $h_{z1}(t)$, and q_{ref} were taken from a more or less passive region of the flow domain. The facts, that q_{ref} never lagged behind q_{obt} and that less than 10 % of β_{cal} were larger than 1, indicates that passive regions were more extensive in the flow domain than the preferred water pathways. We suppose that time series measured in situ at adjacent positions could yield quite different performances of the Buckingham-Darcy method.

Even though we showed that the Darcy-Buckingham method is valid under different edaphic and atmospheric conditions there is still research need concerning this method. The method's sensitivity to measurement errors of soil moisture should be investigated additionally. Another issue is the more general question of representing spatial heterogeneous water fluxes in effective one-dimensional calculations. In addition bridging the gap between the scale of flux observation and larger scales of interest is of major concern when the Buckingham-Darcy method is applied. This is a major issue of actual soil hydrological research (Lin, 2011).

2.5. Conclusions

The aim of this study was to identify conditions of particle size distribution and textural heterogeneity under which the simplified Buckingham-Darcy method of Schindler and Müller (1998) can be used to obtain deep seepage dynamics on the basis of measured soil moisture and matric head time series. Our approach to test the method in a numerical experiment was successful in so far that we could show that the method´s performance is influenced mainly by (i) the soil textural class and (ii) the time period used for flux calibration. The performance of the method was poor in sand and silty texture. Such textural classes were addressed as hotspots of errors. Best performance could be found in sandy loam. The most sensitive van Genuchten parameter was *n*. It exhibited high values in both hotpots of errors. In addition the selection of an adequate calibration period is crucial. Using a period with high variance in seepage fluxes for calibration yielded the best performance. Our findings can also be interpreted in terms of the occurrence of temporally stable soil water flux patterns, which is a precondition for successful calibration of obtained fluxes. This implies that soil texture conditions yielding good performance of the Buckingham-Darcy method did also enhance temporal stability.

Acknowledgements

This study was funded by the *German Research Foundation DFG* (project Li 802/3-1). We thank Uwe Schindler for critical hints and suggestions that improved this work, Anne-Kathrin Schneider and Björn Thomas for proofreading and helpful discussions, Andre Peters for providing the *SHYPFIT 2.0* software and three anonymous reviewers and the associate editor Juan V. Giraldez for their valuable comments.

References

Abdou, H.M., Flury, M., 2004. Simulation of water flow and solute transport in free-drainage lysimeters and field soils with heterogeneous structures. Eur J Soil Sci, 55(2): 229-241.

Bethune, M.G., Selle, B., Wang, Q.J., 2008. Understanding and predicting deep percolation under surface irrigation. Water Resour Res, 44(12).

Bogner, C., Wolf, B., Schlather, M., Huwe, B., 2008. Analysing flow patterns from dye tracer experiments in a forest soil using extreme value statistics. Eur J Soil Sci, 59(1): 103-113.

Brooks, R.H., Corey, A.T., 1964. Hydraulic Properties of Porous Media, Hydrology Paper 3, Colorado State University, Fort Collins, Colorado.

Burgess, T.M., Webster, R., 1980. Optimal interpolation and isarithmic mapping of soil properties. 1. The semi-variogram and punctual kriging. J Soil Sci, 31(2): 315-331.

Cassel, D.K., Wendroth, O., Nielsen, D.R., 2000. Assessing spatial variability in an agricultural experiment station field: Opportunities arising from spatial dependence. Agron J, 92(4): 706-714.

Da Silva, A.L., Reichardt, K., Roveratti, R., Bacchi, O. O. S., Timm, L. C., Oliveira, J. C. M., Dourado-Neto, D., 2007. On the use of soil hydraulic conductivity functions in the field. Soil Till Res, 93(1): 162-170.

De Vries, J.J., Simmers, I., 2002. Groundwater recharge: an overview of processes and challenges. Hydrogeol J, 10(1): 5-17.

Durner, W., 1994. Hydraulic conductivity estimation for soils with heterogeneous pore structure. Water Resour Res, 30(2): 211-223.

Fleckenstein, J.H., Fogg, G.E., 2008. Efficient upscaling of hydraulic conductivity in heterogeneous alluvial aquifers. Hydrogeol J, 16(7): 1239-1250.

Fragala, F.A., Parkin, G., 2010. Local recharge processes in glacial and alluvial deposits of a temperate catchment. J Hydrol, 389(1-2): 90-100.

Gee, G.W., Newman, B. D., Green, S. R., Meissner, R., Rupp, H., Zhang, Z. F., Keller, J. M., Waugh, W. J., van der Velde, M., Salazar, J., 2009. Passive wick fluxmeters: Design considerations and field applications. Water Resour Res, 45, W04420.

Gerke, H.H., van Genuchten, M.T., 1993. A dual-porosity model for simulating the preferential movement of water and solutes in structured porous-media. Water Resour Res, 29(2): 305-319.

Ghiberto, P.J., Libardi, P.L., Brito, A.S., Trivelin, P.C.O., 2011. Components of the water balance in soil with sugarcane crops. Agr Water Manage, 102(1): 1-7.

Goovaerts, P., 1999. Geostatistics in soil science: state-of-the-art and perspectives. Geoderma, 89(1-2): 1-45.

Guber, A.K., Gish, T. J., Pachepsky, Y. A., Van Genuchten, M. T., Daughtry, C. S. T., Nicholson, T. J., Cady, R. E., 2008a. Temporal stability in soil water content patterns across agricultural fields. Catena, 73(1): 125-133.

Guber, A.K., Gish, T. J., Pachepsky, Y. A., Van Genuchten, M. T., Daughtry, C. S. T., Nicholson, T. J., Cady, R. E., 2008b. Temporal stability of estimated soil water flux patterns across agricultural fields. International Agrophysics, 22(3): 209-214.

Hupet, F., Vanclooster, M., 2002. Intraseasonal dynamics of soil moisture variability within a small agricultural maize cropped field. J Hydrol, 261(1-4): 86-101.

Jarvis, N.J., Jansson, P.E., Dik, P.E., Messing, I., 1991. Modeling water and solute transport in macroporous soil .1. Model description and sensitivity analysis. J Soil Sci, 42(1): 59-70.

Jimenez-Martinez, J., Skaggs, T.H., van Genuchten, M.T., Candela, L., 2009. A root zone modelling approach to estimating groundwater recharge from irrigated areas. J Hydrol, 367(1-2): 138-149.

Kamgar, A., Hopmans, J.W., Wallender, W.W., Wendroth, O., 1993. Plotsize and sample number for neutron probe measurements in small-field trials. Soil Sci, 156(4): 213-224.

Köhne, J.M., Köhne, S., Simunek, J., 2009. A review of model applications for structured soils: a) Water flow and tracer transport. J Contam Hydrol, 104(1-4): 4-35.

Kool, J.B., Parker, J.C., 1987. Development and evaluation of closed-form expressions for hysteretic soil hydraulic-properties. Water Resour Res, 23(1): 105-114.

Kosugi, K., 1996. Lognormal distribution model for unsaturated soil hydraulic properties. Water Resour Res, 32(9): 2697-2703.

Kung, K.J.S., 1990. Preferential flow in a sandy vadose zone: 2. Mechanism and implications. Geoderma, 46(1-3): 59-71.

Lin, H., 2011. Hydropedology: Towards new insights into interactive pedologic and hydrologic processes across scales. J Hydrol, 406(3-4): 141-145.

Lu, X.H., Jin, M.G., van Genuchten, M.T., Wang, B.G., 2011. Groundwater recharge at five representative sites in the Hebei Plain, China. Ground Water, 49(2): 286-294.

McCord, J.T., 1991. Application of 2nd-type boundaries in unsaturated flow modeling. Water Resour Res, 27(12): 3257-3260.

Meissner, R., Prasad, M.N.V., Laing, G.D., Rinklebe, J., 2010a. Lysimeter application for measuring the water and solute fluxes with high precision. Curr Sci India, 99(5): 601-607.

Meissner, R., Rupp, H., Seeger, J., Ollesch, G., Gee, G.W., 2010b. A comparison of water flux measurements: passive wick-samplers versus drainage lysimeters. Eur J Soil Sci, 61(4): 609-621.

Miller, E.E., Miller, R.D., 1956. Physical theory for capillary flow phenomena. J Appl Phys, 27(4): 324-332.

Mirus, B.B., Loague, K., Cristea, N.C., Burges, S.J., Kampf, S.K., 2011. A synthetic hydrologic-response dataset. Hydrol Process, 25(23): 3688-3692.

Mittelbach, H., Seneviratne, S.I., 2012. A new perspective on the spatio-temporal variability of soil moisture: temporal dynamics versus time-invariant contributions. Hydrol Earth Syst Sc, 16(7): 2169-2179.

Mohanty, B.P., Skaggs, T.H., 2001. Spatio-temporal evolution and time-stable characteristics of soil moisture within remote sensing footprints with varying soil, slope, and vegetation. Adv Water Resour, 24(9-10): 1051-1067.

Mualem, Y., 1976. New model for predicting hydraulic conductivity of unsaturated porous-media. Water Resour Res, 12(3): 513-522.

Pachepsky, Y.A., Guber, A.K., Jacques, D., 2005. Temporal persistence in vertical distributions of soil moisture contents. Soil Sci Soc Am J, 69(2): 347-352.

Paulo, J., Ribeiro, J., Diggle, P.J., 2001. geoR: a package for geostatistical analysis. R-News, 1(2): 14-18. Version 1.7-4. http://www.leg.ufpr.br/geoR/.

Perkins, K.S., Nimmo, J.R., Rose, C.E., Coupe, R.H., 2011. Field tracer investigation of unsaturated zone flow paths and mechanisms in agricultural soils of northwestern Mississippi, USA. J Hydrol, 396(1-2): 1-11.

Peters, A., Durner, W., 2006. Improved estimation of soil water retention characteristics from hydrostatic column experiments. Water Resour Res, 42(11), W11401.

Peters, A., Durner, W., 2008. Simplified evaporation method for determining soil hydraulic properties. J Hydrol, 356(1-2): 147-162.

R Development Core Team, 2010. R: A Language and Environment for Statistical Computing. R Foundation for Statistical Computing, Vienna, Austria. http://www.R-project.org.

Reichardt, K., Portezan, O., Libardi, P. L., Bacchi, O. O. S., Moraes, S. O., Oliveira, J. C. M., Falleiros, M. C., 1998. Critical analysis of the field determination of soil hydraulic conductivity functions using the flux-gradient approach. Soil Till Res, 48(1-2): 81-89.

Rocha, D., Abbasi, F., Feyen, J., 2006. Sensitivity analysis of soil hydraulic properties on subsurface water flow in furrows. J Irrig Drain E-Asce, 132(4): 418-424.

Ross, P.J., Smettem, K.R.J., 2000. A simple treatment of physical nonequilibrium water flow in soils. Soil Sci Soc Am J, 64(6): 1926-1930.

Sanford, W., 2002. Recharge and groundwater models: an overview. Hydrolgeology Journal, 10(1): 110-120.

Scanlon, B.R., Healy, R.W., Cook, P.G., 2002. Choosing appropriate techniques for quantifying groundwater recharge. Hydrogeol J, 10(1): 18-39.

Schaap, M.G., Leij, F.J., van Genuchten, M.T., 2001. ROSETTA: a computer program for estimating soil hydraulic parameters with hierarchical pedotransfer functions. J Hydrol, 251(3-4): 163-176.

Schelle, H., Durner, W., Schlüter, S., Vogel, H.J., Vanderborght, J., 2013. Virtual soils: Moisture measurements and their interpretation by inverse modeling. Vadose Zone J, 12(3).

Schindler, U., Fank, J., Müller, L., 2008. Alternativlösung zur Quantifizierung der Tiefensickerung in situ, 13. Gumpensteiner Lysimetertagung. Lehr- und Forschungszentrum für Landwirtschaft Raumberg-Gumpenstein, Gumpenstein, pp. 93-98.

Schindler, U., Müller, L., 1998. Calculating deep seepage from water content and tension measurements in the vadose zone at sandy and loamy soils in North-East Germany. Archives of Agronomy and Soil Science 43(3): 233-243.

Schindler, U., Müller, L., 2005. Comparison of deep seepage estimations of a virtual with a real lysimeter by means of TDR-measurements. International Agrophysics, 19(1): 69-73.

Schindler, U., Müller, L., 2010. Data of hydraulic properties of North East and North Central German soils. Earth System Science Data, 2(2): 189-194.

Schlather, M., 2011. RandomFields: Simulation and Analysis of Random Fields. R package version 2.0.45. http://CRAN.R-project.org/package=RandomFields.

Schlüter, S., Vogel, H.J., 2011. On the reconstruction of structural and functional properties in random heterogeneous media. Adv Water Resour, 34(2): 314-325.

Schlüter, S., Vogel, H. J., Ippisch, O., Bastian, P., Roth, K., Schelle, H., Durner, W., Kasteel, R., Vanderborght, J., 2012. Virtual soils: Assessment of the effects of soil structure on the hydraulic behavior of cultivated soils. Vadose Zone J, 11(4).

Selle, B., Lischeld, G., Huwe, B., 2008. Effective modelling of percolation at the landscape scale using data-based approaches. Comput Geosci, 34(6): 699-713.

Simunek, J., van Genuchten, M.T., Sejna, M., 2011. The HYDRUS Software Package for Simulating Two- and Three-Dimensional Movement of Water, Heat, and Multiple Solutes in Variably-Saturated Media, Version 2. Technical Manual. PC Progress, Prague, Czech Republic.

Twarakavi, N.K.C., Simunek, J., Schaap, M.G., 2009. Development of pedotransfer functions for estimation of soil hydraulic parameters using support vector machines. Soil Sci Soc Am J, 73(5): 1443-1452.

Vachaud, G., Desilans, A.P., Balabanis, P., Vauclin, M., 1985. Temporal stability of spatially measured soil-water probability density-function. Soil Sci Soc Am J, 49(4): 822-828.

Van Genuchten, M.T., 1980. A closed-form equation for predicting the hydraulic conductivity of unsaturated soils. Soil Sci Soc Am J, 44(5): 892-898.

Van Genuchten, M.T., Leij, F.J., Yates, S.R., 1991. The RETC Code for Quantifying the Hydraulic Functions of Unsaturated Soils, Version 1.0. EPA Report 600/2-91/065, U.S. Salinity Laboratory, USDA, ARS, Riverside, California.

van Schaik, N.L.M.B., 2009. Spatial variability of infiltration patterns related to site characteristics in a semi-arid watershed. Catena, 78(1): 36-47.

Vanderlinden, K., Vereecken, H., Hardelauf, H., Herbst, M., Martinez, G., Cosh, M. H., Pachepsky, Y. A., 2012. Temporal stability of soil water contents: A review of data and analyses. Vadose Zone J, 11(4).

Vogel, T., Cislerova, M., Hopmans, J.W., 1991. Porous-media with linearly variable hydraulic-properties. Water Resour Res, 27(10): 2735-2741.

Weiler, M., Flühler, H., 2004. Inferring flow types from dye patterns in macroporous soils. Geoderma, 120(1-2): 137-153.

Weiler, M., McDonnell, J., 2004. Virtual experiments: a new approach for improving process conceptualization in hillslope hydrology. J Hydrol, 285(1-4): 3-18.

Wessolek, G., Duijnisveld, W.H.M., Trinks, S., 2008. Hydro-pedotransfer functions (HPTFs) for predicting annual percolation rate on a regional scale. J Hydrol, 356(1-2): 17-27.

Wösten, J.H.M., Lilly, A., Nemes, A., Le Bas, C., 1998. Using Existing Soil Data to Derive Hydraulic Parameters for Simulation Models in Environmental Studies and in Land Use Planning, Report 157, Wageningen, The Netherlands.

3. Does textural heterogeneity matter? Quantifying transformation of hydrological signals in soils[2]

Summary

Textural heterogeneity causes complex water flow patterns and soil moisture dynamics in soils that hamper monitoring and modeling soil hydrological processes. These patterns can be generated by process based models considering soil texture heterogeneities. However, there is urgent need for tools for the inverse approach, that is, to analyze observed dynamics in a quantitative way independent from any model approach in order to identify effects of soil texture heterogeneity. Here, studying the transformation of hydrological input signals (e.g., rainfall, snow melt) propagating through the vadose zone is a promising supplement to the common perspective of mass flux considerations. In this study we applied a recently developed new approach for quantitative analysis of hydrological time series (i) to investigate the effect of soil texture on the signal transformation behavior and (ii) to analyze to what degree soil moisture dynamics from a heterogeneous profile can be reproduced by a corresponding homogenous substrate. We used simulation models to generate three data sets of soil moisture time series considering homogeneous substrates (HOM), homogeneous substrates with noise added (NOISE), and heterogeneous substrates (HET). The soil texture classes sand, loamy sand, clay loam and silt were considered. We applied a principal component analysis (also called empirical orthogonal functions) to identify predominant functional patterns and to measure the degree of signal transformation of single time series. For the HOM case 86.7 % of the soil moisture dynamics were reproduced by the first two principal components. Based on these results a quantitative measure for the degree of transformation of the input signal was derived. The general nature of signal transformation was nearly identical in all textures, but the intensity of signal damping per depth interval decreased from fine to coarse textures. The

same functional patterns occurred in the HET data set. However, here the signal damping of time series did not increase monotonically with soil depth. The analysis succeeded in extracting the same signal transformation behavior from the NOISE data set compared to that of the HOM case in spite of being blurred by random noise. Thus, principal component analysis proved to be a very robust tool to disentangle between independent effects and to measure the degree of transformation of the input signal. The suggested approach can be used for (i) data processing, including subtracting measurement noise (ii) identification of factors controlling soil water dynamics, (iii) assessing the mean signal transformation in heterogeneous soils based on observed soil moisture time series, and (iv) model building, calibration and evaluation.

Keywords: Soil heterogeneity, Soil moisture time series, Principal component analysis, Transformation of hydrological signals, Functional averaging, Numerical experiment

[2] An article with equivalent content has been published as:

Hohenbrink, T.L., Lischeid, G., 2015. Does textural heterogeneity matter? Quantifying transformation of hydrological signals in soils. Journal of Hydrology, 523: 725-738. DOI: 10.1016/j.jhydrol.2015.02.009.

3.1. Introduction

Textural heterogeneity of soils is a widespread phenomenon occurring at almost every location of the subsurface (Schulz et al., 2006). An important consequence is that water fluxes in the vadose zone occur in heterogeneous flow fields. This substantially complicates predicting subsurface fluxes by simulation models. No generally accepted model approach to easily simulate heterogeneous flow fields recently exist (cf.Vereecken et al., 2007). Inherent non-linearities of soil hydrological processes complicate modeling of soil water dynamics. Consequently, spatially aggregating of soil structural properties usually yields different model results than considering explicit small scale soil structure heterogeneities. However, considering such heterogeneities in high spatial resolution is feasible only at very small scales and with great effort. Hence, it is necessary to investigate inherent characteristics of soil moisture time series from heterogeneous flow fields in order to find new efficient ways to consider textural heterogeneity in simulation models.

Effects of soil structure heterogeneity on soil water flow fields has often been studied by physically based models, i.e., generating time series of soil hydrological behavior (e.g. soil water flux q [$L\ T^{-1}$] or soil moisture θ [$L^3\ L^{-3}$]) as a function of soil structure and input fluxes (Köhne et al., 2009; Vereecken et al., 2007). However, the reverse approach, i.e., assessing effects of soil structure heterogeneities based on analysis of observed behavior is hardly feasible due to possible equifinality. Moreover, this approach has scarcely been investigated before. Overcoming this obstacle would allow to determine (i) to what degree properties of soil structure impose characteristic patterns on observed behavior, (ii) to what degree any observed behavior of heterogeneous soils could be modeled using a corresponding homogeneous substrate, and (iii) how the latter could be identified based on observed soil hydrological behavior.

In soil hydrology, soil water dynamics are usually regarded from the aspect of mass fluxes that can be modeled with flow and transport equations (van Genuchten et al., 2014). Here we suggest focusing on the aspect of transformation of a hydrological input signal (e.g. rainfall, snow melt) as it propagates through the soil. We define hydrological signals as spatiotemporal changes of state variables (e.g. pressure head, water level) that are propagated through a sequence of hydrological subsystems (e.g. aquifers or streams). In the vadose zone hydrological signals are processed by a change of soil moisture over time and space. In a homogeneous soil,

an input signal becomes increasingly smoothed (Pan et al., 2011) and delayed (Mahmood et al., 2012) with soil depth.

In contrast, soil moisture dynamics emerging from heterogeneous flow fields are not only determined by soil depth and texture. They are also controlled by the usually randomly chosen position in a network of flow channels surrounded by regions with less mobile water (Schelle et al., 2013). Heterogeneous flow fields or non-uniform water fluxes can occur under various conditions. The most prominent reasons for such preferential flow patterns are macropore flow (Jarvis, 2007; Köhne et al., 2009), finger flow induced by water repellency (Diamantopoulos et al., 2013; Hendrickx et al., 1993; Ritsema and Dekker, 2000), and textural heterogeneity. The latter was investigated by Kung (1990a) and Kung (1990b) who described distinct water pathways emerging from flow concentration at the top of inclined sand layers underlying finer textured substrates. This phenomenon called funneled flow was related to the occurrence of capillary barriers. It was intensively studied in the field (Heilig et al., 2003), in the laboratory (Kung, 1993; Walter et al., 2000) and by means of numerical experiments (Schlüter et al., 2012b). Roth (1995) performed numerical simulations of steady state flow through a Miller-similar medium (Miller and Miller, 1956). He showed that local heterogeneities of soil hydraulic properties in macroscopic homogeneous substrates can also evoke complex networks of flow channels. This approach was frequently used to represent heterogeneous flow fields in numerical models (e.g. Hohenbrink and Lischeid, 2014; Peters and Durner, 2009; Vogel et al., 2010).

Soil moisture dynamics at a specific location depend on the interplay of preceding local fluxes. An interesting question is whether non-linear interaction of preceding fluxes causes dynamics of soil moisture that could not occur in a homogeneous flow field. This would mean that non-linearity increases the complexity of soil moisture patterns. This question is of particular importance for upscaling purposes:

- If this would be the case, seepage fluxes at investigation sites could only be predicted on the basis of detailed information about spatial soil texture distributions. In the last decades great efforts have been made to map soil structures by non-invasive geophysical methods (e.g. Haarder et al., 2011; Koszinski et al., 2013). Resulting structural information has been included to inverse soil hydrological modeling (e.g. Busch et al., 2013; Hinnell et al., 2010; Kowalsky et al., 2004). Vogel et al. (2006) performed a dye tracer experiment in a structured soil and reconstructed geometry of observed struc-

tural components in a three dimensional model domain. They considered soil horizons, mesoscopic heterogeneity and macropores. Afterwards, they simulated water flow and tracer transport using the Richards Equation. Such analyses require much effort that can only be done in single studies at very small spatial scales.

- If this would not be the case, it would be rather possible to replace heterogeneous profiles in models by homogeneous surrogates (e.g. Greco et al., 2013) paving the way for upscaling approaches. Soil profiles showing similar response to input events (similar functional properties) could be aggregated to functional units (Lin et al., 2006). A large number of scientific papers deals with finding effective soil hydraulic properties (e.g. Bayer et al., 2005; Durner et al., 2008) and averaging vadose zone variables (e.g. De Lannoy et al., 2007; Schlüter et al., 2012a; Vogel et al., 2010). Most of these studies aimed at modeling heterogeneous soil water fluxes effectively with the one-dimensional Richards Equation.

Several authors stressed a common need for robust tools to identify and predict spatiotemporal patterns in soil science and hydrology (Grayson et al., 2002; Lin et al., 2006; Schröder, 2006). This includes functional patterns, i.e. principal characteristics of system behavior that can be identified by intrinsic properties of measured time series. A promising way to evaluate functional patterns is to investigate how hydrological input signals propagate through a soil profile. It might be expected that the signal transformation behavior is a function of various processes related to soil properties, their heterogeneities, and soil depth. Transformation of soil moisture signals was more often studied in a meteorological context of atmosphere/subsurface interactions (Mahmood et al., 2012; Oudin et al., 2004; Wu et al., 2002) than with respect to soil hydrological questions like deep seepage (Wu et al., 1997). Lischeid et al. (2010) used a principal component analysis (PCA) to identify basic patterns of water signal transformation in unconfined aquifers and to quantify the intensity of signal damping in measured time series.

The aim of this study was to (i) investigate the effect of soil texture on the signal transformation behavior of homogeneous profiles and to (ii) analyze to what degree soil moisture dynamics simulated at any location of a heterogeneous profile can be reproduced by a corresponding homogenous substrate. For this purpose we performed numerical experiments to investigate and compare transformation characteristics of hydrological signals propagating homogeneous and heterogeneous profiles. In addition, we studied the effect of measurement

errors trying to distinguish these effects from those of soil structure heterogeneities. We only considered flow processes occurring in the soil matrix that can conceptually be modeled by the Richards Equation. This includes uniform flow, finger flow, funneled flow and flow affected by local heterogeneities. Our intention was to investigate signal damping characteristics emerging from purely gravity driven flow without considering effects like root water uptake, capillary rise from groundwater or evaporation. We followed the approach that has recently been introduced by Lischeid et al. (2010). Thus, we used time series simulated for simple model scenarios instead of complex monitoring data in order to avoid confusion introduced by uncertain variables like evapotranspiration. In this paper we used the term functional heterogeneity to describe the variability in signal transformation behavior of soil profiles. Functional heterogeneity can be a function of different soil properties like heterogeneity in texture or soil structure.

3.2. Methods

The propagation of hydrological signals through soil profiles was analyzed by means of modeled data sets of daily soil moisture time series that can be expected at sites with large distance to groundwater. The soil system's reaction on water input signals was simulated by modeling gravity driven water fluxes with the mixed form of the Richards Equation (cf. Celia et al., 1990). Soil moisture time series were simulated at daily time resolution. Different data sets comprising three model scenarios were generated: (i) water flow through a homogeneous soil profile (data set HOM), (ii) water flow through a homogeneous soil profile mimicking meas-

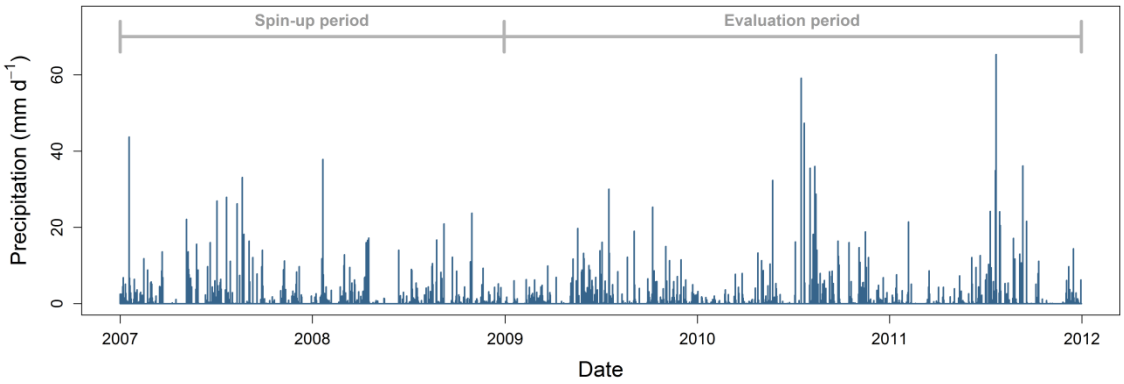

Figure 3.1. Measured precipitation defining the upper flux boundary condition to simulate soil moisture time series. The first two years were used as model spin-up and were not considered in data evaluation.

urement errors of soil moisture (data set NOISE), and (iii) water flow through a heterogeneous soil profile (data set HET). All scenarios were simulated for the USDA texture classes sand (S), loamy sand (LS), clay loam (CL), and silt (Si). A Principal component analysis (PCA) was applied to all time series following the approach of Lischeid et al. (2010) in order to assess the signal transformation behavior of the soil profiles. Results were compared with commonly used measures of signal transformation based on autocorrelation, cross-correlation and the power spectrum of time series. Generation of noise data and statistical analyses were performed with the *R* software package (R Development Core Team, 2010).

3.2.1. Simulating soil moisture time series

Basic model set up

The basic model set up defined all model specifications the three model scenarios HOM, HET and NOISE had in common. Specific features of each model scenario are described in the following sections. A time series of precipitation measured in the years 2007 to 2011 in the Federal State of Brandenburg, Germany was implemented as upper flux boundary condition (Fig. 3.1 and file *UpperBC.txt* of supplementary material). The first two years served as model spin-up time (cf. Ajami et al., 2014). They were simulated only to generate realistic spatial soil moisture distributions over the soil profiles at the beginning of the evaluated time period. Initial conditions at the beginning of the spin-up period were defined by a constant soil water pressure head h = -100 cm at each node of the model domain. Note that the water potential is defined as energy per weight and termed pressure head h [L] in this paper (cf. Durner et al., 2014).

Free drainage conditions were implemented by defining a unit hydraulic gradient I = 1 at the lower boundary as recommended by McCord (1991). We previously analyzed possible influences of the free drainage boundary condition on simulated soil moisture time series (cf. Hohenbrink and Lischeid, 2014). In that pre-study soil moisture time series were simulated in model domains with different vertical extent. They were compared to those from a reference simulation with constant groundwater level at 21 m soil depth (constant head boundary condition). All texture classes were considered. The results of this pre-study showed that the mean percent errors of simulated soil moisture did not exceed 0.5 % when the distance between the observation points and the lower boundary was at least 3 m. Thus, we used 7.5 m deep model domains in this study even if only the upper 4.5 m were of interest. Solving the Richards Equa-

tion requires information about the soil water characteristics defined by the soil water retention function $\theta(h)$ and the function of hydraulic conductivity of the unsaturated soil $k(h)$. We used the models of van Genuchten (1980) and Mualem (1976) to describe both functions by means of the six soil hydraulic parameters: residual and saturated soil water content θ_r and θ_s, the inverse of the pressure head at the air entry point α [L^{-1}], a shape-parameter n [-] related to the width of the pore size distribution, the hydraulic conductivity of the saturated soil k_s [$L\ T^{-1}$], and the tortuosity parameter τ [-]. An overview about the characterization of unsaturated soil hydraulic properties is given by Durner et al. (2014). The different texture classes S, LS, CL, and Si were considered in the model by four realizations of $\theta(h)$ and $k(h)$ (Fig. 3.2). The texture specific soil hydraulic parameters θ_s, θ_r, α, n and K_s (Tab. 3.1) were predicted by the first model of the pedotransfer function *Rosetta* (Schaap et al., 2001). This model provides averaged hydraulic parameters for each USDA texture class based on 2134 soil samples for water retention, 1306 samples for saturated hydraulic conductivity and 235 soil samples for unsaturated hydraulic conductivity. The tortuosity parameter τ was assumed to be 0.5 as it is common practice (Mualem, 1976). Observation points were inserted at 15 depths between 0.3 m and 4.5 m with a distance of 0.3 m each. At these positions soil moisture time series were simulated at daily time resolution.

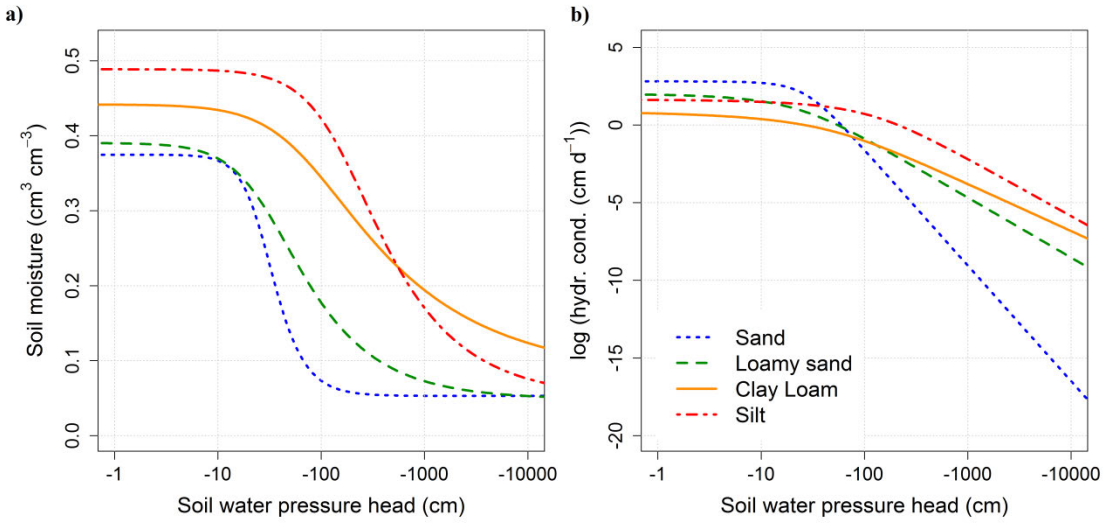

Figure 3.2. Soil hydraulic properties of substrates sand (S), loamy sand (LS), clay loam (CL) and silt (Si) used for simulation of soil moisture time series. Soil water retention curve $\theta(h)$ (a) and hydraulic conductivity of the unsaturated soil $k(h)$ (b). Note that the soil water pressure head h is expressed in the unit cm of equivalent water column which equals the pressure unit hPa.

Table 3.1. Soil hydraulic parameters of the four different USDA texture classes predicted by the pedo-transfer function *Rosetta* (Schaap et al., 2001).

	θ_r ($cm^3\ cm^{-3}$)	θ_s ($cm^3\ cm^{-3}$)	α (cm^{-1})	n (-)	K_s ($cm\ d^{-1}$)	τ (-)
Sand (S)	0.053	0.375	0.035	3.18	643.0	0.5
Loamy sand (LS)	0.049	0.390	0.035	1.75	105.1	0.5
Clay loam (CL)	0.079	0.442	0.016	1.41	8.2	0.5
Silt (Si)	0.050	0.489	0.007	1.68	43.7	0.5

Table 3.2. Properties of three data sets of soil moisture used to investigate the signal transformation behavior in soil profiles. The time series were generated with simulation models.

Data set ID	Texture classes	Soil depths	Soil heterogeneity	Measuring noise	Replicates	Simulation model	Number of time series
HOM	4 texture classes: Sand (S), Loamy sand (LS), Clay loam (CL), Silt (Si)	15 depths: 30 to 450 cm, Δ_z = 30 cm	Homogeneous	No noise	1 Profile	*Hydrus 1D*	60
NOISE			Homogeneous	With noise	4 Noise realizations	*Hydrus 1D*	240
HET			Heterogeneous	No noise	4 Profiles in each 2D domain	*Hydrus 2D*	240

Data set HOM

The data set HOM (*DataSetHOM.txt* of supplementary material) comprised 60 soil moisture time series representing 15 depths between 0.3 m and 4.5 m for four soils with homogeneous but different texture classes each (Tab. 3.2). Water flux and soil moisture were modeled with the software package *Hydrus 1D* (Simunek et al., 2008). The 7.5 m deep one dimensional model domain was spatially discretized by 0.05 m spaced nodes. The total number of nodes was 151. In Fig. 3.3 time series simulated for S and CL are shown for 0.3 m, 2.4 m, and 4.5 m depth. A clear response to rainfall events around day 550 and day 950 became apparent by increasing soil moisture. In both soils peaks exhibited increasingly smaller amplitudes, smoother shape and greater time lags with increasing soil depth. The same signal transformation behavior with increasing soil depth could be observed in cases of the other texture classes Ls and Si (not shown). However, the intensity of signal transformation per depth unit varied between the different textures. This becomes clear with the example of the time series simulated in 4.5 m

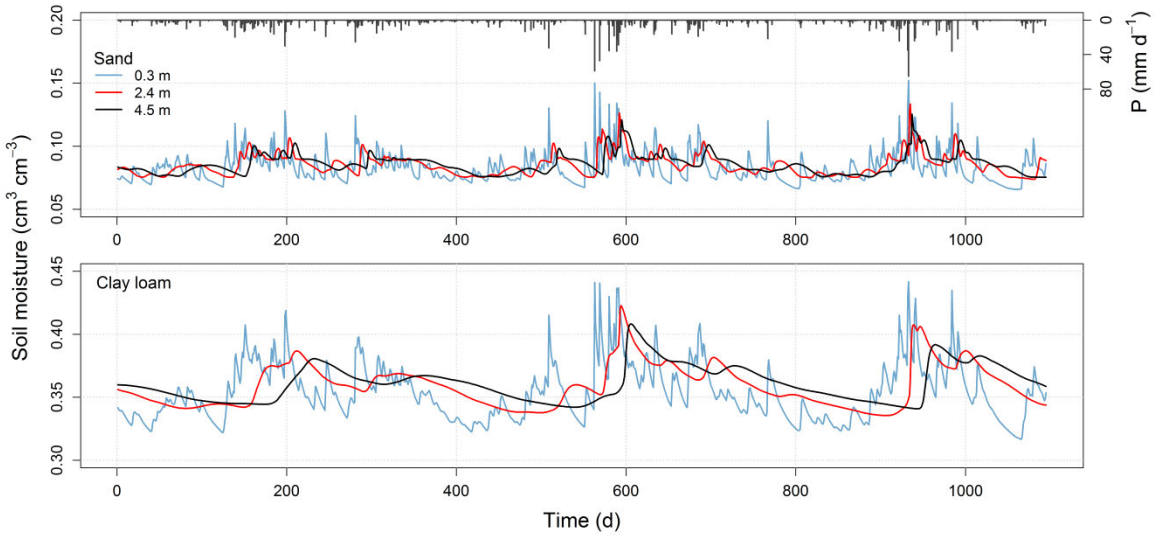

Figure 3.3. Soil moisture time series simulated for the homogeneous case (HOM). Time series at soil depths 0.3 m, 2.4 m and 4.5 m are shown for sand and clay loam. The soil moisture axes (left) are scaled in the same range although the values differ. The bars showing precipitation inputs (P) refer to the right axis.

soil depth where the time series from CL was more smoothed and shifted in time than that from S.

Data set NOISE

The data set NOISE (*DataSetNOISE.txt* of supplementary material) aimed at mimicking uncorrelated measurement errors. This was realized by adding random numbers to the time series from data set HOM. Each set of random numbers was normally distributed (mean: 0 % soil moisture; standard deviation σ: 1 % soil moisture) in order to mimic realistic measurement noise where large deviations are less likely than small ones. The standard deviation was set to σ = 1 % soil moisture because measurement errors of dielectric-based techniques to determine soil moisture can be less than 1.5 % soil moisture in mineral soils (Romano, 2014). Each time series from data set HOM was blurred four times yielding four replicates of noise realization. Overall data set NOISE comprised 240 time series (Tab. 3.2). Sets of random numbers were generated independently to assure that noise components of single time series were not correlated. The generated time series exhibited clear reactions of soil moisture to input signals (Fig. 3.4), although they were substantially blurred by the random fluctuations.

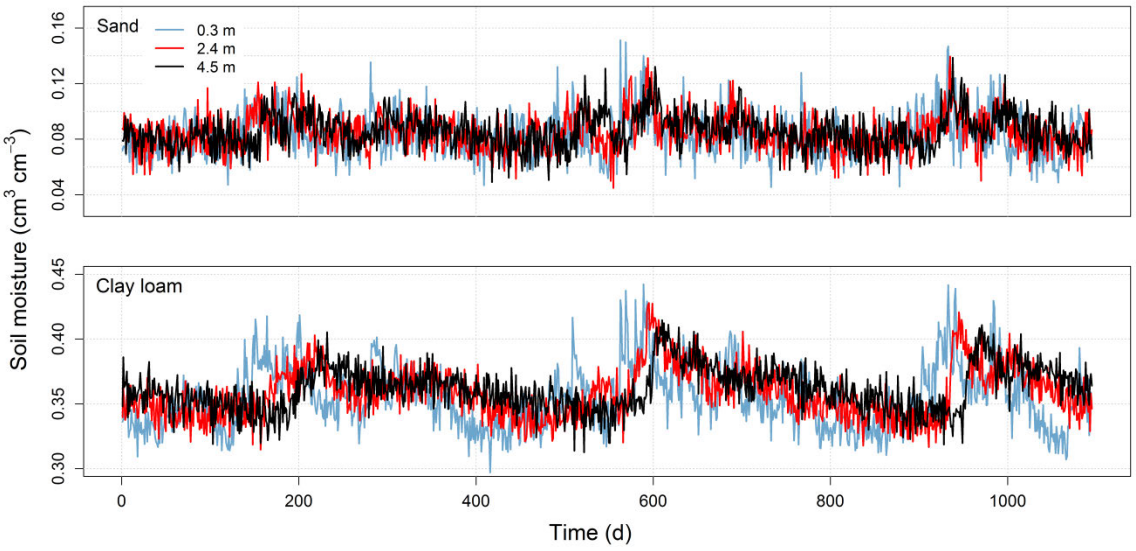

Figure 3.4. Soil moisture time series simulated for the homogeneous case and manipulated by random noise (NOISE). Time series at soil depths 0.3 m, 2.4 m and 4.5 m are shown for sand and clay loam. The soil moisture axes are scaled in the same range although the values differ.

Data set HET

In the data set HET (*DataSetHET.txt* of supplementary material) the influence of soil textural heterogeneity was considered. The software package *Hydrus 2D* (Simunek et al., 2011) was used to simulate two dimensional heterogeneous flow fields (Fig. 3.5). The model domain was x = 4 m wide and z = 7.5 m deep. Node spacing was 0.05 m in both directions and the total number of nodes was 12,231.

Textural heterogeneity was considered in the upper 5 m of the model domain based on the scaling theory of Miller and Miller (1956). This theory describes a relation between soil hydraulic properties from two pore systems with similar internal geometry but different scales. The soil water retention curve $h(\theta)$ and the soil hydraulic conductivity curve $k(h)$ of a porous medium can be derived from corresponding curves $h^*(\theta)$ and $k^*(h)$ of a Miller similar reference medium. Fields of spatial variable soil hydraulic properties can be generated by scaling the reference curves differently at each position of a two dimensional model domain. This concept was frequently used to model spatial variable water fluxes through soils (e.g. Hohenbrink and Lischeid, 2014; Roth, 1995; Schlüter et al., 2012b). We used the soil water retention curves and the soil hydraulic conductivity curves of S, LS, CL, and Si (Fig. 3.2) as reference functions $h^*(\theta)$ and $k^*(h)$. They were manipulated at each node by a scaling factor $\varphi_{x,z}$. In consequence each

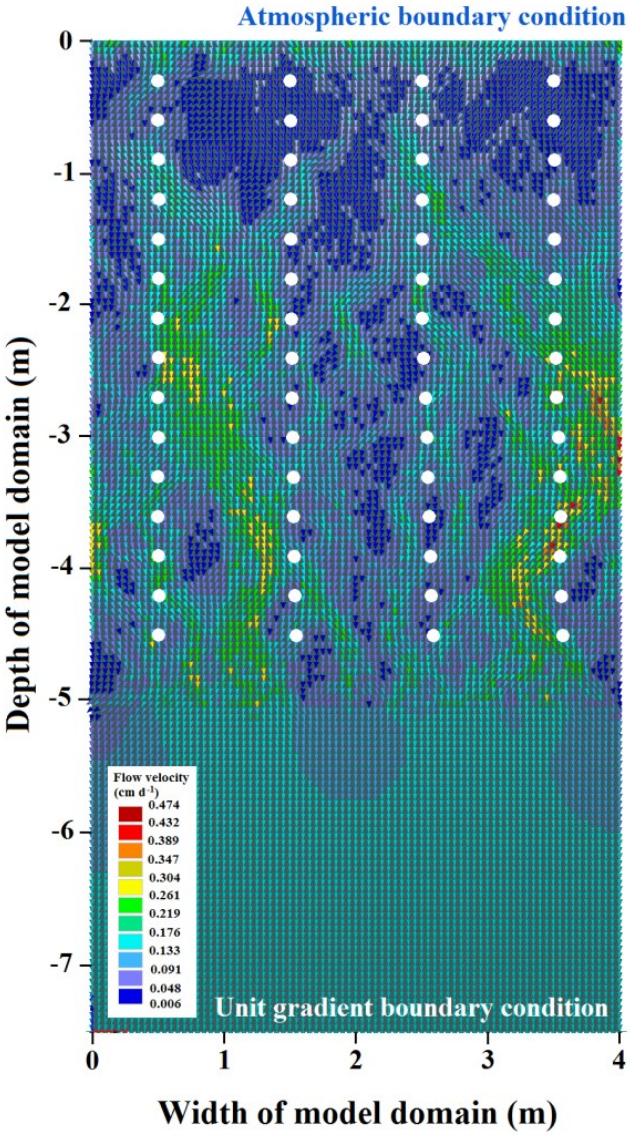

Figure 3.5. Heterogeneous flow field emerging from Miller scaling of the soil hydraulic parameters shown for the loamy sand under wet conditions. White dots show positions where soil moisture time series were generated. Note that a snapshot in time after an input flux through the upper boundary is shown. The peak of the seepage water was located in a soil depth around 3 m at that time.

location was characterized by individual soil hydraulic functions. Scaling factors for the retention curve φ_h and the hydraulic conductivity curve φ_k were related via $\varphi_h = \varphi_k^{-0.5}$ and θ was not scaled $\varphi_\theta = 1$. Thus it was possible to scale both hydraulic functions with one set of φ (cf. Abdou and Flury, 2004; Vogel et al., 1991)

$$h_{x,z}(\theta) = \frac{h^*(\theta)}{\sqrt{\varphi_{x,z}}} \tag{3.1}$$

and

$$k_{x,z} = \varphi_{x,z} \cdot k^*(h)\,. \tag{3.2}$$

We defined φ to be log-normal distributed (median: $\tilde{\varphi} = 0$, variance: $\sigma^2(\log_{10}(\varphi)) = 1$) according to the observation, that pore size distributions are typically log-normal (cf. Schlüter and Vogel, 2011). The spatial distribution of φ was defined by an exponential covariance function (cf. Abdou and Flury, 2004; Peters and Durner, 2009) with a range parameter of $l = 0.325$ m. We used the R routine *grf()* from the package *geoR* (Paulo et al., 2001) to generate spatial Gaussian random fields of φ.

Observation points were inserted to the model domain on four vertical transects with a lateral distance of 1 m (Fig. 3.5). This distance was set fairly large, so the four transects could be treated as quasi replicates. Spacing within each transect was 0.3 m. Soil moisture time series were simulated at these positions. Thus data set HET comprised 240 time series including four heterogeneous profiles in each model domain (Tab. 3.2). The simulated water contents varied spatially in the model domain. Water infiltrating homogeneously through the upper boundary was concentrated in vertical flow channels (Fig. 3.5). This corresponds with flow patterns observed in field by dye tracer experiments (e.g. van Schaik, 2009). The HET time series also showed a reaction of soil moisture to precipitation inputs. However, a relation between signal transformation and soil depth was less obvious than for the HOM data.

3.2.2. Functional analysis of simulated soil moisture time series

Autocorrelation, cross-correlation and power spectrum

Various tools to characterize and compare functional properties of hydrological time series exist that are more common than applying a PCA to time series. We computed different measures of signal transformation based on autocorrelation, cross-correlation and power spectrum for the HOM data set and compared them with our results from a PCA. The autocorrelation function $\rho_{ac}(k)$ describes the correlation between an equidistant time series $\theta(t)$ and replications $\theta(t+k)$ shifted by time lags of k time steps (c.f. Shumway and Stoffer, 2011)

$$\rho_{ac}(k) = \frac{\mathrm{cov}[\theta(t), \theta(t+k)]}{\sigma_\theta \cdot \sigma_\theta}. \quad (3.3)$$

The smoothness of a time series is quantified by $\rho_{ac}(k)$ (e.g. Thomas et al., 2012). We characterized the signal damping behavior of the HOM profile by comparing autocorrelation functions of soil moisture time series from different depths. Time series from two different depths can be compared directly by the cross-correlation function $\rho_{cc}(k)$ (c.f. Mahmood et al., 2012; Shumway and Stoffer, 2011)

$$\rho_{cc} = \frac{\mathrm{cov}[\theta_{z1}(t), \theta_{z2}(t+k)]}{\sigma_{\theta,z1} \cdot \sigma_{\theta,z2}}. \quad (3.4)$$

The time series $\theta_{z1}(t)$ and $\theta_{z2}(t+k)$ are shifted relatively to each other in both directions, because k can be either positive or negative. The time lag where $\rho_{cc}(k)$ is maximal measures the time shift between two time series (c.f. Hohenbrink and Lischeid, 2014). We used the time series from 30 cm soil depth as references and computed their cross-correlations with time series from every depth of the HOM profile.

Another common way to investigate the degree of signal damping is based on the power spectrum of time series. It is a tool of spectral analysis to characterize the low-pass filtering behavior of hydrological systems (e.g. Gall et al., 2013; Katul et al., 2007; Kirchner et al., 2010) rather than analyzing specific frequencies (e.g. annual cycle). The power spectrum describes the distribution of frequencies of oscillations occurring in a time series. It is computed by a Fourier transformation of $\rho_{ac}(k)$. When the power is drawn against frequency in a log-log plot, the slope β of the high frequency part (in this study >0.025 d^{-1}) characterizes the strength of low-pass filtering. We computed β for all time series of the HOM data set and used it as a measure of signal damping.

Principal Component Analysis of time series

The idea of a PCA is to identify prevailing patterns by aggregating most relevant information in a multivariate data set, e.g., a matrix of time series. This is done by decomposing the total variance of an n-dimensional data set containing all time series into few linearly independent principal components that explain most of the variance.

To achieve equal weighing of the single time series they are scaled separately to zero mean $\overline{\theta}$ = 0 and unit variance $\sigma_{\theta z}^2$ = 1 (z-transformation) prior the analysis

$$\theta_z(t) = \frac{\theta(t) - \bar{\theta}(t)}{\sigma_\theta}. \quad (3.5)$$

Thus, information about absolute values and amplitudes of fluctuations is not considered. The z-transformed time series are organized in one matrix Θ where the variables are arranged in columns and the values for single dates in rows.

The PCA performs a multivariate ordination that aims at finding an orthonormal basis for the multidimensional data space spanned by all time series where maximal fraction of total variance σ^2_{expl} is covered by a minimum number of axes. This is done by linear transformation of Θ into a matrix P containing independent components ordered by the fraction of variance they explain (cf. Jolliffe, 2002)

$$\Theta \rightarrow P = \Lambda^T \Theta. \quad (3.6)$$

The matrix Λ contains the eigenvectors of the correlation matrix of Θ ordered by their corresponding eigenvalues which represent the fraction of variance explained by the specific components. The similarity between single time series and a component of the k^{th} order can be evaluated by their correlations that are called loadings L_k. The loadings can be used to calculate the fraction of variance σ^2_{expl} of a time series explained by the *m* first components (cf. Lischeid et al., 2012)

$$\sigma_{\exp l} = \sum_{k=1}^{m} L_k^2 \leq 1. \quad (3.7)$$

A PCA performs a bijective transformation of a data set that is fully reversible when all components are considered ($k = n$). We refer to Jolliffe (2002) for detailed information, examples and discussions about principal component analyses. That textbook also contains a chapter about PCA for time series. Algorithms to perform a PCA are implemented in most statistical software packages.

Every component can be interpreted as a time series describing an independent temporal pattern occurring in the dataset. The loadings provide a basis for identifying specific controls that provoke the patterns described by single components. If the input time series share a large fraction of variance only few principal components are needed to represent a major part of the total information content. The PCA can only detect linear structures in the data space. It overestimates the dimensionality of data sets exhibiting non-linear patterns (Lee and Verleysen, 2007). Thus, a nonlinear structure could only be represented by piece-wise approximation by a

set of linear components. In that case single principal components would underestimate the fraction of variance explained by a single effect.

In this study we used the R routine *princomp()* to apply a PCA to the z-transformed simulated soil moisture series. It is recommended to apply a PCA only to normally distributed data (cf. Jolliffe, 2002). A Shapiro-Wilk test showed that the simulated moisture time series were not normal distributed. But, it is almost impossible to proof normal distribution for such big data sets, because the common tests are very selective in terms of large samples. Moreover, Jolliffe (2002) argued that the precondition of normally distributed input data is much less relevant when a PCA is considered as a mainly descriptive technique.

Assessing signal transformation behavior by PCA

Lischeid et al. (2010) applied a PCA to a set of time series of groundwater head data. They found that the first component described the mean behavior of all time series. The second component reflected the effect of thickness of the overlying vadose zone. They assessed the relative damping of the input signal in each time series from the relation of their loadings with both principal components. Each symbol in a plot showing L_1 on the x-axis and L_2 on the y-axis represents a single time series. In such a plot all symbols usually form a curved trajectory. The position on that one-dimensional trajectory indicates the damping status of a time series. Hence, a damping coefficient D [-] quantifying the intensity of signal damping can be defined (Lischeid et al., 2010)

$$D = \arctan(\alpha). \tag{3.8}$$

The angle α between the x-axis and the line from the origin to the symbol of a time series is defined in radians. Note that D is a relative measure that can only be interpreted in the context of the specific data set analyzed by the PCA. This approach to determine D considers information from the first two components only. The effects described by the remaining components are neglected.

3.3. Results

3.3.1. Autocorrelation, cross-correlation and power spectrum

The depth profiles of autocorrelation (ρ_{ac}) at time lags of k = 1 d and k = 10 d for sand and clay loam (Fig. 3.6a) show an increase of ρ_{ac} with depth. Hence, soil moisture time series appeared to be more strongly damped in greater depths of homogeneous soils. In fine textured soils this

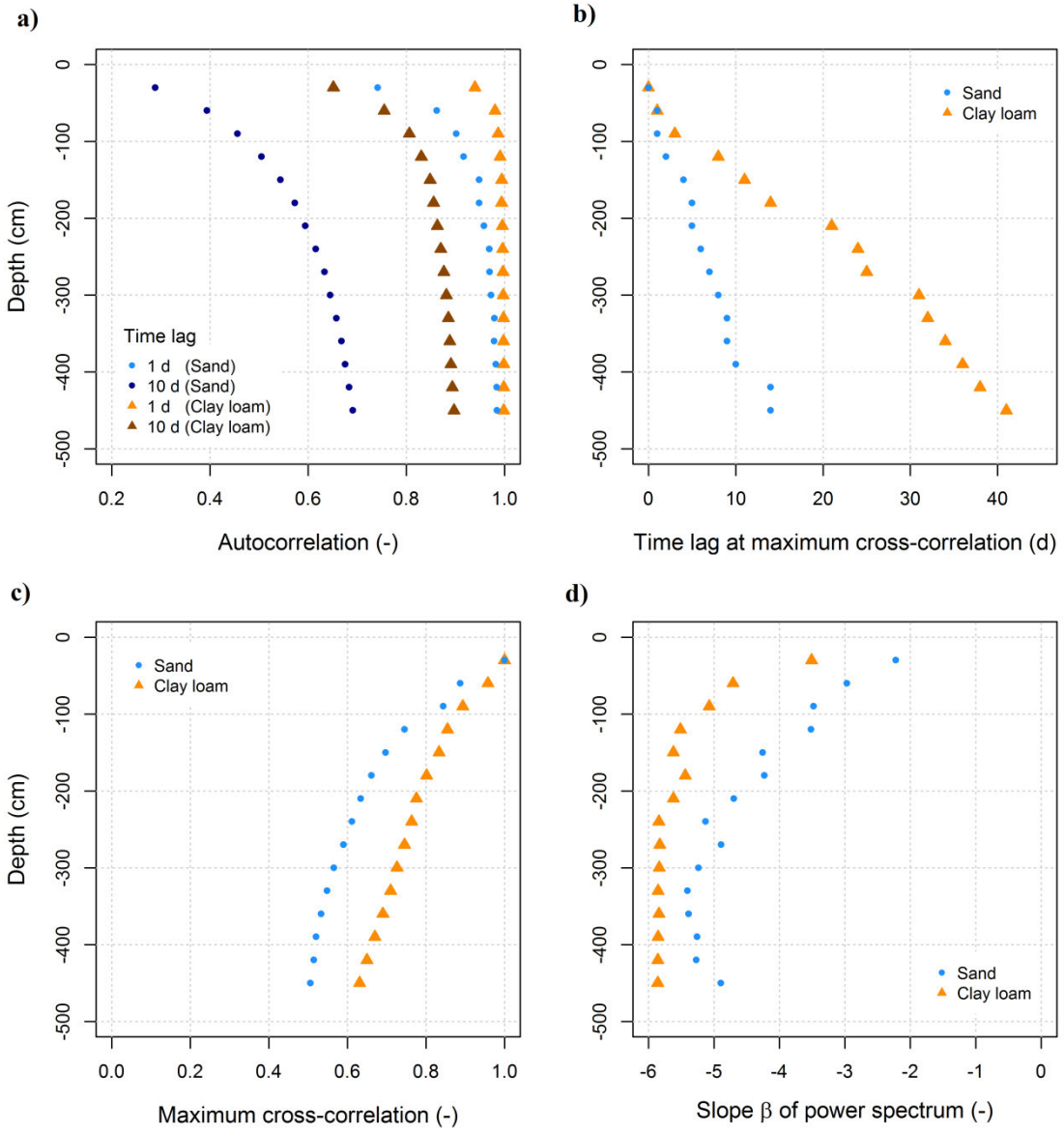

Figure 3.6. Depth profiles of autocorrelation at time lags of 1 d and 10 d shown for sand and clay loam (a). Depth profiles of time lags at the maximum of the cross-correlation function (b) and values of maximum cross-correlation (c). The moisture time series in 30 cm depth were used as reference in all cross-correlation analyses. Depth profiles of the slope β of the power spectrum (d).

effect was stronger than in coarse substrates as shown exemplarily for CL and S (Fig. 3.6a). All depth profiles of ρ_{ac} showed monotonous but non-linear shapes.

The cross-correlation analyses showed that all moisture time series from the HOM data set were increasingly time delayed with larger soil depth. This was clearly reflected by the depth profiles of time lags at maximum cross-correlation between the reference time series (z = 30 cm) and time series from all other depths (shown for CL and S in Fig. 3.6b). The time delay per depth unit increased from coarse to fine textures. Lags of time series simulated in the deepest depth (z = 450 cm) were less than 15 d for S and more than 40 d for CL. The depth profiles of time lags were approximately linear but exhibited irregular steps, although the time series were simulated in homogeneous substrates. Values of maximum cross-correlation decreased with soil depth (Fig. 3.6c). This showed that besides time delaying also other ways of signal transformation exist.

The slopes β of the power spectrum were always negative in the HOM case. Hence, all time series exhibited stronger prevalence of low frequencies compared to high frequencies. The values of β decreased with soil depth (Fig. 3.6d) showing that the soil profiles act as low-pass filters yielding more strongly damped time series with increasing depth. Similar to the autocorrelation (Fig. 3.6a) the intensity of signal damping increased from coarse to fine textures. The depth profiles of β showed both non-linear shapes and irregular steps.

3.3.2. Principal Components

The principal component analysis aimed at a quantitative description of soil hydrological behavior in order to disentangle between different effects. When PCAs were applied separately on the data sets HOM, NOISE, and HET the resulting 1st components were very similar (r^2 > 0.99 in any combination). The same appeared for the 2nd components where correlations were always larger than r^2 = 0.98. Hence, neither textural heterogeneity nor measurement errors influenced the two most dominant patterns of moisture dynamics, even if the relevance of these patterns differed between the three data sets. For that reason there was no benefit for applying PCAs separately on each data set. Hence, we present in the following the first two components of a merged data set MERGED containing all 540 time series of the data sets HOM, HET and NOISE.

Table 3.3. Fraction of variance σ^2_{expl} explained by the first two principal components (PC) for each of the three data sets HOM, NOISE and HET and the entire data set MERGED. Note that the number of time series was 60 in data set HOM but 240 in data sets NOISE and HET.

	σ_{expl} (%)		
	1st PC	2nd PC	Sum
HOM	64.9	21.8	86.7
NOISE	43.6	14.3	64.0
HET	68.3	20.4	88.7
MERGED	57.0	17.8	74.8

The first component explained 64.9 % of the total variance of the HOM data and the 2nd component another 21.8 % (Tab. 3.3). Thus, data set HOM could be summarized by two representative time series maintaining σ^2_{expl} = 86.7 % of the total information content. Consequently, the time series of data set HOM exhibited a large share of common temporal patterns, although they were simulated in different soil depths with a wide range of soil hydraulic properties (Fig. 3.2). This was different for the NOISE data where only σ^2_{expl} = 57.9 % could be expressed by the first two components due to the uncorrelated random noise added to the time series from data set HOM. Correspondingly, the noisy time series shared a smaller fraction of common dynamics that could be detected by a PCA. In the case of the HET data σ^2_{expl} was 88.7 %. Data set HET could be represented by the first two principal components to a similar

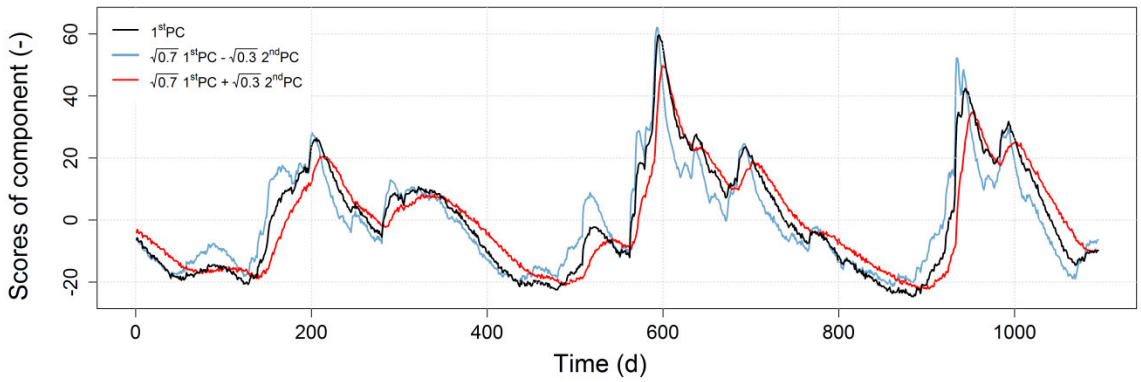

Figure 3.7. First two principal components (PC) shown as time series. Red and blue lines display different combinations of the 1st and 2nd component.

extent like data set HOM, although the number of time series was four times larger and they were simulated in a heterogeneous model domain.

The 1st component represented a time series that was highly correlated with a time series of the arithmetic mean values for each date of all 540 time series (r^2>0.99). Each moisture time series loaded positively on the 1st component. Thus, this component represented an averaged time series reflecting the mean temporal dynamics (Fig. 3.7).

About a half of the moisture time series from data set HOM loaded positively on the 2nd component and the others negatively. The loadings increased with increasing soil depth within each texture class. Correlation between loadings and soil depth was r^2 = 0.76 (S) and r^2>0.96 (LS, Cl, and Si). Thus, the 2nd component obviously captures the effect of increasing damping and delay with soil depth in a homogeneous profile. More precisely, it describes the corresponding deviations from the mean soil moisture dynamics (1st component). This in turn means that any measured time series, irrespective of soil depth, can be approximated by linear regression with the 1st and 2nd components. The regression coefficients are equal to the loadings as long as normalized data are used. Combining both components yields time series that reflect only those temporal patterns described by the components. In this way temporal patterns caused by single factors can be extracted from entire data sets. The ratio used to combine the components determines the weighting of both patterns in the constructed time series. In the two examples in Fig. 3.7 the 1st and the 2nd component were combined in a ratio of 70:30 according to Eq. 3.7. Adding the 2nd component to the 1st component in this ratio (red line in Fig. 3.7) resulted a time series smoother than the mean temporal dynamics (1st component). It also clearly lagged behind the mean dynamics. Such strongly damped moisture time series can be expected in large depths of homogeneous profiles. Subtracting the 2nd component from the mean dynamics yielded a less strongly damped time series (blue line in Fig. 3.7). The peaks preceded those from the 1st component. This temporal pattern can be expected in shallow depths.

3.3.3. Signal transformation behavior assessed by PCA

In the previous section the first two principal components were used to reproduce time series with different degrees of damping. Conversely, the damping intensity of a time series can be measured by the loadings on the first two components. In Fig. 3.8a each symbol represents one specific time series. The closer a symbol is to the unit circle, the larger is the fraction of variance explained by the first two components σ^2_{expl}. The distance to the unit circle indicates the fraction of variance 1-σ^2_{expl} that is not covered by the first two components and thus explained by components of higher order. Symbols of each texture class plot along curved lines with increasing soil depth in anticlockwise direction. They are all close to a single common trajectory. This trajectory describes the evolution of hydrological input signals. Symbols of time series from equal depths but different textures are located at different positions on the trajectory. Time series from S were concentrated in the lower left part of the trajectory, whereas those from Si were arranged more in the upper part. Within each texture class of the HOM data set the damping coefficient *D* (Eq. 3.8) increased with increasing soil depth. Resulting damping profiles were slightly s-shaped (Fig. 3.8b). They can be used to characterize the signal transformation behavior of the different substrates. Their slopes decreased in the order S, LS, Cl, and Si, showing that signal transformation per depth interval is by far weakest in S and strongest in Si.

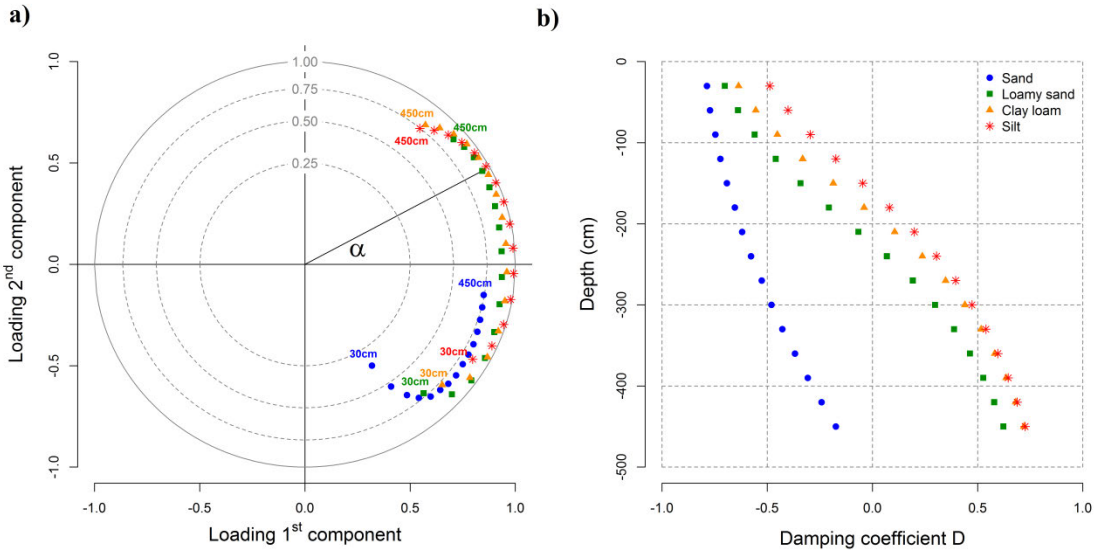

Figure 3.8. Loadings on the first two principal components for all HOM time series (a). Symbols represent single moisture time series. Gray circles denote the fraction of variance σ^2_{expl} explained by both components. Resulting depth profiles of signal damping for the different texture classes (b).

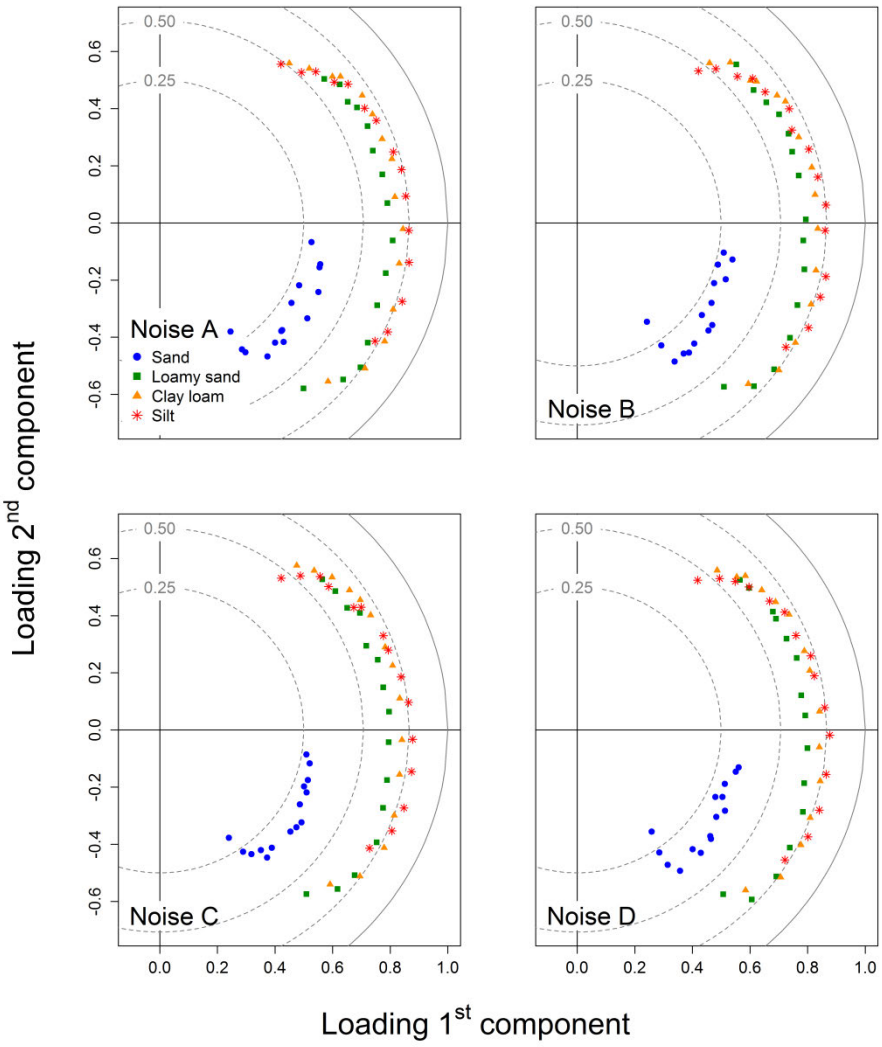

Figure 3.9. Loadings on the first two principal components for all NOISE time series. Each panel corresponds to one noise realization. Symbols represent single moisture time series. Gray circles denote the fraction of variance σ^2_{expl} explained by both components.

Loadings on the 1st and 2nd component for the NOISE data set show a similar pattern (Fig. 3.9). However, compared to the HOM data they were more distant from the unit circle, which is consistent with the smaller values of σ^2_{expl} (Tab. 3.3). Especially for moisture series from S the explained fraction of variance was low (σ^2_{expl} slightly larger than 0.25). Consequently, symbols of the S time series were arranged on a separate curve parallel to the trajectory of the symbols from the other texture classes. Symbols from both sandy substrates S and LS scattered in the direction orthogonal to their trajectory. Damping coefficients from the four NOISE realizations scattered slightly within each texture class (Fig. 3.10). The damping profiles were highly corre-

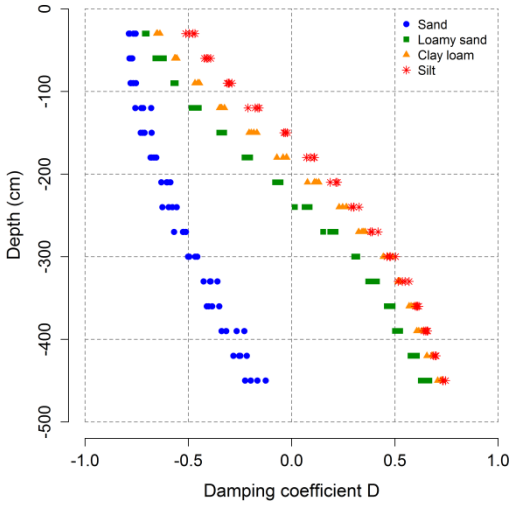

Figure 3.10. Depth profiles of signal damping for the different texture classes of the NOISE data set.

lated (r^2 > 0.975) with those obtained from the HOM data within each texture group. A Wilcoxon signed-rank test (cf. Hollander et al., 2014) showed that the median values of *D* differed in only two out of 16 cases significantly from the HOM case (significance level: 0.05).

Loadings on the first two components of the HET data set plotted close to the unit circle (Fig. 3.11). They also plotted close to a common trajectory, very similar to the HOM case. However, the distances between adjacent symbols within the texture classes of single profiles were more irregular than in the HOM case. This resulted in less clear damping profiles for single texture classes. Correlations of single damping profiles with the HOM reference profiles were r^2 > 92.4 for S and r^2 > 99.2 for the other texture classes. The absolute values of *D* differed in 12 out of 16 cases significantly from those of the HOM reference profiles (Wilcoxon signed-rank test, significance level: 0.05). Especially in the sand substrate *D* scattered substantially with increasing variability at greater depths (Fig. 3.12). The extent of signal damping was not increasing monotonically with soil depth in the heterogeneous flow field. The two time series marked with “a” in Fig. 3.12 exhibited the same degree of damping, although they correspond to different depths of 300 cm and 420 cm, respectively. Conversely, the time series marked with “b” were simulated at the same depth of 360 cm but exhibited different damping degrees of *D* = -0.42 and *D* = 0.04, respectively.

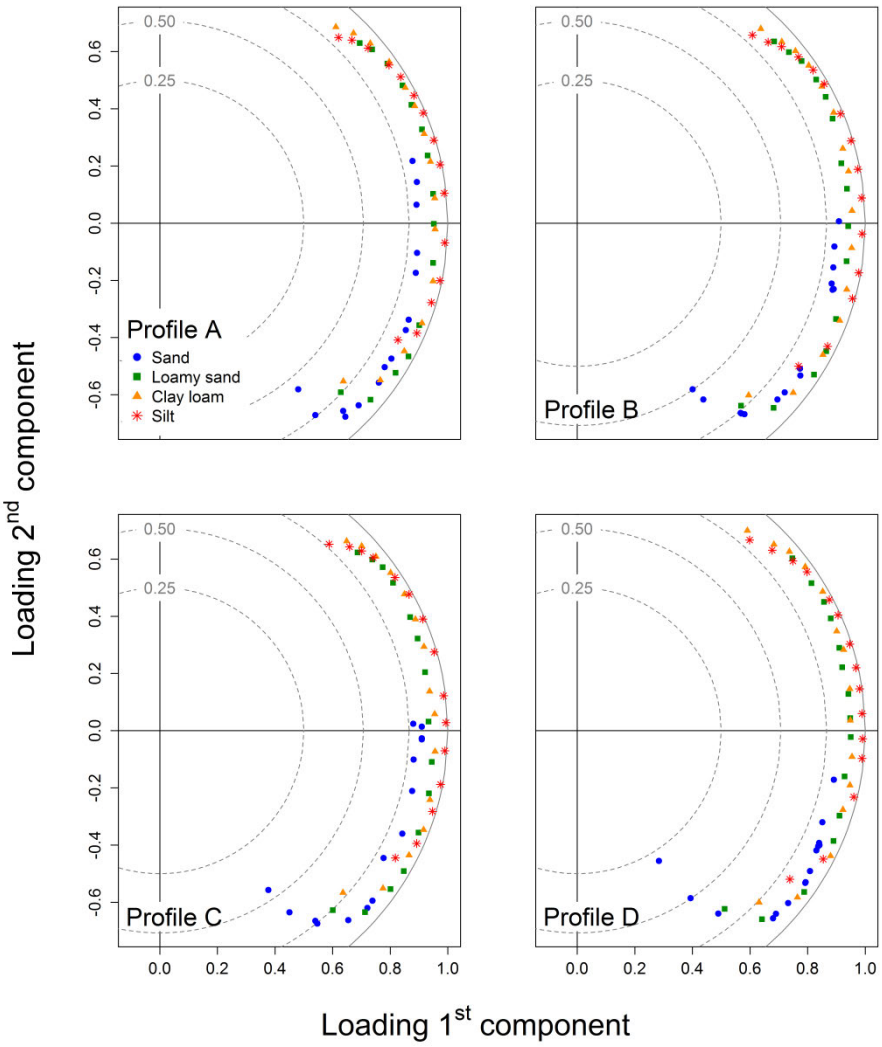

Figure 3.11. Loadings on the first two principal components for all HET time series. Each panel corresponds to one profile. Symbols represent single moisture time series. Gray circles denote the fraction of variance σ^2_{expl} explained by both components.

3.4. Discussion

3.4.1. Analyzing simulated soil moisture time series by PCA

We introduced and tested a method to evaluate hydrological signal transformation in a soil profile by means of simulated data. This had the advantages that (i) the investigated scenarios could be defined to be very simple, (ii) purely gravity driven water flux could be considered without unknown influences like evaporation or root water uptake, (iii) all properties of gener-

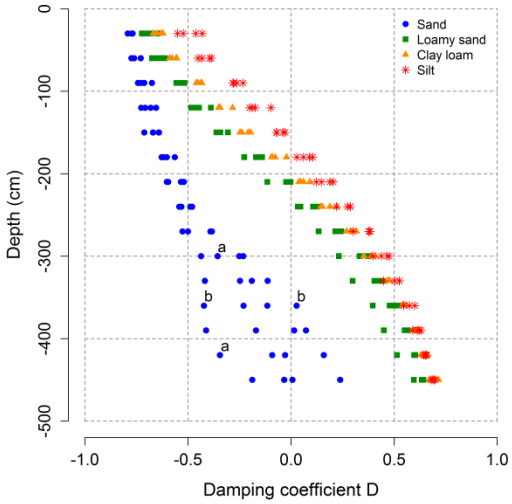

Figure 3.12. Depth profiles of signal damping for the different texture classes of the HET data set.

ated textural heterogeneity and generated random noise were known, and (iv) the precipitation was identical for all data sets. However, these advantages are accompanied by the question about transferability of results from a “simulated world” to the “real world”. The models we used to generate time series are based on various assumptions such as rigid pore systems or unimodal pore distributions. Several processes like macropore flow or hysteresis were ignored. However, these constraints correspond to those of most soil hydrological models for deep seepage flux below the rooting zone. In this study it was not the intention to simulate specific scenarios observed in field, but rather to set up a data set with certain spatial heterogeneity. Nevertheless it remains indispensable to test the method with soil moisture time series measured under filed conditions like inclined soil surfaces or spatially heterogeneous precipitation inputs. For more detailed discussions about advantages and limitations of numerical experiments in the fields of hydrology and soil physics we refer to Schlüter et al. (2012b) and Weiler and McDonnell (2004).

We characterized the soil system behavior by analyzing soil moisture time series and interpreting the results in terms of soil water fluxes. In a numerical study it would also be possible to analyze flux dynamics directly. We decided for the indirect way because soil moisture is likely the most predominant variable in existing soil water monitoring programs and it can be expected that researchers will have better access to such data resources in future (Vereecken et al., 2008). The approach presented in this paper can be directly applied to such monitoring data sets in order to identify first order controls.

The phenomenon of macropore flow was not considered in this study. In contrast to matrix flow many different approaches exist to model macropore flow in structured soils (Köhne et al., 2009). A PCA would probably detect functional differences between time series simulated by different macropore flow models. This would further complicate disentangling between all emerging effects and would require much more comprehensive efforts. On the other hand, our results suggest that macropore flow would merely reduce the damping intensity per depth unit in a soil profile rather than generating a completely different kind of transformation of the input signal. This should be further investigated in a separate study.

3.4.2. Signal transformation in homogeneous soils with different textures

Two independent functional patterns detected by a PCA sufficed to explain σ^2_{expl} = 86.7 % of the total variance of the HOM data set comprising soils of quite different textures. Most of the soil moisture dynamics at any depth and any texture could be reconstructed by simply combining two principal components. Both patterns did not occur in random combination spread over the profile. Their ratios were strictly ordered by soil depth as it could be described by one single trajectory in the vector space of the loadings. Hydrological signals can only be transformed to a more damped status with reduced variance while they are processed through the system. Consequently, the modeled soil systems possess only one degree of freedom to transform hydrological input signals. The only difference between textures was the damping intensity per depth unit indicated by the slopes of the damping profiles in Fig. 3.8b. As a consequence the moisture series in 120 cm (Si), 150 cm (CL), 180 cm (LS), and 450 cm (S) were equally damped although they were simulated at different depths.

All of the remaining components together accounted for another 13.3 % of the HOM variance. As stated above, non-linearities of the signal transformation might be hidden in some of the remaining components. Non-linear patterns could be detected by single components when a non-linear ordination method like Isometric Feature Mapping (Tenenbaum et al., 2000) is used, but this was beyond the scope of this study. On the other hand, a Kruskal-Wallis test (cf. Hollander et al., 2014) showed that there were several of the remaining components where the loadings from at least one texture group differed significantly from the others. In total these components accounted for 3.4 % (significance level: 0.05) or 0.9 % (significance level: 0.01) of HOM variance, respectively. That numbers represent an upper limit of the variance that could be ascribed to substrate-specific kind of transformation of the input signal.

Hauhs and Lange (1996) concluded from thermodynamic considerations that the information content of input fluxes is lowered during the passage through ecosystems. They further stated that ecosystems act as filters smoothing input data, increasing with depth. Our results showed that the vadose zone can also be seen as a low-pass filter for soil moisture signals where the characteristics of filtering are almost identical but the intensity of filtering strongly depends on soil texture.

Both alternative damping measures autocorrelation ρ_{ac} and low-pass damping β assessed by power spectrum analysis yielded strong non-linear depth profiles. Hence, both measures are very sensitive in shallow sections of a soil, but fail in describing signal transformation in larger depths. The cross-correlation ρ_{cc} measuring time lags is linearly scaled over the whole range of soil depth. However, ρ_{cc} represents a non-monotonous measure due to irregular steps in the depth profile. In contrast to all three presented alternative measures the PCA makes full use of the shape of the time series, including both time lags as well as smoothing effects. Resulting depth profiles of D are adequate to describe signal transformation in soils, because D increases almost linearly and monotonously with soil depth.

Soils with homogeneous textures occur very rarely in nature. Usually soil profiles exhibit horizontal layers. If layered profiles are assumed to be comprised of several homogeneous layers with different textures, it can be expected on the basis of our results that no new independent functional patterns of soil moisture would emerge. Hence, all time series occurring in a layered profile could also be described by the same trajectory. However, the damping profiles would exhibit abrupt changes in slopes at the layer boundaries.

Pressure head conditions typical for sites with large distance to groundwater (free drainage lower boundary condition) were considered in this study. However, sites with shallow depths of groundwater tables also occur frequently in nature. In such cases water content profiles are imposed to reach saturation above the groundwater table. It can be supposed that different signal transformation intensities between the four textural classes would also be observed under very wet or even saturated conditions, because hydraulic conductivities do also vary between soil textures under wet conditions. However, this should explicitly be analyzed in a separate study.

3.4.3. Effects of random noise and textural heterogeneity

In the NOISE and HET data sets time series were manipulated in different ways. The NOISE data were blurred by adding independent random noise producing larger variance among the moisture series. This consequently yielded more functional heterogeneity. But it is worth noting that the first two components and the resulting damping profiles were nearly identical to the HOM case, although the fraction of explained variance was much smaller. This showed that *D* is a very robust measure of the signal damping status.

In contrast, for the HET data spatial variance in texture distribution was generated firstly and then considered in each simulation run. Hence, the HET data set contained information about the system response to textural heterogeneity. The explained variance σ_{expl}^2 was similar to the HOM case and input signals were also transformed in only one direction along a common trajectory. This means that random patterns in soil texture did not yield random patterns in soil moisture dynamics. In other words, textural heterogeneity did not cause functional heterogeneity, because no additional functional patterns occurred in the HET time series. This is consistent with Basu et al. (2010) who stated for the catchment scale that structural heterogeneity does not necessarily translate to functional heterogeneity. In contrast to the HOM case the damping status of time series did not change monotonically with depth. The distances between adjacent symbols on the trajectory were less regular yielding less distinct damping profiles (Fig. 3.12). Obviously, water fluxes occur along various pathways with different signal damping intensities. The damping status of a time series at any position of the profile results from the superposition of effects along the respective flow paths. This implies that the damping status at any position could be used to assess characteristics of the flow field above. Consequently, a heterogeneous flow field can be analyzed by means of time series measured at different positions. In the best case, the spatial distribution of soil texture could be predicted on the basis of such functional analyses.

Roth (1995) showed by means of numerical simulations that low-flux regions can become high-flux regions and vice versa when a threshold of effective saturation is exceeded. This effect was not considered in this study because a PCA represents a global measure of signal transformation behavior that does not distinguish between different states of a soil system. It is worth analyzing if time series simulated at identical positions in a heterogeneous soil but under different degrees of saturation would be located at identical positions on the trajectory. However, this was beyond the scope of this study.

3.4.4. Potential fields of application

The vadose zone plays a preeminent role for transformation of the input signal given by precipitation or snowmelt. It is usually the first link in a sequence of hydrological subsystems like aquifers, the riparian zone or streams where hydrological signals are propagated and transformed. In addition, signal transformation in the vadose zone is far more intensive than in saturated substrates due to the large water displacement space in the unsaturated pore system. It is likely that the vadose zone determines signal propagation through the whole hydrological system (Lischeid et al., 2010). Thus, investigating the signal transformation behavior of the vadose zone is of outermost importance for various application fields like groundwater balance calculation or even flood forecasting. The presented approach allows analyzing and quantifying this function of the vadose zone within the hydrological cycle. It is worth investigating if similar patterns can be found in observed data where additional influences like evaporation, root water uptake or capillary rise occur. This could be done by means of moisture time series measured in different soils that are exposed to identical atmospheric conditions like it was done in the TERENO-SOILCan project (Zacharias et al., 2011). Some fields of application are outlined in the following.

First, the presented approach can be used performing data plausibility tests, gap filling and identification of potential outliers. It is a powerful and robust tool to distinguish valuable information from uncorrelated background noise as it was shown for the NOISE case. Systematic and correlated errors might be summarized by single components that can then be eliminated from the data set easily.

Second, the approach might be used to assess the mean damping per depth in heterogeneous soils. This “functional averaging” might then be used to define a corresponding homogeneous substrate that could easily be used to simulate mean damping per depth at a larger scale rather than aiming at mimicking the observed heterogeneity to a full extent. Thus an effective 1D model representation of heterogeneous flow fields could be achieved. Parameters of such a 1D model could be fitted to the mean damping behavior rather than trying to mimic any single observed time series. We feel that this is a very promising approach for upscaling from small-scale observations. This approach would circumvent the problems known to be ascribed to the wide-spread approach to average properties of the soils prior to inputting them into a model (e.g. Ahuja et al., 2010; Vereecken et al., 2007; Zhu and Mohanty, 2002). The resulting functional averaged time series could then be used both for model calibration and model testing.

Third, the approach can easily be extended to identify additional causes of heterogeneity in observed data. In contrast to process based modeling approaches the PCA does not require any prior assumptions about underlying processes. Instead, processes identified by PCA help to constrain the structure of process based models right from the beginning of the modeling process. In fact, that approach has been successful in analyzing groundwater head data (Böttcher et al., 2014; Lewandowski et al., 2009) as well as discharge data (Thomas et al., 2012).

3.5. Conclusions

This study presents and tests an approach to determine the kind and degree of transformation of a hydrological input signal in soils. Soil moisture time series simulated at different depths and for different soil textures were analyzed in a quantitative way. The results provide strong evidence that different soils differ only with respect to the degree of damping per depth interval rather than with respect to the kind of transformation of the input signal. Consequently, for any heterogeneous soil a corresponding homogeneous soil can be defined that yields exactly the same mean behavior for a given depth. Thus observed data from heterogeneous soils can be used for performing a "functional averaging". Functional averaged time series can be used for calibration and testing large scale models with regard to upscaling from small scale observations.

This study was restricted to simulated data that presumably reflect only part of the variance inherent in observed data. In a next step it will be applied to observed data. However, our results give at least strong evidence that the models based on the Richards equation exhibit only very limited degrees of freedom with respect to the kind of transformation of hydrological signals in soils. Thus, for this type of models at least there is no need to account for different soil textures as long as only mean behavior at a certain depth is of interest.

In contrast to other approaches, the PCA makes full use of the information provided by observed time series. Thus it seems to be a very powerful approach for efficient extraction of information from observed data, and to describe hydrological behavior in heterogeneous systems in a quantitative way. We feel that this approach could yield much information supplementing the usual modeling approaches.

Acknowledgements

This study was funded by the *German Research Foundation DFG* (project Li 802/3-1). We thank Anne-Kathrin Schneider, Dr. Björn Thomas, Steven Böttcher and Christian Lehr for proofreading and helpful discussions. We also thank three anonymous reviewers for their valuable comments and suggestions.

References

Abdou, H.M., Flury, M., 2004. Simulation of water flow and solute transport in free-drainage lysimeters and field soils with heterogeneous structures. Eur J Soil Sci, 55(2): 229-241.

Ahuja, L.R., Ma, L., Green, T.R., 2010. Effective soil properties of heterogeneous areas for modeling infiltration and redistribution. Soil Sci Soc Am J, 74(5): 1469-1482.

Ajami, H., McCabe, M.F., Evans, J.P., Stisen, S., 2014. Assessing the impact of model spin-up on surface water-groundwater interactions using an integrated hydrologic model. Water Resour Res, 50(3): 2636-2656.

Basu, N.B., Rao, P.S.C., Winzeler, H.E., Kumar, S., Owens, P., Merwade, V., 2010. Parsimonious modeling of hydrologic responses in engineered watersheds: Structural heterogeneity versus functional homogeneity. Water Resour Res, 46, W04501.

Bayer, A., Vogel, H.J., Ippisch, O., Roth, K., 2005. Do effective properties for unsaturated weakly layered porous media exist? An experimental study. Hydrol Earth Syst Sc, 9(5): 517-522.

Böttcher, S., Merz, C., Lischeid, G., Dannowski, R., 2014. Using Isomap to differentiate between anthropogenic and natural effects on groundwater dynamics in a complex geological setting. J Hydrol, 519: 1634-1641.

Busch, S., Weihermuller, L., Huisman, J.A., Steelman, C.M., Endres, A.L., Vereecken, H., van der Kruk, J., 2013. Coupled hydrogeophysical inversion of time-lapse surface GPR data to estimate hydraulic properties of a layered subsurface. Water Resour Res, 49(12): 8480-8494.

Celia, M.A., Bouloutas, E.T., Zarba, R.L., 1990. A general mass-Conservative numerical-solution for the unsaturated flow equation. Water Resour Res, 26(7): 1483-1496.

De Lannoy, G.J.M., Houser, P.R., Verhoest, N.E.C., Pauwels, V.R.N., Gish, T.J., 2007. Upscaling of point soil moisture measurements to field averages at the OPE3 test site. J Hydrol, 343(1-2): 1-11.

Diamantopoulos, E., Durner, W., Reszkowska, A., Bachmann, J., 2013. Effect of soil water repellency on soil hydraulic properties estimated under dynamic conditions. J Hydrol, 486: 175-186.

Durner, W., Diamantopoulos, E., Iden, S.C., Scharnagl, B., 2014. Hydraulic Properties and Non-equilibrium Water Flow in Soils. In: Teixeira, W.G., Ceddia, M.B., Donnagema, G.K., Ottoni, M.V. (Eds.), Application of Soil Physics in Environmental Analyses. Springer International Publishing.

Durner, W., Jansen, U., Iden, S.C., 2008. Effective hydraulic properties of layered soils at the lysimeter scale determined by inverse modelling. Eur J Soil Sci, 59(1): 114-124.

Gall, H.E., Park, J., Harman, C.J., Jawitz, J.W., Rao, P.S.C., 2013. Landscape filtering of hydrologic and biogeochemical responses in managed catchments. Landscape Ecol, 28(4): 651-664.

Grayson, R.B., Blöschl, G., Western, A.W., McMahon, T.A., 2002. Advances in the use of observed spatial patterns of catchment hydrological response. Adv Water Resour, 25(8-12): 1313-1334.

Greco, R., Comegna, L., Damiano, E., Guida, A., Olivares, L., Picarelli, L., 2013. Hydrological modelling of a slope covered with shallow pyroclastic deposits from field monitoring data. Hydrol Earth Syst Sc, 17(10): 4001-4013.

Haarder, E.B., Looms, M.C., Jensen, K.H., Nielsen, L., 2011. Visualizing unsaturated flow phenomena using high-resolution reflection ground penetrating radar. Vadose Zone J, 10(1): 84-97.

Hauhs, M., Lange, H., 1996. Ecosystem dynamics viewed from an endoperspective. Sci Total Environ, 183(1-2): 125-136.

Heilig, A., Steenhuis, T.S., Walter, M.T., Herbert, S.J., 2003. Funneled flow mechanisms in layered soil: field investigations. J Hydrol, 279(1-4): 210-223.

Hendrickx, J.M.H., Dekker, L.W., Boersma, O.H., 1993. Unstable wetting fronts in water-repellent field soils. J Environ Qual, 22(1): 109-118.

Hinnell, A.C., Ferre, T.P.A., Vrugt, J.A., Huisman, J.A., Moysey, S., Rings, J., Kowalsky, M.B., 2010. Improved extraction of hydrologic information from geophysical data through coupled hydrogeophysical inversion. Water Resour Res, 46: W00D40.

Hohenbrink, T.L., Lischeid, G., 2014. Texture-depending performance of an in situ method assessing deep seepage. J Hydrol, 511: 61-71.

Hollander, M., Wolfe, D.A., Chicken, E., 2014. Nonparametric statistical methods. Wiley series in probability and statistics. John Wiley & Sons, Inc., Hoboken, New Jersey.

Jarvis, N.J., 2007. A review of non-equilibrium water flow and solute transport in soil macropores: principles, controlling factors and consequences for water quality. Eur J Soil Sci, 58(3): 523-546.

Jolliffe, I.T., 2002. Principal Component Analysis. Springer Series in Statistics. Springer, New York, 489 pp.

Katul, G.G., Porporato, A., Daly, E., Oishi, A. C., Kim, H.S., Stoy, P.C., Juang, J.Y., Siqueira, M. B., 2007. On the spectrum of soil moisture from hourly to interannual scales. Water Resour Res, 43: W05428.

Kirchner, J.W., Tetzlaff, D., Soulsby, C., 2010. Comparing chloride and water isotopes as hydrological tracers in two Scottish catchments. Hydrol Process, 24(12): 1631-1645.

Köhne, J.M., Köhne, S., Simunek, J., 2009. A review of model applications for structured soils: a) Water flow and tracer transport. J Contam Hydrol, 104(1-4): 4-35.

Koszinski, S., Gerke, H.H., Hierold, W., Sommer, M., 2013. Geophysical-based modeling of a kettle hole catchment of the morainic soil landscape. Vadose Zone J, 12(4).

Kowalsky, M.B., Finsterle, S., Rubin, Y., 2004. Estimating flow parameter distributions using ground-penetrating radar and hydrological measurements during transient flow in the vadose zone. Adv Water Resour, 27(6): 583-599.

Kung, K.J.S., 1990a. Preferential flow in a sandy vadose zone .1. Field observation. Geoderma, 46(1-3): 51-58.

Kung, K.J.S., 1990b. Preferential flow in a sandy vadose zone: 2. Mechanism and implications. Geoderma, 46(1-3): 59-71.

Kung, K.J.S., 1993. Laboratory observation of funnel flow mechanism and its influence on solute transport. J Environ Qual, 22(1): 91-102.

Lee, J.A., Verleysen, M., 2007. Nonlinear dimensionality reduction. Information Science and Statistics. Springer, New York, 308 pp.

Lewandowski, J., Lischeid, G., Nutzmann, G., 2009. Drivers of water level fluctuations and hydrological exchange between groundwater and surface water at the lowland River Spree (Germany): field study and statistical analyses. Hydrol Process, 23(15): 2117-2128.

Lin, H. et al., 2006. Hydropedology: Synergistic integration of pedology and hydrology. Water Resour Res, 42: W05301.

Lischeid, G., Natkhin, M., Steidl, J., Dietrich, O., Dannowski, R., Merz, C., 2010. Assessing coupling between lakes and layered aquifers in a complex Pleistocene landscape based on water level dynamics. Adv Water Resour, 33(11): 1331-1339.

Lischeid, G., Steidl, J., Merz, C., 2012. Functional versus trend analysis to assess anthropogenic impacts on groundwater heads. Grundwasser, 17(2): 79-89.

Mahmood, R., Littell, A., Hubbard, K.G., You, J.S., 2012. Observed data-based assessment of relationships among soil moisture at various depths, precipitation, and temperature. Appl Geogr, 34: 255-264.

McCord, J.T., 1991. Application of 2nd-type boundaries in unsaturated flow modeling. Water Resour Res, 27(12): 3257-3260.

Miller, E.E., Miller, R.D., 1956. Physical theory for capillary flow phenomena. J Appl Phys, 27(4): 324-332.

Mualem, Y., 1976. New model for predicting hydraulic conductivity of unsaturated porous-media. Water Resour Res, 12(3): 513-522.

Oudin, L., Andreassian, V., Perrin, C., Anctil, F., 2004. Locating the sources of low-pass behavior within rainfall-runoff models. Water Resour Res, 40(11), W11101.

Pan, F., Pachepsky, Y.A., Guber, A.K., Hill, R.L., 2011. Information and complexity measures applied to observed and simulated soil moisture time series. Hydrolog Sci J, 56(6): 1027-1039.

Paulo, J., Ribeiro, J., Diggle, P.J., 2001. geoR: a package for geostatistical analysis. R-News, 1(2): 14-18. (Version 1.7-4., http://www.leg.ufpr.br/geoR/).

Peters, A., Durner, W., 2009. Large zero-tension plate lysimeters for soil water and solute collection in undisturbed soils. Hydrol Earth Syst Sc, 13(9): 1671-1683.

R Development Core Team, 2010. R: A Language and Environment for Statistical Computing. R Foundation for Statistical Computing, Vienna, Austria. (Version 3.1.0, http://www.R-project.org).

Ritsema, C.J., Dekker, L.W., 2000. Preferential flow in water repellent sandy soils: principles and modeling implications. J Hydrol, 231: 308-319.

Romano, N., 2014. Soil moisture at local scale: Measurements and simulations. J Hydrol, 516: 6-20.

Roth, K., 1995. Steady-state flow in an unsaturated, 2-Dimensional, macro-scopically homogeneous, miller-similar medium. Water Resour Res, 31(9): 2127-2140.

Schaap, M.G., Leij, F.J., van Genuchten, M.T., 2001. ROSETTA: a computer program for estimating soil hydraulic parameters with hierarchical pedotransfer functions. J Hydrol, 251(3-4): 163-176.

Schelle, H., Durner, W., Schlüter, S., Vogel, H.J., Vanderborght, J., 2013. Virtual soils: moisture measurements and their interpretation by inverse modeling. Vadose Zone J, 12(3).

Schlüter, S., Vanderborght, J., Vogel, H.J., 2012a. Hydraulic non-equilibrium during infiltration induced by structural connectivity. Adv Water Resour, 44: 101-112.

Schlüter, S., Vogel, H.J., 2011. On the reconstruction of structural and functional properties in random heterogeneous media. Adv Water Resour, 34(2): 314-325.

Schlüter, S., Vogel, H. J., Ippisch, O., Bastian, P., Roth, K., Schelle, H., Durner, W., Kasteel, R., Vanderborght, J., 2012b. Virtual soils: Assessment of the effects of soil structure on the hydraulic behavior of cultivated soils. Vadose Zone J, 11(4).

Schröder, B., 2006. Pattern, process, and function in landscape ecology and catchment hydrology - how can quantitative landscape ecology support predictions in ungauged basins? Hydrol Earth Syst Sc, 10(6): 967-979.

Schulz, K., Seppelt, R., Zehe, E., Vogel, H.J., Attinger, S., 2006. Importance of spatial structures in advancing hydrological sciences. Water Resour Res, 42(3).

Shumway, R.H., Stoffer, D.S., 2011. Time Series Analysis and Its Applications. Springer Texts in Statistics. Springer, New York, 376 pp.

Simunek, J., Sejna, M., Saito, H., Sakai, M., Van Genuchten, M.T., 2008. The Hydrus-1D Software Package for Simulating the Movement of Water, Heat, and Multiple Solutes in Variably Saturated Media. Department of Environmental Sciences, University of California Riverside, Riverside. (Version 4.16.0080, http://www.pc-progress.com/en/Default.aspx?hydrus-1d).

Simunek, J., van Genuchten, M.T., Sejna, M., 2011. The HYDRUS software package for simulating two- and three-dimensional movement of water, heat, and multiple solutes in variably-saturated media. Technical Manual. PC Progress, Prague, Czech Republic. (Version 2.04.0440,
http://www.pc-progress.com/en/Default.aspx?hydrus-3d).

Tenenbaum, J.B., de Silva, V., Langford, J.C., 2000. A global geometric framework for nonlinear dimensionality reduction. Science, 290: 2319-2323.

Thomas, B., Lischeid, G., Steidl, J., Dannowski, R., 2012. Regional catchment classification with respect to low flow risk in a Pleistocene landscape. J Hydrol, 475: 392-402.

van Genuchten, M.T., 1980. A closed-form equation for predicting the hydraulic conductivity of unsaturated soils. Soil Sci Soc Am J, 44(5): 892-898.

van Genuchten, M.T., Naveira-Cotta, C., Skaggs, T.H., Raoof, A., Pontedeiro, E.M., 2014. The Use of Numerical Flow and Transport Models in Environmental Analyses. In: Teixeira, W.G., Ceddia, M.B., Donnagema, G.K., Ottoni, M.V. (Eds.), Application of Soil Physics in Environmental Analyses. Springer International Publishing.

van Schaik, N.L.M.B., 2009. Spatial variability of infiltration patterns related to site characteristics in a semi-arid watershed. Catena, 78(1): 36-47.

Vereecken, H., Huisman, J.A., Bogena, H., Vanderborght, J., Vrugt, J.A., Hopmans, J. W., 2008. On the value of soil moisture measurements in vadose zone hydrology: A review. Water Resour Res, 44: W00D06.

Vereecken, H., Kasteel, R., Vanderborght, J., Harter, T., 2007. Upscaling hydraulic properties and soil water flow processes in heterogeneous soils: A review. Vadose Zone J, 6(1): 1-28.

Vogel, H.J., Cousin, I., Ippisch, O., Bastian, P., 2006. The dominant role of structure for solute transport in soil: experimental evidence and modelling of structure and transport in a field experiment. Hydrol Earth Syst Sc, 10(4): 495-506.

Vogel, H.J., Weller, U., Ippisch, O., 2010. Non-equilibrium in soil hydraulic modelling. J Hydrol, 393(1-2): 20-28.

Vogel, T., Cislerova, M., Hopmans, J.W., 1991. Porous-media with linearly variable hydraulic-properties. Water Resour Res, 27(10): 2735-2741.

Walter, M.T. et al., 2000. Funneled flow mechanisms in a sloping layered soil: Laboratory investigation. Water Resour Res, 36(4): 841-849.

Weiler, M., McDonnell, J., 2004. Virtual experiments: a new approach for improving process conceptualization in hillslope hydrology. J Hydrol, 285(1-4): 3-18.

Wu, L., Jury, W.A., Chang, A.C., Allmaras, R.R., 1997. Time series analysis of field-measured water content of a sandy soil. Soil Sci Soc Am J, 61(3): 736-742.

Wu, W.R., Geller, M.A., Dickinson, R.E., 2002. The response of soil moisture to long-term variability of precipitation. J Hydrometeorol, 3(5): 604-613.

Zacharias, S. Bogena, H., Samaniego, L., Mauder, M., Fuss, R., Putz, T., Frenzel, M., Schwank, M., Baessler, C., Butterbach-Bahl, K., Bens, O., Borg, E., Brauer, A., Dietrich, P., Hajnsek, I., Helle, G., Kiese, R., Kunstmann, H., Klotz, S., Munch, J.C., Papen, H., Priesack, E., Schmid, H.P., Steinbrecher, R., Rosenbaum, U., Teutsch, G., Vereecken, H., 2011. A network of terrestrial environmental observatories in Germany. Vadose Zone J, 10(3): 955-973.

Zhu, J.T., Mohanty, B.P., 2002. spatial averaging of van Genuchten hydraulic parameters for pteady-ptate flow in heterogeneous soils: a numerical study. Vadose Zone J, 1(2): 261-272.

4. Disentangling the effects of land management and soil heterogeneity on soil moisture dynamics[3]

Summary

Soil moisture is the essential control of water and energy dynamics at arable sites. Time series of soil moisture reflect the interplay of various processes, each of which influences the overall soil moisture dynamics. In this study we tested an approach to break down observed soil moisture behavior into the respective contributions of individual processes. We applied a principal component analysis to soil moisture time series from a field experiment comprising two crop rotation systems and two different soil tillage practices. We concentrated on 57 soil moisture time series measured over nearly four years at 12 plots and five soil depths, down to 1.5 m. About 77.9 % of the variance was reflected by the first component being almost identical to a time series of averaged soil moisture. It described the effect of the meteorological boundary conditions. The second component described the effect of the input signal damping increasing with soil depth and accounted for 7.8 % of total variance. The signal transformation over depth proved to be more or less uniform throughout the test site, despite considerable soil heterogeneity. Another 3.6 % of the total variance (third component) was unambiguously explained by the different cropping systems. On the contrary, different soil tillage practices had no significant effect. The suggested approach opens up many possibilities to analyze and better understand complex soil system behavior. The data-based approach of time series analysis provides model-independent, quantitative information about the key factors and processes controlling soil-water dynamics. Hence, it is especially valuable for model building, calibration and evaluation.

Keywords: Soil moisture time series, Crop rotation systems, Soil tillage, Transformation of hydrological signals, Hydropedology

[3] An article with equivalent content has been published as:

Hohenbrink, T.L., Lischeid, G., Schindler, U., Hufnagel, J., 2016. Disentangling the Effects of Land Management and Soil Heterogeneity on Soil Moisture Dynamics. Vadose Zone Journal, 15(1). DOI: 10.2136/vzj2015.07.0107.

4.1. Introduction

Soil moisture θ [L^3 L^{-3}] is probably the most important measurable status variable to evaluate the water and energy budgets of arable sites (Vereecken et al., 2008). However, soil moisture usually exhibits considerable spatial heterogeneity (Corradini, 2014; Vereecken et al., 2014), making all means of data evaluation more complicated. This heterogeneity can be caused by natural effects, e.g. the spatial variability of soil texture (e.g. Hohenbrink and Lischeid, 2014; Jawson and Niemann, 2007; Schlüter et al., 2012) as well as by different land use practices, such as soil tillage techniques (e.g. Perfect and Caron, 2002; Schwen et al., 2011). The impacts of land use practices on soil moisture dynamics must be quantified in order to evaluate the efficacy of specific management decisions. Interactions between different land management effects are usually investigated using simulation models (an overview of which is provided by Boote et al., 2013). However, this always requires *a priori* knowledge or assumptions about the governing processes. Therefore, model-independent diagnostic tools to disentangle the different sources of soil moisture heterogeneity are urgently needed to analyze existing monitoring data sets. Such tools could even be used to reduce uncertainty in numerical models.

There are several approaches to determine the patterns hidden in moisture data sets (for an overview see Vereecken et al., 2014), each emphasizing different features of soil moisture patterns. Classical geostatistical methods are used to characterize the spatial distribution of soil moisture. The spatial covariance of soil moisture from different locations is usually expressed as a function of distance illustrated by variograms (e.g. Baroni et al., 2013; Joshi and Mohanty, 2010; Korres et al., 2015). More recently, more sophisticated methods such as wavelet analysis (e.g. Biswas, 2014; Peng et al., 2013; Rivera et al., 2014), self-organizing maps (e.g. Zou et al., 2012) or fractal analysis (Korres et al., 2015) were used to investigate the spatial distribution of soil moisture. Temporal stability analyses of soil moisture patterns (Vachaud et al., 1985) are designed to identify locations with soil moisture dynamics representative of the whole observation site. This approach is based on the observation that the ranks of soil moisture values from different locations remain almost constant over time (see the overview by Vanderlinden et al., 2012). Standard methods of time series analysis, such as autocorrelation and cross-correlation analyses, have been used to compare soil moisture dynamics from various depths (De Lannoy et al., 2006; Hohenbrink and Lischeid, 2015; Mahmood and Hubbard, 2007) and relate them to other variables such as precipitation and temperature (Mahmood et al., 2012). Low-pass filtering behavior, i.e. changing periodicity of soil moisture oscillations,

was investigated for vadose zones (Hohenbrink and Lischeid, 2015; Katul et al., 2007) and entire catchments (Gall et al., 2013). Slopes of the power-spectra were used to characterize and compare the periodicity distributions of time series from different locations. Principal component analysis (PCA), also known as empirical orthogonal functions analysis (cf. Vereecken et al., 2014), was frequently used to decompose the variance in soil moisture data sets from arable fields into uncorrelated patterns and relate them to specific explanatory variables (e.g. Baroni et al., 2013; Korres et al., 2010; Qiu et al., 2014).

Applying the presented methods to monitoring data sets from various investigation sites revealed that soil moisture patterns can be controlled by topography (e.g. Qiu et al., 2014; Yoo and Kim, 2004), soil textural properties (e.g. Baroni et al., 2013; Jawson and Niemann, 2007; Yoo and Kim, 2004), soil organic carbon content (Korres et al., 2010), vegetation (e.g. Baroni et al., 2013; Korres et al., 2015), land management (e.g. Korres et al., 2010; Korres et al., 2015) and meteorological conditions (e.g. Joshi and Mohanty, 2010; Qiu et al., 2014). However, most researchers only investigated spatiotemporal moisture patterns from a shallow soil depth on a few selected dates. Hupet and Vanclooster (2002) stressed the importance of using measurements from the entire hydrologically active zone to investigate soil moisture spatial variability. However, few studies analyze long-term soil moisture dynamics in vertical profiles deeper than one meter (De Lannoy et al., 2006; Hu and Si, 2014). Hohenbrink and Lischeid (2015) proposed to apply a PCA on soil moisture time series from different locations in vertical soil profiles. They investigated the effects of textural heterogeneity on the transformation of hydrological signals (e.g. rainfall, snow melt) propagating through the vadose zone. Furthermore, they stated that the approach has great potential to distinguish independent effects contributing to hydrological behavior observed in soil systems. Their approach was introduced with the example of simulated time series resulting from a numerical experiment. However, the transferability of their results from a “simulated world” to the “real world” still has to be proven based on soil moisture time series measured under field conditions. In fact, that approach has already been successfully applied to groundwater head time series (Böttcher et al., 2014; Lehr et al., 2015; Lischeid et al., 2010; Page et al., 2012).

Our objectives were to identify and describe the specific effects of soil heterogeneity and land management practices on soil moisture dynamics. To achieve this, we decomposed the total variance of measured soil moisture time series by PCA as suggested by Hohenbrink and Lischeid (2015). An adequate monitoring data set of soil moisture time series was required to

apply the approach. We used a monitoring data set from a multifactorial field experiment in Northeast Germany as it had the following features: (i) intensive instrumentation, (ii) large number of replicates, (iii) different well documented soil treatments, (iv) spatially homogeneous precipitation inputs due to the small size of the test site and (v) large soil heterogeneity spatially uncorrelated with the experimental set-up. In this paper the term “hydrological signal” designates spatiotemporal changes in the soil moisture which are propagated through the vadose zone (cf. Hohenbrink and Lischeid, 2015). We use the term “functional heterogeneity” to express the variability among measured time series (cf. Basu et al., 2010; Hohenbrink and Lischeid, 2015) bearing information about the hydrological system behavior of the soils investigated.

4.2. Methods

4.2.1. Field experiment

The experimental test site (52° 31′ 01′′ N, 14° 07′ 27′′ E, 62 m a.s.l.) was situated in the lowlands of Northeastern Germany close to the city of Müncheberg. It is located in the transition area between a maritime climate and a continental climate. Between 1981/01/01 and 2012/01/01, the annual sums of precipitation and potential evaporation were 529 mm and 659 mm and the mean annual temperature was 9.1°C (DWD, 2014). The experimental site is covered by a layer of sediment from the Late Pleistocene, with a flat surface. Sand layers alternate at short distances with glacial till containing clay and marl, resulting in large textural heterogeneity. More information about the depth distribution of soil texture at the experimental site can be found in a data set published by Mirschel et al. (2010). The predominant FAO soil type at the test site is Orthic Luvisol.

Twelve experimental plots with an area of 788 m^2 each were arranged on an experimental field (Fig. 4.1). Six plots were managed using a cultivation system designed to stabilize the organic carbon content of the soil. This featured a four-year crop rotation system of winter rye (*Secale cereale*), forage sorghum (*Sorghum bicolor*), winter triticale (*xTriticale*), a mixture of alfalfa, clover and grass (*Medicago sativa*, *Trifolium pretense* and *Lolium perenne*), and maize (*Zea mays*) each harvested as whole plants. This system is hereafter referred to as "CropRo4". The other six plots were cultivated using a one-year crop rotation system of maize and winter

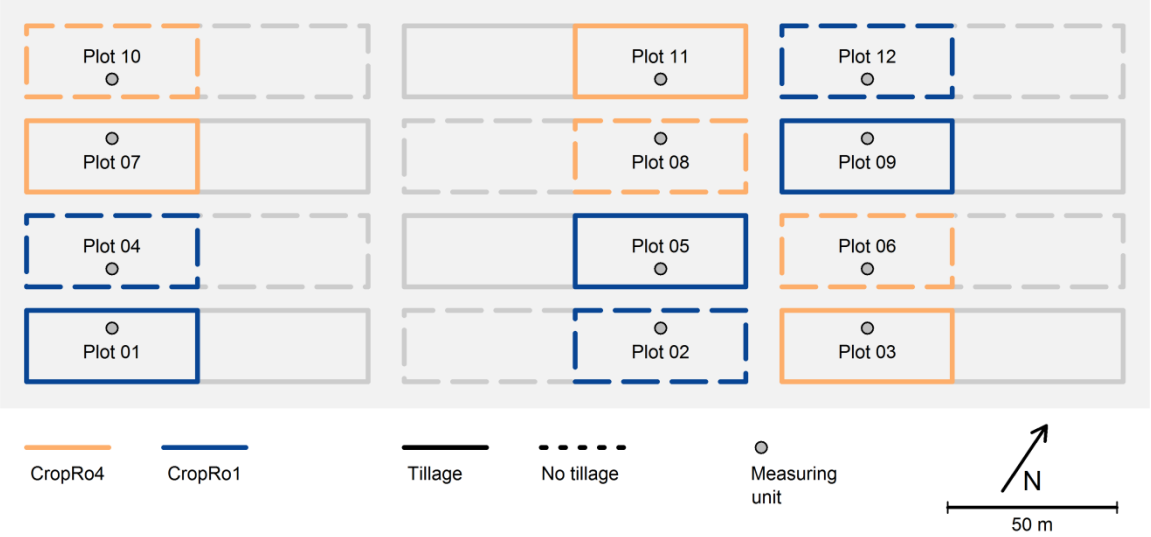

Figure 4.1. Experimental design of the long-term field experiment in Northeast Germany comprising two crop rotation systems and two different soil tillage practices. At each plot, soil moisture time series were measured at different soil depths.

rye designed to maximize the yield of biomass (hereafter referred to as "CropRo1"). The maize was harvested as a whole plant. The winter rye was only grown for erosion protection in the winter (as a cover crop) and was removed at an early stage of growth. Thus, its soil water consumption was marginal. Half of the plots were managed by plowing and the others were not tilled (direct seeding). Thus, each combination of cultivation system and tillage practices was carried out in three replicates. Each experimental plot was equipped with seven FDR soil moisture sensors (ThetaProbe ML2x, Delta-T Devices, England) at depths of 0.3 m, 0.6 m, 0.9 m, 1.2 m, 1.5 m, 2.0 m, and 3.0 m. All devices and cables were installed at least 30 cm below the ground to ensure that the upper 25 cm of the soil could be plowed. The soil moisture was measured for nearly four years between 2008/05/01 and 2012/04/23 with an hourly time resolution and aggregated to daily data.

4.2.2. Data preparation

The measured time series were initially plotted in a diagram and checked visually for plausibility. They cannot be shown here, due to their large number. Time periods with frozen soil water had to be omitted from the data set, because the FDR probes were calibrated for non-frozen soils only. Thus, an exclusion criterion was defined on the basis of soil temperature time series measured by DWD (2014). Soil moisture values were not considered when the soil temperature at either 0.2 m or 0.5 m was smaller than 1°C, yielding four data gaps during the winter.

Two additional time periods of 30 d (from 2009/05/20 to 2009/06/18) and 41 d (from 2011/07/14 to 2011/08/23) were omitted due to data gaps in several time series caused by malfunctioning data loggers. The time series measured at 150 cm at Plot 03, Plot 06 and Plot 10, and at 200 cm at Plot 11, had to be omitted totally as those sensors malfunctioned. Any measurement gaps in all the remaining time series were smaller than 6 d. An autocorrela-

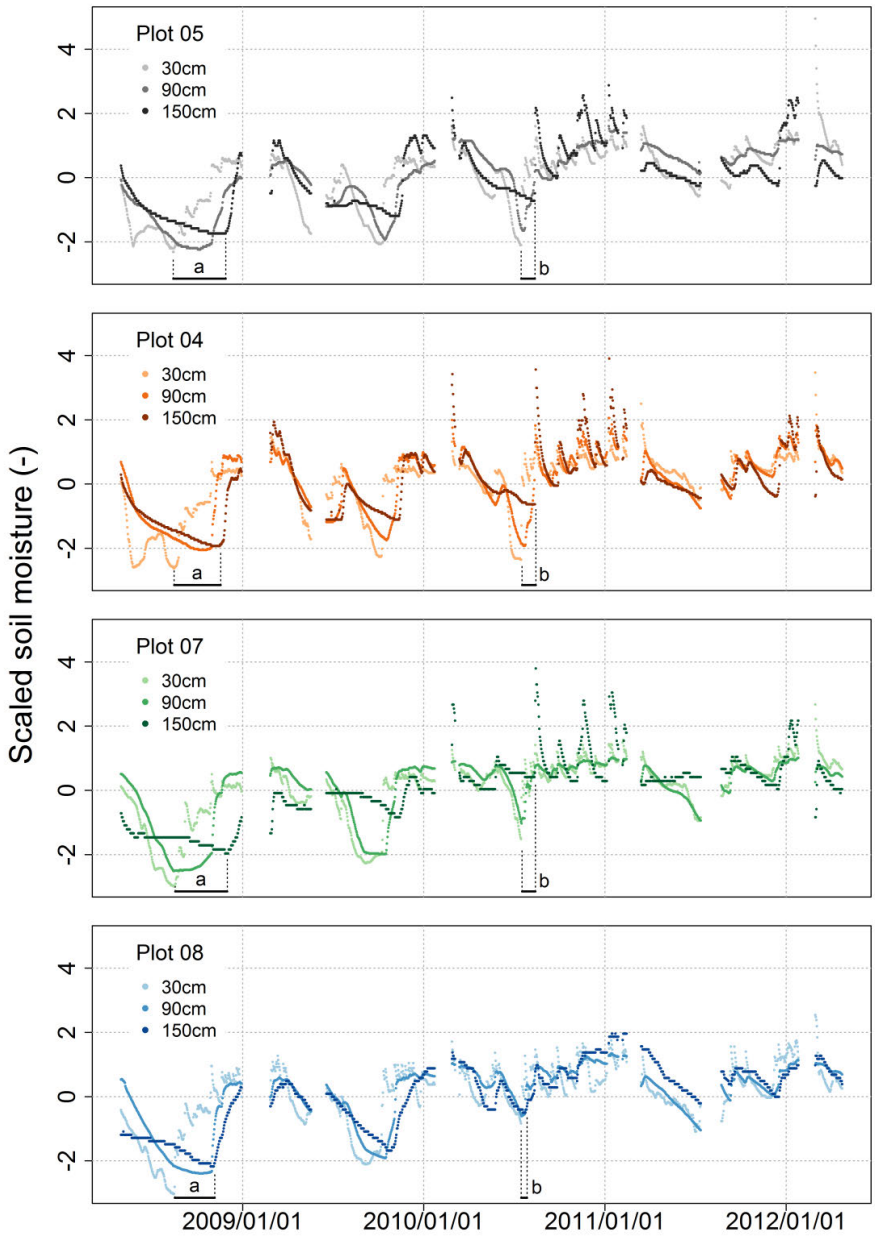

Figure 4.2. Z-transformed soil moisture time series shown as an example for three soil depths at four experimental plots. Time shifts in two local soil moisture minima between shallow and great depths are highlighted with an “a” and a “b”.

tion analysis of all time series showed that the minimum autocorrelation for time lags of 6 d was 0.80. This means that missing values can be predicted by existing with an accuracy of at least 80 %. Thus, all gaps smaller than 6 d were interpolated linearly. The fraction of interpolated data points considered in the analysis was 1.24 %.

Each individual moisture time series $\theta(t)$ was scaled to zero mean and unit variance (z-transformation)

$$\theta^*(t) = \frac{\theta(t) - \bar{\theta}(t)}{\sigma_\theta}. \qquad (4.1)$$

Information about the absolute values and amplitudes of $\theta(t)$ are lost during z-transformation, but it makes the scaled moisture time series $\theta^*(t)$ comparable and they are weighed equally. In the first step, only data from the upper five depths (z≤150cm) were considered for detailed analyses and discussion, because plant effects were presumably more significant here compared to greater depths. The z-transformed moisture series exhibited annual fluctuations with maxima in winter and minima in summer (Fig. 4.2). As the soil depth increased, the time series became smoother and lagged in time. However, time lags varied between different time periods. In Fig. 4.2 time shifts between the shallow and great depths are highlighted for two local minima. Time lags of soil moisture time series were much larger in the autumn of 2008 (marked with an “a”) compared to the summer of 2010 (marked with a “b”), although they were measured at identical positions. All z-transformed time series were organized in an input matrix Θ where each column represented a time series and each row a date.

4.2.3. Principal component analysis of time series

A PCA was applied to the input matrix of time series. This is an ordination method to analyze the structure of a multivariate data set and to identify common temporal patterns among time series. A PCA finds a new orthonormal basis for the multivariate data space spanned by all input time series. The total variance of the input data is decomposed into independent fractions. This results a set of uncorrelated principal components (PCs). Here, the target is to identify a first component which explains most of the total variance, a second component which explains most of the remaining variance and so on. All the resulting PCs are summarized in a matrix P in the order of the fraction of variance they explain. The transformation of the input matrix Θ into P can be computed by

$$\Theta \rightarrow P = \Lambda^T \Theta \,. \tag{4.2}$$

The matrix Λ contains the eigenvectors of the correlation matrix of Θ ordered by their corresponding eigenvalues. The fraction of total variance explained by a PC can be calculated by dividing the corresponding eigenvalue by the sum of all eigenvalues. Often only few PCs are needed to explain much of the total variance. We refer to Jolliffe (2002) for a detailed mathematical description of PCA. One important limitation of PCA is that only linear patterns are detected. Nonlinear patterns in a data set can only be approximated by gradually superposing several linear PCs (cf. Lee and Verleysen, 2007). The input time series should ideally be normally distributed but this condition is less important when PCA is considered a mainly descriptive technique (Jolliffe, 2002).

The PCs represent time series describing uncorrelated temporal patterns which presumably reflect different effects on the observed dynamics. Pearson correlation coefficients among PCs and the measured time series are known as loadings, *L*. The fraction of variance σ^2_{expl} of individual time series explained by the *m* first components can be calculated by the loadings

$$\sigma^2_{\mathrm{exp}l} = \sum_{k=1}^{m} L_k^2 \leq 1 \tag{4.3}$$

We calculated the arithmetic mean values $\overline{\sigma^2_{expl}}$ of the explained variances σ^2_{expl} of all individual time series from each measuring plot. The means of explained variances $\overline{\sigma^2_{expl}}$ were used to quantify the prevalence of temporal patterns described by single or several PCs at the individual measuring plots. On the basis of σ^2_{expl}, $\overline{\sigma^2_{expl}}$, *L*, and additional information (e.g. the measuring depth of the moisture time series), the temporal patterns described by individual components can be related to specific factors causing the observed patterns. We systematically tested whether all PCs were associated with effects of the following factors (significance level: 0.01):

1. Mean soil moisture behavior: the Pearson correlation was calculated between the daily arithmetic mean values of all input time series and the scores of each PC. A *t*-test was performed to see whether the resulting correlation coefficients *r* differed from 0.
2. Soil depth: the Pearson correlation was calculated between the installation depth of single sensors and the loadings of the corresponding time series for each PC. A *t*-test was performed to see whether the resulting correlation coefficients *r* differed from 0.

3. Cropping system: a Wilcoxon-Mann-Whitney test was performed for each PC to see whether the loadings from the CropRo1 and CropRo4 plots differ.

4. Soil tillage: a Wilcoxon-Mann-Whitney test was performed for each PC to see whether the loadings from the tilled and non-tilled plots differed.

In cases where the first component describes the mean course of all the considered soil moisture time series and another component represents an effect of soil depth, Hohenbrink and Lischeid (2015) suggested evaluating the input signal transformation behavior of the vadose zone on the basis of both components. A signal damping coefficient *D* [-] quantifying the extent of smoothing and time lagging in each moisture series can be derived from the ratio of the loadings L_1 and L_2 as described by Hohenbrink and Lischeid (2015) and Lischeid et al. (2010). The damping coefficient *D* represents a dimensionless relative measure that can only be interpreted in the context of the data set evaluated by the PCA. Temporal dynamics explained by components of a higher order are neglected by *D* because it is only based on the first two components. In this study all calculations and statistical analyses were performed with the *R* software package (R Development Core Team, 2010).

Table 4.1. Arithmetic mean values $\overline{\sigma^2_{expl}}$ of the explained variances of all individual time series from each measuring plot. The mean values $\overline{\sigma^2_{expl}}$ provide a measure of the prevalence of temporal patterns described by the principal components (PCs) at each measuring plot.

	Mean of expl. variances $\overline{\sigma^2_{expl}}$		
	1st PC	2nd PC	3rd PC
Plot 01	0.792	0.110	0.014
Plot 05	0.774	0.111	0.027
Plot 09	0.653	0.090	0.094
Plot 02	0.812	0.098	0.009
Plot 04	0.805	0.073	0.026
Plot 12	0.753	0.092	0.039
Plot 03	0.837	0.044	0.048
Plot 07	0.719	0.075	0.046
Plot 11	0.718	0.055	0.021
Plot 06	0.841	0.059	0.024
Plot 08	0.832	0.066	0.028
Plot 10	0.808	0.058	0.055

4.3. Results

4.3.1. Mean behavior of soil moisture and effect of soil depth

First principal component

The first PC explained 77.9 % of the data set's total variance. The mean values of explained variances ranged from $\overline{\sigma^2_{expl}}$ = 0.653 at Plot 09 to $\overline{\sigma^2_{expl}}$ = 0.841 at Plot 06 (Tab. 4.1). All loadings were positive (Fig. 4.3a). The absolute values of the loadings were between 0.697 and 0.960. Thus, the first PC described a temporal pattern that was apparent in every single time series. At each plot, the largest loadings appeared at medium depths, showing that the pattern described by the first PC was most predominant in the center of the soil profiles. The first PC was nearly identical (r^2>0.999, p-value≪0.01) to a time series representing the daily arithmetic mean values of all input time series. Thus, the first PC described the mean behavior of soil moisture, which was strongly influenced by atmospheric controls.

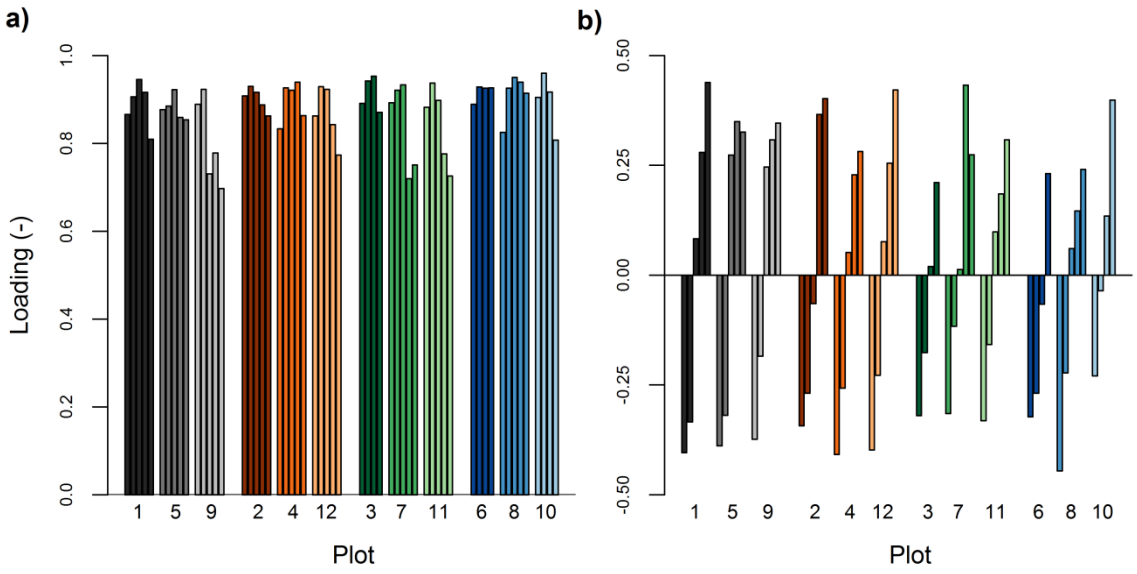

Figure 4.3. Loadings of all time series on the first (a) and second (b) principal components. Bars represent individual time series grouped by measuring plot. Plots are ordered by the management options CropRo1/tillage (grey), CropRo1/no tillage (reddish colors), CropRo4/tillage (green) and CropRo4/no tillage (blue). Within each plot, the time series are sorted by measuring depth, which increases from left to right.

Figure 4.4. Time series showing the scores of the first two principal components (PCs) superposed in different ratios. Time shifts in two local minima are highlighted with an "a" and a "b".

Second principal component

The fraction of total variance explained by the second PC was 7.8 %. The loadings of the time series on the second PC varied between -0.446 and 0.439 and were correlated (r^2 = 0.884, p-value≪0.01) with soil depth. Loadings increased with the depth, from negative values in the topsoil to positive values at greater depths (Fig. 4.3b). Thus, the second PC reflected deviations from the mean behavior (first component) depending on the soil depth. Combining the first two PCs by linear combination according to the principle of superposition resulted in reconstructed time series. They represented approximations of moisture dynamics that could be expected if soil depth were the only influencing factor. Different desired soil depths were specified using the ratio of combination. Adding the second PC to the first one yielded a time series (blue line in Fig. 4.4) that was more strongly damped (smoother) and time lagged compared to the mean behavior (black line). Temporal patterns of this kind were observed at large soil depths, where loadings of the second PC were positive. On the contrary, subtracting the second PC from the first one yielded a more weakly damped time series (orange line) with temporally preceding dynamics compared to the mean behavior. Such moisture time series were observed at shallow depths and loaded positively on the second PC. The variances of the first and second component were combined in the ratio 70:30 to construct the moisture dynamics shown in Fig. 4.4. Following Eq. 4.3 this corresponds to the loadings $L_1 = \sqrt{0.7} = 0.83$ and $L_2 = \sqrt{0.3} = \pm 0.54$. Soil depth had a slightly stronger effect in the constructed time series than in the observed ones, since the absolute values of L_2 were slightly larger than those of the time series measured at shallow and great depths (Fig. 4.3).

Time shifts between the moisture dynamics reconstructed for shallow and great soil depths varied between different time periods similarly to the measured moisture series. In Fig. 4.4, different time lags of local minima in the autumn of 2008 and the summer of 2010 are highlighted with “a” and “b” as in Fig. 4.2.

Signal damping

It was possible to calculate signal damping coefficients *D* quantifying the damping status of each measured time series, since the loadings on the second PC were correlated with the soil depth. The calculation of *D* was based on the loadings of the first two components only. Thus, the determination of *D* made use of 85.7 % of the data set’s total variance. The mean value of

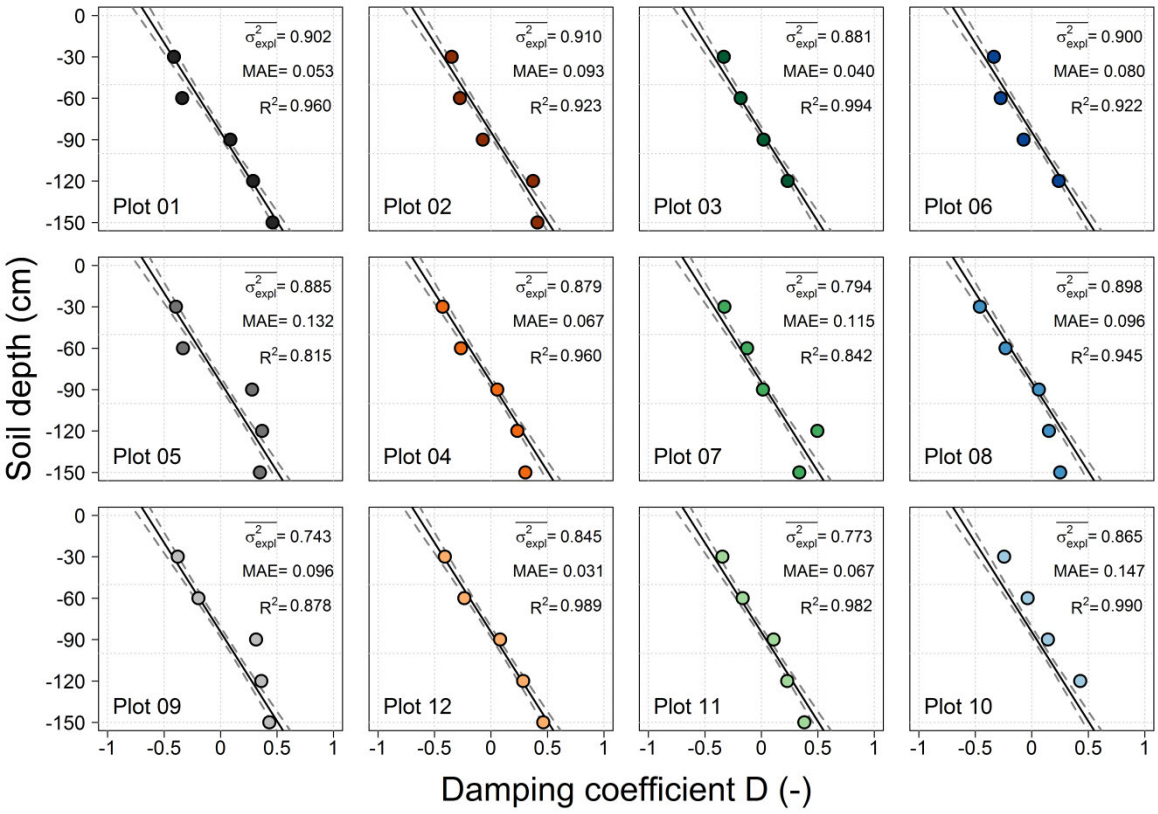

Figure 4.5. Depth profiles of the signal damping coefficient *D* for each measuring plot. The panels are ordered into columns based on the management options CropRo1/tillage (grey), CropRo1/no tillage (reddish colors), CropRo4/tillage (green) and CropRo4/no tillage (blue). The black lines describe the averaged damping behavior of the vadose zone. The three quality criteria indicate the mean value of variances explained by the first two components ($\overline{\sigma^2_{expl}}$), as well as the mean absolute error (*MAE*) and correlation (R^2) between the individual and averaged damping profiles.

variances explained by the first two PCs used to calculate *D* varied between $\overline{\sigma^2_{expl}}$ = 0.743 at Plot 09 and $\overline{\sigma^2_{expl}}$ = 0.910 at Plot 02 (Tab. 4.1). At each plot *D* increased along with the soil depth; in other words, time series measured at a greater soil depth were more strongly damped compared to those from shallow depths (Fig. 4.5). The relation between *D* and soil depth was almost linear. A regression line (intersect: -84.5 cm, slope: -129.4 cm per unit of *D,* r^2 = 0.88) described the field-averaged signal damping status of the measured time series. Its slope indicated the averaged signal transformation intensity and thus characterized the signal transformation behavior of the vadose zone. Moisture dynamics showing the averaged damping state can be reconstructed for any soil depth by combining the first two components. That way, the measured soil moisture time series can be functionally averaged. This means averaging the signal transformation behavior of the vadose zone at the experimental site (cf. Hohenbrink and Lischeid, 2015). The damping coefficients of individual time series differed only slightly from the field average, showing that hydrological signals were similarly transformed at all plots. Mean absolute errors (*MAEs*) and correlation coefficients (R^2) between individual and averaged damping profiles were used to evaluate deviations from the averaged behavior. Plot 12 (*MAE* = 0.031, R^2 = 0.989) and Plot 03 (*MAE* = 0.040, R^2 = 0.994) behaved most similarly to the average while the largest deviations from the mean behavior occurred at Plot 10 (*MAE* = 0.147, R^2 = 0.990) and Plot 05 (*MAE* = 0.132, R^2 = 0.815). All time series from Plot 10 were more strongly damped than the field average. Hence, the damping profile ran parallel to the averaged one. Note that the mean values of explained variances $\overline{\sigma^2_{expl}}$ were correlated neither with *MAE* (r^2 < 0.005) nor with R^2 (r^2 < 0.04). This shows that moisture dynamics deviating from the field-averaged damping status can be approximated by the first two components to the same extent as those representing the average behavior.

4.3.2. Effect of cropping system

The third PC covered 3.6 % of the data set's total variance. In contrast to the first two components, the mean value of explained variances (Tab. 4.1) was largest at Plot 09 ($\overline{\sigma^2_{expl}}$ = 0.094) and smallest at Plot 02 ($\overline{\sigma^2_{expl}}$ = 0.009). The loadings were clustered in two groups (Wilcoxon-Mann-Whitney Test, p-value$\ll$0.01). The time series measured at the CropRo1 plots were positively correlated with the third PC (Fig. 4.6), and those measured at the CropRo4 plots were negatively correlated. In consequence, the third PC discriminated between the cropping systems with respect to differences in the soil moisture dynamics between the CropRo4 and the

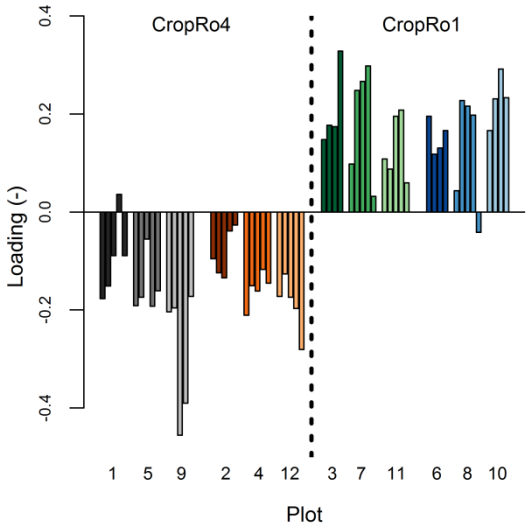

Figure 4.6. Loadings on the third component. Bars represent individual time series grouped by measuring plot. Plots are ordered based on the management options CropRo1/tillage (grey), CropRo1/no tillage (reddish colors), CropRo4/tillage (green) and CropRo4/no tillage (blue). Within each plot, the time series are sorted by measuring depth, which increases from left to right.

CropRo1 plots (Fig. 4.7). Positive scores of the third PC indicate that the z-transformed soil moisture values were greater at the CropRo1 plots than at the CropRo4 plots. The opposite was true during time periods with negative scores. Color bars at the top and bottom of Fig. 4.7 indicate the plants grown at the CropRo1 (top) and CropRo4 (bottom) plots during different time periods. In May 2008 the rye plants at the CropRo4 plots consumed more water than the very young maize plants at theCropRo1 plots. Hence, soil moisture at the CropRo4 plots decreased compared to the CropRo1 plots, as indicated by increasing scores of this component. This development promptly reversed after the rye harvest (marked with an “a” in Fig. 4.7). The scores decreased until the maize was harvested at the CropRo1 plots (marked with a “b”). During this time period, the maize plants built up much of their biomass, consuming more water than the millet plants at the CropRo4 plots. The same interplay of plant growth and water consumption was observed in the following year, 2009 (turning points marked “c” and “d”). The course of the third PC also showed a response to the alfalfa-clover-grass mixture being mowed (marked “e” and “f”). The scores increased before the mowing dates, showing that water consumption was higher at the CropRo4 plots. After mowing, the water consumption of the alfalfa-clover-grass mixture was reduced, leading to decreasing scores. This effect was not clearly visible when the mowing date was shortly before or after maize harvesting at the CropRo1

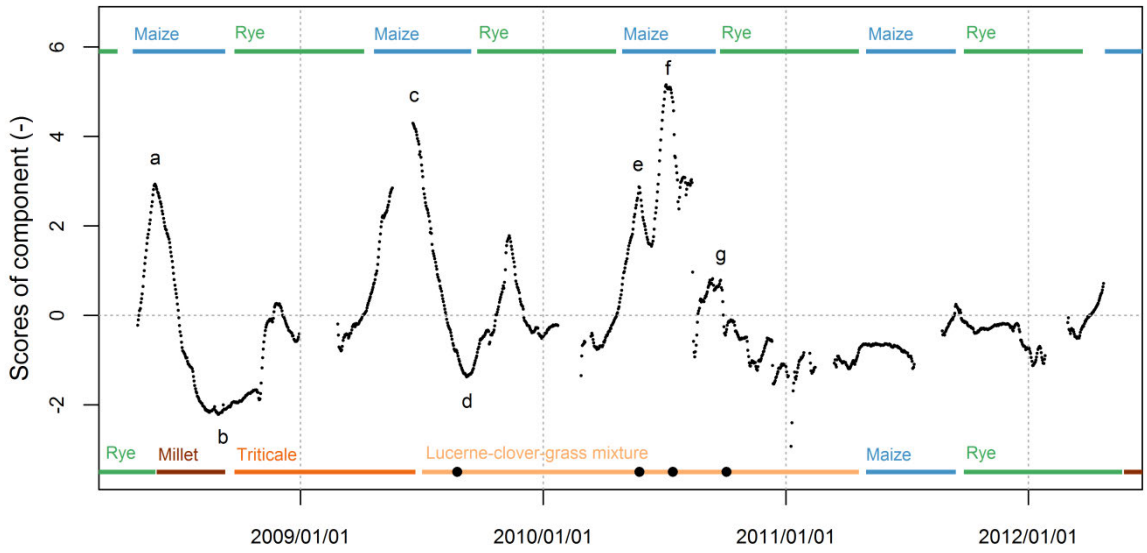

Figure 4.7. Scores of the third component shown as time series. Color bars indicate plants grown in the different cropping systems CropRo1 (top) and CropRo4 (bottom). Black dots indicate the dates when the alfalfa-clover-grass mixture was mowed.

plots (marked “d” and “g”). In the last observed season in 2011 and 2012, all plots were uniformly cultivated with maize followed by rye in the winter. During this time span, the scores of the third component were close to zero. Thus, there were no major differences in soil moisture dynamics between the CropRo4 and CropRo1 plots. It is worth mentioning that the third component described relative soil moisture dynamics instead of providing information about absolute soil moisture values, since each input time series was z-transformed (Eq. 4.1).

The first three PCs can be combined to reconstruct time series approximating the soil moisture dynamics that could be expected if only the soil depth and cropping system affected soil moisture. Such reconstructed time series aggregate the most pronounced effects of soil depth and the cropping system. They can be used both for (i) detailed analyses of the specific effects and (ii) upscaling purposes. The time series shown in Fig. 4.8 were composed by superposing the first three PCs. The third PC was considered both positively (CropRo1) and negatively (CropRo4). The ratios for combination were determined by their fraction of explained total variance, where the sum of explained total variance of 89.2% was set to 100 %. Thus, the third PC accounted for 4.03 %. The remaining 95.97% were then assigned to the first (95.80 %) and second PC (0.17 %) in a ratio determined by the field-averaged value of *D* for a depth of 90 cm. Note that the second PC only accounted for 0.17 %, because the pattern represented by this

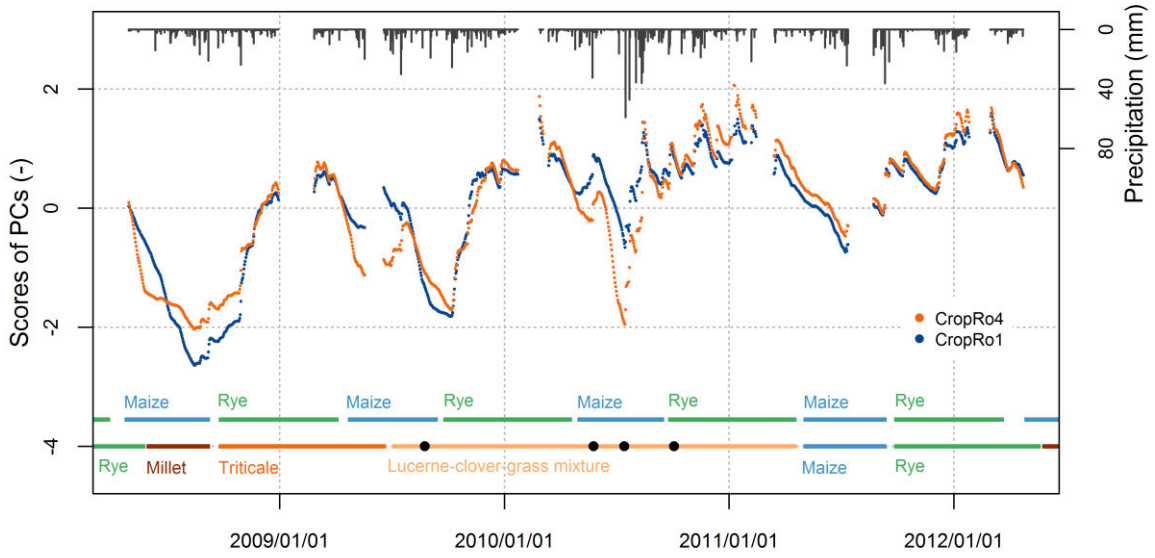

Figure 4 8. Functional averaged time series at a medium depth of 90 cm reconstructed for CropRo4 and CropRo1 plots. The time series are composed by superposing the first (95.80%), second (0.17%) and third component (4.03%). Color bars indicate plants grown in the different cropping systems CropRo1 (top) and CropRo4 (bottom). Black dots indicate the dates when the alfalfa-clover-grass mixture was mowed.

PC was almost non-existent in the middle of the soil profile (cf. Fig. 4.3b). The time series show reconstructed soil moisture dynamics that can be expected for both cropping systems at a soil depth of 90 cm. The temporal patterns emerging from mean behavior, soil depth and cropping system were functionally averaged for the whole experimental field. The moisture dynamics are controlled by precipitation and plant transpiration. The most significant differences between the cropping systems appeared in the summer months when transpiration rates were highest and soil moisture deficits were not rapidly compensated by precipitation.

4.3.3. Effect of soil tillage

The design of the field experiment included two soil tillage options (Fig. 4.1). The loadings of the time series from tilled and non-tilled plots differed significantly for the 27th component (Wilcoxon-Mann-Whitney Test, p-value$\ll$0.01) indicating that it provides information about soil tillage effects. However, it only accounted for 0.046 % of the total variance. This fraction is too small for reasonable process interpretations. Nevertheless, it provides an estimation of the maximal fraction of total soil moisture variance below the plowing zone that could be caused by soil tillage effects.

Table 4.2. Effect of the number of soil depths considered on the fraction of total variance explained by the first three principal components (PCs).

Considered soil depths (cm)	Number of time series	Fraction of total variance explained by			
		1.PC Mean behavior	2.PC: Signal damping	3.PC: Water consumption of plants	Sum
30, 60, 90	36	0.849	0.052	0.038	0.939
30, 60, 90, 120, 150	57	0.779	0.078	0.036	0.893
30, 60, 90, 120, 150, 200, 300	80	0.720	0.090	0.030	0.840

4.3.4. Considering data from different soil depths

The previous sections showed the results from analyses of the upper five measuring depths between 30 cm and 150 cm. The described effects of mean behavior, signal damping, and plant water consumption were also detected using PCA when different numbers of measuring depths were considered. However, their relevance differed. The fraction of variance explained by the mean behavior decreased from 84.9 % (upper three depths) to 72.0 % (all seven depths) when time series from more soil depths were considered (Tab. 4.2). Conversely, the effect of signal damping was strongest (explained total variance: 9.0 %) when all measuring depths were considered. The effect of water consumption of plants slightly became weaker with increasing number of considered measuring depths. The total amount of variance that could clearly be assigned to specific influencing factors decreased from 93.9 % (upper three depths) to 84.0 % (all seven depths).

4.4. Discussion

4.4.1. Decomposing the soil moisture variance

Applying PCA to the z-transformed input data set yielded three meaningful components accounting for 89.3 % of the total variance in the upper five soil depths. A large share of the observed temporal dynamics recurs in each time series, showing that soil moisture dynamics exhibited only a small degree of functional heterogeneity at the experimental site. This becomes particularly obvious when looking at the first component. More than three quarters of

the total variance could already be aggregated by one single temporal pattern that was almost identical to a time series of mean values from all measuring locations. These findings are in good agreement with the results of Korres et al. (2010), who analyzed spatiotemporal soil moisture patterns at shallow soil depths using empirical orthogonal functions. They also found a PC reflecting the mean soil moisture dynamics at a pasture site and an arable field. Similarly to our results, this main pattern explained more than 70 % of soil moisture variance from the arable site, although Korres et al. (2010) considered only ten measuring dates.

The explanatory power of a PCA to identify specific effects strongly depends on the information content of the analyzed data set. Thus, the experimental design already determines the applicability of a PCA. Our results have shown that the fraction of variance explained by specific effects was determined by the number of soil depths considered. However, the nature of the resulting PCs and, thus, the specific effects identified by the PCA were similar for all the numbers of soil depths considered. This underlines how robustly PCA identifies first-order controls.

A PCA is often used as a dimensionality reduction tool. In that case it is necessary to test how many components contain significant information and can thus be considered for interpretation (Peres-Neto et al., 2005). Our purpose, however, was to identify and extract the effects of specific factors known beforehand. Thus, we systematically tested whether each PC contained information about the factor of interest, notwithstanding the fraction of variance it explained.

4.4.2. Signal transformation behavior

The second component described the part of the deviation from the mean behavior (first PC) that can be explained by effects of soil depth. The fraction of total variance explained by the first two components (85.7 %) was very similar to the results of Hohenbrink and Lischeid (2015). In their study both components explained 88.7 % of soil moisture dynamics simulated in a heterogeneous soil profile. It is noteworthy that the measured dynamics are no more complex than the simulated ones, although the latter were generated for strongly idealized and simplified model cases. However, it is worth mentioning that Hohenbrink and Lischeid (2015) considered model cases covering nearly the whole range of possible soil textures, while the soils at the monitoring site were dominated by sandy textures.

Time series with different degrees of signal transformation were reconstructed by combining the scores of the first two components (Fig. 4.4) as proposed by Hohenbrink and Lischeid

(2015). This was a prerequisite to derive *D* from the loadings of the first two components. The depth profiles of *D* (Fig. 4.5) provided evidence that hydrological input signals were continuously transformed into a more strongly damped status while propagating through the soil profiles. This might be a trivial result known before (e.g. Mahmood et al., 2012; Pan et al., 2011), but the novelty of this approach is that *D* represents a robust measure to quantify the signal transformation behavior of soil systems. The fact that *D* mostly increased linearly with the soil depth easily enables the functional averaging of soil moisture dynamics, i.e. averaging the signal transformation behavior irrespective of small scale heterogeneities.

The damping coefficients of single time series only deviated slightly from the field-averaged damping profile. Furthermore, the slopes of the damping profiles from all measuring plots were very similar. Thus it can be concluded that the general signal transformation behavior of the vadose zone proceeds relatively homogeneously at the field scale. Similarly to temporal stability analyses (cf. Vachaud et al., 1985; Vanderlinden et al., 2012) the concept of signal transformation analysis can be used to identify measuring locations which reflect the mean behavior of the whole investigation site.

At some plots, *D* increased linearly with the soil depth, indicating that water flow was relatively uniform. At other plots, *D* was scattered around the mean damping profile, as indicated by larger values of the mean absolute errors *MAE* and the correlation coefficients R^2 between the individual and averaged damping profiles (Fig. 4.5). This shows that heterogeneous water flow fields occurred at plot scale, i.e. hydrological signals were preferentially propagated along distinct water pathways. This effect can be caused by small-scale textural heterogeneity. In heterogeneous flow fields, the signal transformation along preferred water pathways is less intensive than in surrounding regions with a reduced water flow (Hohenbrink and Lischeid, 2015). Thus, time series measured at a certain depth can be less strongly damped than others from shallower depths. However, the prevalence of both temporal patterns captured by *D* was not reduced upon the occurrence of heterogeneous flow fields, since $\overline{\sigma_{expl}^2}$ was neither correlated with *MAE* nor with the correlation coefficients R^2. Soil moisture dynamics emerging in heterogeneous flow fields were still composed of the first two components to the same extent as under uniform flow conditions. Similarly to Hohenbrink and Lischeid (2015), this shows that textural heterogeneity does not necessarily cause functional heterogeneity, since no additional, more complex temporal patterns were generated by heterogeneous water flow. Soil heterogeneity merely caused different signal transformation intensities per depth unit instead of

inducing completely different kinds of signal transformation. Thus, the effect of textural heterogeneity is much more systematic than e.g. random noise added to the data (cf. Hohenbrink and Lischeid, 2015).

Effects of local heterogeneities, i.e. different intensities of signal transformation, can balance each other out. This can be visualized using the example of layered soil profiles. Input signals entering any soil layer correspond to the output signal of the layer above. An input signal entering the soil surface is propagated in this way through several layers with different thicknesses, textures and small-scale heterogeneities. Given that (i) the general kind of signal transformation does not differ between different layers and that (ii) signals can only be transformed to a more strongly damped status, it is possible to find a corresponding homogeneous soil with the same average signal transformation behavior as the layered soil. This is a basic condition for applying the concept of temporal averaging for different purposes, e.g., upscaling soil moisture dynamics by averaging the signal transformation behavior of the vadose zone.

The calculation of *D* makes use of the first two PCs, representing linear approximations of the two most prevalent uncorrelated temporal patterns, that is, the mean soil moisture behavior and the effect of soil depth. If all depth effects occurring cannot fully be described by the second principal component, there is a risk of neglecting some parts of relevant variance which are also induced by soil depth. This typically happens if signal transformation induces nonlinear structures that can only be approximated by stepwise superposition of several linear components (Hohenbrink and Lischeid, 2015). There is further need for research into the nonlinear behavior of signal transformation. We could not find Pearson correlations between the soil depth and the loadings on higher-order PCs. However, loadings of the fourth component (data not shown) seemed to have a curve-shaped dependency on depth. Thus, more sophisticated measures for nonlinear dependence, such as mutual information (as defined by Shannon (1948), for its estimation see Fraser and Swinney (1986) or Kraskov et al. (2004)), would be needed to detect further non-linear relations between loadings and soil depth. However this would go beyond the scope of our study.

4.4.3. Effects of cropping system and soil tillage

The effect of the cropping systems represented by the third PC accounted for 3.6 % of the total variance. This fraction was smaller than we would have expected beforehand, since both cropping systems comprised plants with different water demands, varying harvest times and non-

parallel growing seasons. The third component nevertheless described a clear and unambiguously interpretable temporal pattern. This holds true for both (i) the clustering of loadings in the two groups of CropRo1 and CropRo4 and (ii) the interpretation of the temporal dynamics described by the scores of the third component. The clarity of these results highlights the great potential of PCA in detecting minimal but significant patterns hidden in data sets of time series (cf. Thomas et al., 2012). Soil moisture temporal patterns accounting for only small fractions of variance can still be interesting and can even have important impacts on dominant soil water processes. This can be illustrated by the example of threshold-controlled processes such as macropore flow occurring under particular moisture conditions. It can be the main reason for solute leaching (reviewed by Jarvis, 2007), although it often accounts for only small fractions of the total soil moisture variance.

Korres et al. (2015) used various analyzing tools to reveal spatio-temporal soil moisture patterns emerging under different land uses. With regard to arable sites they found large spatial soil moisture variability among neighboring fields. They explained this effect by strongly varying evaporation rates due to shifted periods of maximum water uptake by different crops and different agricultural management (e.g. planting dates, harvesting dates, field sizes). It is worth noting that we identified very similar effects of crops on soil moisture patterns by time series analysis such as Korres et al. (2015) found by spatial analysis. Baroni et al. (2013) performed a PCA on a data set containing soil moisture measured at a shallow depth in an agricultural field. Among other PCs they identified a component describing a plant effect. It was spatially correlated with the crop factors leaf area index and plant height. This vegetation-controlled pattern prevailed when the soil became dryer. Our third component also revealed that soil moisture differences between the cropping systems were the greatest in dry conditions, because the scores showed the highest absolute values during the dry summer months (Fig. 4.7).

There is agreement in the literature that in comparison to plowing, non-tillage causes (i) greater bulk density, (ii) more stable soil aggregates, (iii) increased soil biota abundance generating macropores, and (iv) higher soil carbon contents (e.g. Arai et al., 2014; Holland, 2004; Soane et al., 2012). Tillage-induced alterations of these substantial soil characteristics can have various effects on soil hydraulic properties (e.g. Schwen et al., 2011; Strudley et al., 2008). Thus, it might be expected that soil moisture dynamics would also differ between different tillage practices. However, we could not detect significant differences between tilled and non-tilled plots. Some authors reported tillage effects on spatial soil moisture patterns at shallow soil

depths (e.g. Korres et al., 2010; Perfect and Caron, 2002). Similar effects could possibly also be found at very shallow depths at our investigation site. However, we only analyzed time series from greater soil depths, since it is not possible to measure long-term data with sensors placed at fixed positions when the surrounding soil is regularly tilled.

4.5. Conclusions

By applying a principal component analysis to measured soil moisture time series, we achieved our objectives of identifying, describing and evaluating the specific effects of soil heterogeneity and land management on soil moisture dynamics. The method turned out to be powerful as long as relative temporal dynamics are of interest rather than absolute values. Based on the results that three meaningful components accounted for 89.2 % of the total soil moisture variance, we can draw the following conclusions.

Firstly, contrary to common assumption, the interactions of infiltration, soil heterogeneity, and different land management practices do not necessarily induce complex soil moisture dynamics in deeper soil layers. Nearly 78 % of the observed soil moisture variance was identical at all measuring locations. Thus, functional heterogeneity, i.e. variability among all soil moisture time series, only accounted for the remaining 22 % of variance. About 35 % of that was unambiguously attributed to the deterministic effect of input signal transformation with increasing soil depth. The large textural heterogeneities at the test site had no effect on the general nature of signal transformation, but did affect its intensity, which varied at different sites. Land management only slightly affected soil moisture dynamics, since the different cropping systems induced 16.3 % of functional heterogeneity. Soil tillage was not found to have any significant effect.

Secondly, the suggested approach opens up new possibilities to analyze and better understand complex soil system behavior. Functional averaging, i.e. averaging the signal transformation behavior of the vadose zone, provides time series representing the most relevant characteristics of the system behavior. The approach does not require *a priori* assumptions about the nature of physical processes, since it is solely based on information provided by the data. Thus, it provides model-independent information on how individual effects contribute to the observed dynamics, making it especially valuable for model building, calibration and evaluation.

Acknowledgements

This study was funded by the *German Research Foundation DFG* (project Li 802/3-1). We would like to thank Wilfried Hierold for providing soil description data, Ralf Dannowski for preparing information about climatic conditions and Dietmar Barkusky for providing land management data. We are also grateful to Anne-Kathrin Schneider, Christian Lehr, Steven Böttcher, Florian Reverey and Björn Thomas for proofreading and fruitful discussions as well as two anonymous reviewers for their valuable comments and suggestions.

References

Arai, M., Minamiya, Y., Tsuzura, H., Watanabe, Y., Yagioka, A., Kaneko, N., 2014. Changes in water stable aggregate and soil carbon accumulation in a no-tillage with weed mulch management site after conversion from conventional management practices. Geoderma, 221: 50-60.

Baroni, G., Ortuani, B., Facchi, A., Gandolfi, C., 2013. The role of vegetation and soil properties on the spatio-temporal variability of the surface soil moisture in a maize-cropped field. J Hydrol, 489: 148-159.

Basu, N.B., Rao, P.S.C., Winzeler, H.E., Kumar, S., Owens, P., Merwade, V., 2010. Parsimonious modeling of hydrologic responses in engineered watersheds: Structural heterogeneity versus functional homogeneity. Water Resour Res, 46(4): W04501.

Biswas, A., 2014. Scaling analysis of soil water storage with missing measurements using the second-generation continuous wavelet transform. Eur J Soil Sci, 65(4): 594-604.

Boote, K.J., Jones, J.W., White, J.W., Asseng, S., Lizaso, J.I., 2013. Putting mechanisms into crop production models. Plant Cell Environ, 36(9): 1658-1672.

Böttcher, S., Merz, C., Lischeid, G., Dannowski, R., 2014. Using Isomap to differentiate between anthropogenic and natural effects on groundwater dynamics in a complex geological setting. J Hydrol, 519, Part B(0): 1634-1641.

Corradini, C., 2014. Soil moisture in the development of hydrological processes and its determination at different spatial scales. J Hydrol, 516: 1-5.

De Lannoy, G.J.M., Verhoest, N.E.C., Houser, P.R., Gish, T.J., Van Meirvenne, M., 2006. Spatial and temporal characteristics of soil moisture in an intensively monitored agricultural field (OPE3). J Hydrol, 331(3-4): 719-730.

DWD, 2014. German Meteorological Service. http://www.dwd.de/.

Fraser, A.M., Swinney, H.L., 1986. Independent coordinates for strange attractors from mutual Information. Phys Rev A, 33(2): 1134-1140.

Gall, H.E., Park, J., Harman, C.J., Jawitz, J.W., Rao, P.S.C., 2013. Landscape filtering of hydrologic and biogeochemical responses in managed catchments. Landscape Ecol, 28(4): 651-664.

Hohenbrink, T.L., Lischeid, G., 2014. Texture-depending performance of an in situ method assessing deep seepage. J Hydrol, 511: 61-71.

Hohenbrink, T.L., Lischeid, G., 2015. Does textural heterogeneity matter? Quantifying transformation of hydrological signals in soils. J Hydrol, 523: 725-738.

Holland, J.M., 2004. The environmental consequences of adopting conservation tillage in Europe: reviewing the evidence. Agr Ecosyst Environ, 103(1): 1-25.

Hu, W., Si, B.C., 2014. Can soil water measurements at a certain depth be used to estimate mean soil water content of a soil profile at a point or at a hillslope scale? J Hydrol, 516: 67-75.

Hupet, F., Vanclooster, M., 2002. Intraseasonal dynamics of soil moisture variability within a small agricultural maize cropped field. J Hydrol, 261(1-4): 86-101.

Jarvis, N.J., 2007. A review of non-equilibrium water flow and solute transport in soil macropores: principles, controlling factors and consequences for water quality. Eur J Soil Sci, 58(3): 523-546.

Jawson, S.D., Niemann, J.D., 2007. Spatial patterns from EOF analysis of soil moisture at a large scale and their dependence on soil, land-use, and topographic properties. Adv Water Resour, 30(3): 366-381.

Jolliffe, I.T., 2002. Principal Component Analysis. Springer Series in Statistics. Springer, New York, 489 pp.

Joshi, C., Mohanty, B.P., 2010. Physical controls of near-surface soil moisture across varying spatial scales in an agricultural landscape during SMEX02. Water Resour Res, 46(12): W12503.

Katul, G.G., Porporato, A., Daly, E., Oishi, A.C., Kim, H.S., Stoy, P.C., Juang, J.Y., Siqueira, M.B., 2007. On the spectrum of soil moisture from hourly to interannual scales. Water Resour Res, 43(5): W05428.

Korres, W., Koyama, C.N., Fiener, P., Schneider, K., 2010. Analysis of surface soil moisture patterns in agricultural landscapes using Empirical Orthogonal Functions. Hydrol Earth Syst Sc, 14(5): 751-764.

Korres, W., Koyama, C.N., Fiener, P., Schneider, K., 2010. Analysis of surface soil moisture patterns in agricultural landscapes using Empirical Orthogonal Functions. Hydrol Earth Syst Sc, 14(5): 751-764.

Kraskov, A., Stogbauer, H., Grassberger, P., 2004. Estimating mutual information. Phys Rev E, 69(6).

Lee, J.A., Verleysen, M., 2007. Nonlinear Dimensionality Reduction. Information Science and Statistics. Springer, New York, 308 pp.

Lehr, C., Pöschke, F., Lewandowski, J., Lischeid, G., 2015. A novel method to evaluate the effect of a stream restoration on the spatial pattern of hydraulic connection of stream and groundwater. J Hydrol, 527: 394-401.

Lischeid, G., Natkhin, M., Steidl, J., Dietrich, O., Dannowski, R., Merz, C., 2010. Assessing coupling between lakes and layered aquifers in a complex Pleistocene landscape based on water level dynamics. Adv Water Resour, 33(11): 1331-1339.

Mahmood, R., Hubbard, K.G., 2007. Relationship between soil moisture of near surface and multiple depths of the root zone under heterogeneous land uses and varying hydroclimatic conditions. Hydrol Process, 21(25): 3449-3462.

Mahmood, R., Littell, A., Hubbard, K.G., You, J.S., 2012. Observed data-based assessment of relationships among soil moisture at various depths, precipitation, and temperature. Appl Geogr, 34: 255-264.

Mirschel, W., Wenkel, K.O., Wegehenkel, M., Kersebaum, K.C., Schindler, U., 2010. Comprehensive multivariable field data set for agro-ecosystem modelling from Muencheberg Experimental Stations in 1992 - 1998. Leibniz-Zentrum für Agrarlandschaftsforschung (ZALF) e.V. http://dx.doi.org/10.4228/ZALF.1992.167.

Page, R.M., Lischeid, G., Epting, J., Huggenberger, P., 2012. Principal component analysis of time series for identifying indicator variables for riverine groundwater extraction management. J Hydrol, 432: 137-144.

Pan, F., Pachepsky, Y.A., Guber, A.K., Hill, R.L., 2011. Information and complexity measures applied to observed and simulated soil moisture time series. Hydrolog Sci J, 56(6): 1027-1039.

Peng, J., Shen, H., He, S.W., Wu, J.S., 2013. Soil moisture retrieving using hyperspectral data with the application of wavelet analysis. Environ Earth Sci, 69(1): 279-288.

Peres-Neto, P.R., Jackson, D.A., Somers, K.M., 2005. How many principal components? stopping rules for determining the number of non-trivial axes revisited. Comput Stat Data An, 49(4): 974-997.

Perfect, E., Caron, J., 2002. Spectral analysis of tillage-induced differences in soil spatial variability. Soil Sci Soc Am J, 66(5): 1587-1595.

Qiu, J.X., Mo, X.G., Liu, S.X., Lin, Z.H., 2014. Exploring spatiotemporal patterns and physical controls of soil moisture at various spatial scales. Theor Appl Climatol, 118(1-2): 159-171.

R Development Core Team, 2010. R: A Language and Environment for Statistical Computing. R Foundation for Statistical Computing, Vienna, Austria. (Version 3.1.0, http://www.R-project.org).

Rivera, D., Lillo, M., Granda, S., 2014. Representative locations from time series of soil water content using time stability and wavelet analysis. Environ Monit Assess, 186(12): 9075-9087.

Schlüter, S., Vogel, H.J., Ippisch, O., Bastian, P., Roth, K., Schelle, H., Durner, W., Kasteel, R., Vanderborght, J., 2012. Virtual soils: assessment of the effects of soil structure on the hydraulic behavior of cultivated soils. Vadose Zone J, 11(4).

Schwen, A., Bodner, G., Scholl, P., Buchan, G.D., Loiskandl, W., 2011. Temporal dynamics of soil hydraulic properties and the water-conducting porosity under different tillage. Soil Till Res, 113(2): 89-98.

Shannon, C.E., 1948. A Mathematical Theory of Communication. At&T Tech J, 27(4): 379-423; 623-656.

Soane, B.D., Ball, B.C., Arvidsson, J., Basch, G., Moreno, F., Roger-Estrade, J., 2012. No-till in northern, western and south-western Europe: A review of problems and opportunities for crop production and the environment. Soil Till Res, 118: 66-87.

Strudley, M.W., Green, T.R., Ascough, J.C., 2008. Tillage effects on soil hydraulic properties in space and time: State of the science. Soil Till Res, 99(1): 4-48.

Thomas, B., Lischeid, G., Steidl, J., Dannowski, R., 2012. Regional catchment classification with respect to low flow risk in a Pleistocene landscape. J Hydrol, 475: 392-402.

Vachaud, G., Desilans, A.P., Balabanis, P., Vauclin, M., 1985. Temporal stability of spatially measured soil-water probability density-function. Soil Sci Soc Am J, 49(4): 822-828.

Vanderlinden, K., Vereecken, H., Hardelauf, H., Herbst, M., Martinez, G., Cosh, M.H., Pachepsky, Y.A., 2012. Temporal stability of soil water contents: a review of data and analyses. Vadose Zone J, 11(4).

Vereecken, H., Huisman, J.A., Bogena, H., Vanderborght, J., Vrugt, J.A., Hopmans, J.W., 2008. On the value of soil moisture measurements in vadose zone hydrology: A review. Water Resour Res, 44: W00D06.

Vereecken, H., Huisman, J.A., Pachepsky, Y., Montzka, C., van der Kruk, J., Bogena, H., Weihermuller, L., Herbst, M., Martinez, G., Vanderborght, J., 2014. On the spatio-temporal dynamics of soil moisture at the field scale. J Hydrol, 516: 76-96.

Yoo, C., Kim, S., 2004. EOF analysis of surface soil moisture field variability. Adv Water Resour, 27(8): 831-842.

Zou, W.X., Biswas, A., Han, X.Z., Si, B.C., 2012. Extracting soil water storage pattern using a self-organizing map. Geoderma, 177: 18-26.

5. Synthesis

5.1. Achievements of the thesis

In this section the main achievements of this dissertation are evaluated with regard to efficiently describing and making use of the spatial heterogeneities in field data. It is structured into three subsections summarizing the contributions of the single studies to achieve the main objectives introduced in Chapter 1 and discussing their limitations.

5.1.1. Using point information of moisture dynamics for seepage estimation

The Buckingham-Darcy method provides a simple approach to estimate deep seepage fluxes from one soil moisture time series measured in the permanent seepage zone where only downward fluxes occur (Schindler and Müller, 1998). This way, the complex interactions of root-zone processes taking place above can be neglected, since soil moisture dynamics at large depths represent an integrative result of these processes. However, ignoring spatial heterogeneities of subsoil texture might induce substantial errors. Thus, the first study of this dissertation aimed at investigating the effects of soil texture and textural heterogeneity in the deep vadose zone on the performance of that method.

The study presented in Chapter 2 showed that the Buckingham-Darcy method performed well for most soil texture classes. Especially in sandy loam the seepage dynamics obtained from point information could be considered representative for larger scales of interest, indicating that moisture dynamics from different locations were very similar. However, the method was imprecise in pure sand where heterogeneous flow fields were particularly pronounced. The method strictly follows the bottom-up approach, since observations made at the small scale are transferred to larger scales. Additionally, the physically based Buckingham-Darcy law is *a priori* chosen for water flux description. The results from that study clearly demonstrate the advantages and disadvantages of bottom-up approaches. On the one hand, the Buckingham-Darcy law allows for deterministically linking soil moisture dynamics to soil water fluxes. This is

helpful for many purposes, since local soil moisture dynamics can be measured much easier in the field (Robinson et al., 2008) than seepage fluxes (e.g. Meissner et al., 2010). The latter is an important target variable for many purposes such as estimating groundwater recharge (Scanlon et al., 2002) or solute leaching (van Genuchten et al., 2014). On the other hand, there is the risk of neglecting important controls on the target variable by using a predefined process description (e.g. Kirchner, 2006; Savenije, 2009). In pure sand where seepage fluxes were dominated by heterogeneous flow fields the Buckingham-Darcy method turned out to be not applicable, because it simply neglects the effect of water flow heterogeneity. This problem does not only concern the performance of the specific Buckingham-Darcy method presented in Chapter 2, but also the general applicability of one-dimensional process models to simulate the integrative dynamics of heterogeneous flow fields (cf. Durner et al., 2008; Schlüter et al., 2012).

Results from the numerical study were limited to a strongly conceptualized description of textural heterogeneity. Under field conditions various additional factors and processes, e.g. macropore flow, might control the seepage dynamics. This has been the motivation to investigate soil water dynamics in heterogeneous soils from a top-down perspective in the following studies. That way the first order controls on soil moisture dynamics and seepage fluxes can be identified in order to constrain a respective parsimonious seepage flux model.

5.1.2. Analyzing the signal transformation behavior of soils

The second objective of this dissertation was to test the concept of low-dimensional transformation of hydrological signals in heterogeneous soils and to test an efficient approach for grasping and quantifying that transformation behavior. This means analyzing how hydrological signals (e.g. rainfall, snow melt) are transformed while they are propagated through the vadose zone. In Chapter 3 the idea behind that approach was introduced, and the general characteristics of signal transformation in heterogeneous soils were derived from simulated soil moisture time series. Chapter 4 contains an example for its application to monitoring data from a long term field experiment.

It is commonly known that input signals become increasingly smoothed (Pan et al., 2011) and delayed (Mahmood et al., 2012) with soil depth for which the somehow simplifying term “damping” was coined. In this dissertation the approach to derive the damping status of single time series from the loadings on the first two principal components (Lischeid et al., 2010) was applied for the first time in a soil hydrological context. It has already successfully been used in

a few studies dealing with groundwater dynamics (Lehr et al., 2015; Lischeid et al., 2012). Proving the applicability of the damping coefficient *D* as a robust measure to quantify the transformation status of soil moisture time series in the vadose zone is an achievement of this dissertation.

Chapter 3 showed that the moisture time series simulated in different homogeneous soils were very similar. This indicated that the kind of signal transformation is nearly identical in all textures. The only difference between the textures was the intensity of signal damping per depth interval. In fine textured soils the hydrological signals were transformed much more strongly per depth interval than in coarse substrates. In Chapter 3 it was shown that hydrological signals are progressing in a uni-directional way a common trajectory of possible damping states irrespective of soil texture. In contrast to spectral analysis of time series investigating the low pass filtering behavior of the vadose zone (e.g. Katul et al., 2007), PCA additionally considers the time delaying and smoothing of single peaks. In Chapter 3 it was also shown that *D* increased almost linearly over the whole profile, whereas the intensity of low-pass filtering strongly decreased with soil depth. This demonstrated that *D* is an adequate and applicable measure of signal transformation.

Applying a PCA on time series simulated in both homogeneous and heterogeneous model domains yielded the same principal components, showing that the interplay of various local water fluxes in heterogeneous flow fields does not induce totally new temporal soil moisture patterns. This is an important basis for the applicability of one-dimensional models to estimate water fluxes in heterogeneous soils. It implies that moisture dynamics observed in heterogeneous flow fields can generally be simulated with effective soil hydraulic parameters without considering the explicit textural heterogeneity. However, another important finding from Chapter 3 was that in contrast to homogeneous soils the transformation state of time series did not increase monotonically with soil depth. For example, time series simulated at locations along preferential pathways were less strongly transformed than others from adjacent regions. This would suggest that even pronounced preferential flow phenomena only reduce mean damping per depth interval rather than induce completely new features, thus paving the way for efficient modelling mean behavior at larger scales. On the other hand, it is not assured, as assumed by the Buckingham-Darcy method, that soil moisture dynamics observed at one position in a heterogeneous flow field are generally representative for all locations at the same soil depth. The correlation between *D* and soil depth was weakest in sand where the performance

of the Buckingham-Darcy method was also poor (chapter 2). Thus, this more theoretical study helped to better understand the results of the preceding study.

The perspective of signal transformation provides a conceptual framework to investigate the effects of various interacting soil hydrological processes. No *a priori* assumptions about determining processes are required since *D* is based on information provided by observed moisture time series. Indeed, that approach cannot be used to exactly quantify soil water fluxes, but it is well suited to compare soil moisture dynamics observed at different locations. For that reason, it rather provides a valuable supplement to the common mass flux considerations. Additionally, it is neither restricted to the vadose zone nor to a specific scale. Hydrological signals passing the vadose zone are subsequently propagated through other subsystems of the hydrological cycle, such as aquifers or the riparian zones of streams (Hauhs and Lange, 1996; Lischeid et al., 2016; Loik et al., 2004). Therefore, the concept of signal transformation is suitable to bring together observations from different scales and disciplines. It has been stated many times before that there is an urgent need for such approaches linking various disciplines (e.g. Asbjornsen et al., 2011; Lin et al., 2015; Lin, 2003). Although the signal transformation concepts is very suitable for this purpose it is, however, worth mentioning that *D* represents a relative measure that can only be interpreted and compared within the context of the observed data set.

The signal transformation described by the second principal component is only one out of many potential processes and factors determining soil moisture dynamics. The finding from this study that the effects of soil heterogeneity are very low dimensional, increases the chance of additionally identifying effects of other controls accounting for very small fractions of total variance.

5.1.3. Identifying the controls on observed soil moisture dynamics

In this section the third objective of this dissertation is addressed, i.e. identifying and describing the main controls on soil moisture dynamics observed in a real-world data set. For this purpose an extensive data set from a multifactorial long-term field experiment was used. Additionally, the applicability of the followed approach to break down the information contents of large soil moisture datasets to a concise and manageable description is discussed based on the findings from Chapter 3 and 4.

The soil moisture dynamics analyzed in this study were mainly composed of one common temporal pattern described by the scores of the first component. It accounted for more than three quarters of the total variance and could be assigned to atmospheric controls that were assumed to be identical for all measuring plots. It is common knowledge that atmospheric conditions control temporal soil moisture dynamics (e.g. Korres et al., 2010; Mahmood et al., 2012). But the large proportion of the variance that all time series had in common was surprising.

The second component explained additionally 7.8 % of variance and described the effect of signal transformation with increasing soil depth, which has been discussed intensively in the previous section. All measuring plots showed a very similar signal transformation behavior despite of large textural heterogeneities. This showed that large spatial heterogeneities do not necessarily cause large functional heterogeneities, which is in line with the observations made by Basu et al. (2010) at the catchment scale. It furthermore provides experimental evidence for the statement of Baveye and Laba (2015) that it is not always reasonable to concentrate on detailed investigation of spatial structural heterogeneities when the interest is primarily on functional aspects.

The third component of the study in chapter 4 could unambiguously be assigned to the different cropping systems, although it accounted for only 3.6 % of the total variance. A time series of the component scores clearly described the differences in the soil moisture dynamics caused by the cropping systems. Effects of different cropping systems or vegetation covers on soil moisture dynamics have been detected several times before (e.g. Baroni et al., 2013; Korres et al., 2015). However, these studies usually aimed at investigating spatial patterns of near surface soil moisture with large spatial but very low temporal resolutions. The functionally averaged time series presented in Chapter 4 provided valuable detailed descriptions of the cropping system effects in a high temporal resolution.

In addition to the cropping system two different soil tillage practices were explicitly considered in the field experiment. In Chapter 4 it was shown that the fraction of total soil moisture variance caused by soil tillage did not exceed 0.05 %. The information that soil tillage in fact had no considerable effect on soil moisture dynamics below the plowing zone at the investigated site was a surprising result. It implies that tillage effects can be neglected in models predicting deep seepage fluxes for the particular field experiment. Please note that this would not neces-

sarily hold for steep topographical gradients where surface runoff might play a much larger role.

In this dissertation PCA proved to be a powerful tool to systematically learn from soil moisture data in the sense of the top-down approach. It has been used to break down the information content of large data sets of moisture time series to a concise and manageable description of the most relevant dynamics. This applied equally to both investigated cases, the numerically simulated data set (Chapter 3) as well as the monitoring data from a long term field experiment (Chapter 4). Particular objectives that can be achieved by PCA are (i) identifying the main controls on the hydrological behavior of soils, (ii) quantifying their relevance by the fraction of total variance they explain, and (iii) providing explicit descriptions of their specific effects in the form of functionally averaged time series.

An important limitation of PCA is that only relative soil moisture dynamics can be analyzed. However, practical soil hydrological questions often aim at quantifying absolute values of different water balance components, such as deep drainage rates (Scanlon et al., 2002; Silburn et al., 2013) or amounts of root water uptake (Green et al., 2006). For that reason, it might be useful for many purposes to combine PCA with common methods of mass flux considerations, e.g. process based modeling.

Principal component analysis identifies only linear structures in datasets (Jolliffe, 2002). The fact that the variance of soil moisture time series from data in Chapter 3 and 4 could be explained by only three distinct controls underlines the low complexity in these particular datasets. If several principal components are related to one factor or if one of the main principal components is correlated to several factors, nonlinearities must be considered (Lee and Verleysen, 2007). For example, isometric feature mapping (Tenenbaum et al., 2000), a nonlinear dimensionality reduction method, was successfully applied in a large-scale hydrological study (Böttcher et al., 2014).

It is remarkable that in the study presented in Chapter 4 almost 90 % of the variance of 57 soil moisture time series was caused by only three independent temporal patterns that could be assigned to first order controls. The particular temporal patterns described by functionally averaged time series represent the integral effects of various factors and processes interacting in a continuum of scales. Hence, PCA enables to grasp the relevant hydrological behavior of

soils at a given scale without explicitly considering all subscale controls and their heterogeneities. This has great potential for large-scale modeling.

5.2. Implications for modeling and further research needs

5.2.1. Reducing uncertainties in large scale modeling

In large-scale models spatial heterogeneities are commonly represented by hydrological response units. These are defined by combining spatial information about presumed controls, such as land use and soil texture (e.g. Arnold et al., 2012; Flügel, 1996). The hydrological behavior of single units is determined by upscaled information about the effects of single controls. For example, hydraulic conductivity for a certain soil type is usually predicted by pedotransfer functions (Vereecken et al., 2010). The relations between hydrological behavior and single controls like soil texture, vegetation or land management are based on correlations published in literature (e.g. Baroni et al., 2013; Korres et al., 2010; Yoo and Kim, 2004). However, these correlations are often low. Additionally, it can be expected that the "file drawer problem", i.e. a preference of positive and significant results for publication (Rosenthal, 1979), leads to an overestimation of these controls in literature. This implies that there is a considerable risk of largely overestimating the effects of these controls by such a model approach. Additionally, using only these controls for large-scale hydrological modelling might primarily reflect the sharply delineated patterns provided by the spatial model input information. An explicit verification of the relevance of the presumed controls in a given case is not possible. Instead, PCA makes full use of the integral soil moisture dynamics observed in field to identify the controls being relevant for a particular question. This approach does not require assumptions about the correlations between controls and hydrological behavior because it is purely data-based. The information provided by PCA is of outermost importance with regard to constraining respective models and thus to reduce model uncertainty right from the beginning of the modelling exercise.

An adequate model structure can be determined by comparing principal components of modeled time-series with those of observed data. Furthermore, the fractions of variance explained by the principal components provide valuable information for the weighting between different

sub-models. This approach allows for rigorously testing if a model is generally suitable to simulate an observed hydrological behavior and if the actual controls on that behavior are considered correctly. The model structure has to be adapted iteratively until principal component scores and their explained variances from modeled and observed data achieve minimum differences.

Model calibration can also be done with PCA outputs. Principal component scores and explained variances can be used to define an objective function for a parameter optimization algorithm. By this, simulation of the general hydrological system behavior is targeted instead of trying to reproduce time-series observed at a few locations.

Obviously, the suggested approaches require large data sets of moisture dynamics that have not been accessible in the past. However, it can be expected that they will be increasingly available in the near future (Vereecken et al., 2014).

5.2.2. Experimental evidence for signal transformation characteristics

In the study presented in Chapter 3 conclusions about the low dimensional nature of signal transformation in heterogeneous soils were drawn from the results of a numerical experiment. In the following study (Chapter 4) it was also shown that the concept of signal transformation has large potential to grasp moisture dynamics observed at the field scale. However, up to now no experimental evidence for the particular findings from Chapter 3 has been provided. Thus, there is a need for further research aiming at rigorously investigating the effects of soil texture and different types of heterogeneities on signal transformation characteristics in controlled experimental set ups.

This could, for instance, be achieved by percolation experiments with soil columns in laboratory. The kind and intensity of signal transformation in various well defined soil textures could systematically be determined. Additionally, signal transformation characteristics could also be related to explicit descriptions of soil structure including macropores. In the laboratory environment it is also possible to examine if damping profiles determined by PCA are sensitive to the degree of saturation. However, it should always be critically questioned if the findings from such a small scale provide reliable implications for field applications.

Weighing lysimeters filled with different soils but exposed to identical atmospheric conditions (e.g. Zacharias et al., 2011) provide many options to investigate signal transformation charac-

teristics at the pedon scale. They also allow for exploring the relation between signal propagation derived from moisture dynamics and seepage fluxes determined in situ.

5.3. Conclusions

Soil moisture is controlled by various factors and processes occurring across a broad continuum of scales. The resulting variability among soil moisture dynamics observed at different locations was in the focus of this dissertation. It was shown that deep seepage estimation using the Buckingham-Darcy law was weak for pure sand because of this variability. The main achievement of this dissertation was to present an approach to turn this problem into a solution: Principal component analysis was applied to make use of the variability among soil moisture time series for analyzing apparently complex soil hydrological systems. The method turned out to be a powerful approach to identify the main controls, quantify their relevance, and describe their particular effects by functionally averaged time series. It clearly showed that both simulated and observed soil moisture dynamics were rather low dimensional. This means they were composed of only a few clear temporal patterns that could furthermore be traced back to their specific causes.

The first two principal components allow for characterizing the transformation of hydrological input signals (e.g., rainfall, snow melt) propagating through the vadose zone. This perspective is a valuable supplement to common mass flux considerations. Neither different textures nor spatial heterogeneities affected the general kind of signal transformation showing that complex spatial heterogeneities do not necessarily evoke a complex hydrological behavior.

The approach presented in this dissertation provides model free information about the main controls on soil hydrological behavior, since it does not require a priori assumptions about physical processes. This allows for efficiently considering spatial heterogeneities in large scale modeling. It also offers great opportunities to reduce model uncertainties by constraining the model structure right from the beginning of the model exercise and defining meaningful criteria for model calibration. These are necessary next steps for soil hydrology to solve real-world problems, e.g. efficient soil moisture management for field crop production.

References

Arnold, J.G. et al., 2012. Swat: Model Use, Calibration, and Validation. T ASABE, 55(4): 1491-1508.

Asbjornsen, H. et al., 2011. Ecohydrological advances and applications in plant-water relations research: a review. J Plant Ecol, 4(1-2): 3-22.

Baroni, G., Ortuani, B., Facchi, A., Gandolfi, C., 2013. The role of vegetation and soil properties on the spatio-temporal variability of the surface soil moisture in a maize-cropped field. J Hydrol, 489: 148-159.

Basu, N.B. et al., 2010. Parsimonious modeling of hydrologic responses in engineered watersheds: Structural heterogeneity versus functional homogeneity. Water Resour Res, 46, W04501.

Baveye, P.C., Laba, M., 2015. Moving away from the geostatistical lamppost: Why, where, and how does the spatial heterogeneity of soils matter? Ecol Model, 298: 24-38.

Böttcher, S., Merz, C., Lischeid, G., Dannowski, R., 2014. Using Isomap to differentiate between anthropogenic and natural effects on groundwater dynamics in a complex geological setting. J Hydrol, 519, Part B: 1634-1641.

Durner, W., Jansen, U., Iden, S.C., 2008. Effective hydraulic properties of layered soils at the lysimeter scale determined by inverse modelling. Eur J Soil Sci, 59(1): 114-124.

Flügel, W.A., 1996. Hydrological Response Units (HRUs) as modeling entities for hydrological river basin simulation and their methodological potential for modeling complex environmental process systems. Die Erde, 127: 42-62.

Green, S.R., Kirkham, M.B., Clothier, B.E., 2006. Root uptake and transpiration: From measurements and models to sustainable irrigation. Agr Water Manage, 86(1-2): 165-176.

Hauhs, M., Lange, H., 1996. Ecosystem dynamics viewed from an endoperspective. Sci Total Environ, 183(1-2): 125-136.

Jolliffe, I.T., 2002. Principal Component Analysis. Springer Series in Statistics. Springer, New York, 489 pp.

Katul, G.G. et al., 2007. On the spectrum of soil moisture from hourly to interannual scales. Water Resour Res, 43(5), W05428.

Kirchner, J.W., 2006. Getting the right answers for the right reasons: Linking measurements, analyses, and models to advance the science of hydrology. Water Resour Res, 42(3).

Korres, W., Koyama, C.N., Fiener, P., Schneider, K., 2010. Analysis of surface soil moisture patterns in agricultural landscapes using Empirical Orthogonal Functions. Hydrol Earth Syst Sc, 14(5): 751-764.

Korres, W. et al., 2015. Spatio-temporal soil moisture patterns - A meta-analysis using plot to catchment scale data. J Hydrol, 520: 326-341.

Lee, J.A., Verleysen, M., 2007. Nonlinear Dimensionality Reduction. Information Science and Statistics. Springer New York.

Lehr, C., Pöschke, F., Lewandowski, J., Lischeid, G., 2015. A novel method to evaluate the effect of a stream restoration on the spatial pattern of hydraulic connection of stream and groundwater. J Hydrol, 527: 394-401.

Lin, H., Drohan, P., Green, T.R., 2015. Hydropedology: The Last Decade and the Next Decade. Soil Sci Soc Am J, 79(2): 357-361.

Lin, H.S., 2003. Hydropedology: Bridging disciplines, scales, and data. Vadose Zone J, 2(1): 1-11.

Lischeid, G. et al., 2016. Catchment evapotranspiration and runoff. In: Foken, T. (Ed.), Energy and Matter Fluxes of a Spruce Forest Ecosystem. Springer, Berlin, Heidelberg (in press).

Lischeid, G. et al., 2010. Assessing coupling between lakes and layered aquifers in a complex Pleistocene landscape based on water level dynamics. Adv Water Resour, 33(11): 1331-1339.

Lischeid, G., Steidl, J., Merz, C., 2012. Functional versus trend analysis to assess anthropogenic impacts on groundwater heads. Grundwasser, 17(2): 79-89.

Loik, M.E., Breshears, D.D., Lauenroth, W.K., Belnap, J., 2004. A multi-scale perspective of water pulses in dryland ecosystems: climatology and ecohydrology of the western USA. Oecologia, 141(2): 269-281.

Mahmood, R., Littell, A., Hubbard, K.G., You, J.S., 2012. Observed data-based assessment of relationships among soil moisture at various depths, precipitation, and temperature. Appl Geogr, 34: 255-264.

Meissner, R., Rupp, H., Seeger, J., Ollesch, G., Gee, G.W., 2010. A comparison of water flux measurements: passive wick-samplers versus drainage lysimeters. Eur J Soil Sci, 61(4): 609-621.

Pan, F., Pachepsky, Y.A., Guber, A.K., Hill, R.L., 2011. Information and complexity measures applied to observed and simulated soil moisture time series. Hydrolog Sci J, 56(6): 1027-1039.

Robinson, D.A. et al., 2008. Soil moisture measurement for ecological and hydrological watershed-scale observatories: A review. Vadose Zone J, 7(1): 358-389.

Rosenthal, R., 1979. The file drawer problem and tolerance for null results. Psychol Bull, 86(3): 638-641.

Savenije, H.H.G., 2009. HESS Opinions "The art of hydrology". Hydrol Earth Syst Sc, 13(2): 157-161.

Scanlon, B.R., Healy, R.W., Cook, P.G., 2002. Choosing appropriate techniques for quantifying groundwater recharge. Hydrogeol J, 10(1): 18-39.

Schindler, U., Müller, L., 1998. Calculating deep seepage from water content and tension measurements in the vadose zone at sandy and loamy soils in North-East Germany. Archives of Agronomy and Soil Science 43(3): 233-243.

Schlüter, S. et al., 2012. Virtual soils: Assessment of the effects of soil structure on the hydraulic behavior of cultivated soils. Vadose Zone J, 11(4).

Silburn, D.M., Foley, J.L., Biggs, A.J.W., Montgomery, J., Gunawardena, T.A., 2013. The Australian Cotton Industry and four decades of deep drainage research: a review. Crop Pasture Sci, 64(11-12): 1049-1075.

Tenenbaum, J.B., de Silva, V., Langford, J.C., 2000. A global geometric framework for nonlinear dimensionality reduction. Science, 290(5500): 2319-2323.

van Genuchten, M.T., Naveira-Cotta, C., Skaggs, T.H., Raoof, A., Pontedeiro, E.M., 2014. The Use of Numerical Flow and Transport Models in Environmental Analyses. In: Teixeira, W.G., Ceddia, M.B., Donnagema, G.K., Ottoni, M.V. (Eds.), Application of Soil Physics in Environmental Analyses. Springer International Publishing.

Vereecken, H. et al., 2014. On the spatio-temporal dynamics of soil moisture at the field scale. J Hydrol, 516: 76-96.

Vereecken, H. et al., 2010. Using pedotransfer functions to estimate the van Genuchten-Mualem soil hydraulic properties: A review. Vadose Zone J, 9(4): 795-820.

Yoo, C., Kim, S., 2004. EOF analysis of surface soil moisture field variability. Adv Water Resour, 27(8): 831-842.

Zacharias, S. et al., 2011. A network of terrestrial environmental observatories in Germany. Vadose Zone J, 10(3): 955-973.

Author's declaration

I prepared this dissertation myself and without any illegal assistance. The work is original except where indicated by references in the text and no part of the dissertation has been submitted for any other degree.

This dissertation has not been presented to any other university for examination, neither in Germany nor in any other country.

Berlin, March 17th, 2016

_____

(Tobias Ludwig Hohenbrink)